Roles of Lipid and Protein Receptors in Regulating Polyomavirus Infection

by

Mengding Qian

A dissertation submitted in partial fulfillment
of the requirements for the degree of
Doctor of Philosophy
(Cell and Developmental Biology)
in the University of Michigan
2010

Doctoral Committee:

Associate Professor Billy Tsai, Chair
Professor Michael J. Imperiale
Associate Professor Kristen J. Verhey
Assistant Professor Akira Ono

Acknowledgements

This thesis would not have been possible without the enormous support and encouragement of my Ph.D. advisor Professor Billy Tsai. I am sincerely thankful for his research insight and advice during the past five years. I would like to express my great appreciation to Professor Michael J. Imperiale, Kristen J. Verhey and Akira Ono for serving on my thesis committee, whose advice and help are valuable. I want to thank all members of the Tsai, Verhey, Fingar and Nabeshima labs for the discussion in the lab meeting. I want to thank Kristen Verhey and Dawen Cai for teaching me the imaging techniques. I also want to thank the CDB administrative staff, particularly Kristen Hug, Karen Lang and Ryan Schell, for all of their help. I will miss everyday in the lab with all the talented colleagues and friends.

I cannot finish without saying how grateful I am with my family: my father, Yijun Qian, and my mother, Meili Song, for their unconditional love and support, and most importantly, my husband Hao Xing, whose love and patient encourage me in all matters of life.

I want to thank Billy Tsai for generating the data in Figures 2.3C-D, 2.4B, 2.6A, 2.10, 3.5A-B, 3.5H and 3.6A-B, Dawen Cai for participating in data analysis in Figures 2.4G, 2.6C and 2.12, and Hannah Leanne Townsend for generating the data in Figure 3.8.

Contents

List of Figures

Figure

Abstract

The non-enveloped murine polyomavirus (Py) binds to receptors on the cell surface to gain entry into host cells. The virus then traffics to the endoplasmic reticulum (ER) where it penetrates the membrane and enters the cytosol, finally reaching the nucleus to cause infection. How Py is transported from the plasma membrane to the ER, however, is not clear. The sialic acid-galactose containing gangsliosides GD1a and GT1b have been reported to be the functional receptors for Py to stimulate Py infection in host cells. Many glycoproteins, which also contain terminal sialic acid-galactose moiety, can in principle engage Py to be Py's receptors. However, how these glycolipid and glycoprotein receptors guide Py intracellular transport and regulate Py infection are poorly understood.

We show that GD1a is the functional entry receptor for Py. GD1a binds to Py on the plasma membrane, and the GD1a-Py complex is internalized and transported to the endolysosomes where the low pH triggers a conformational change that promotes the subsequent ER-to-cytosol membrane penetration of Py. GD1a then sorts Py from the endolysosomes to the ER, leading Py to the infectious pathway. By contrast, glycoproteins act as decoy receptors. They compete with GD1a on the cell surface and interact with Py, guiding Py to the endolysosomes where the virus is trapped and infection is restricted. Therefore, glycolipids and glycoproteins, two major constituents of the plasma membrane, act in opposing manners to control Py infection.

Chapter 1

Introduction

Polyomaviruses are noneveloped, icosahedral viruses with double strand DNA. Polyomaviruses are named from their ability to induce multiple tumors. The family of polyomaviruses includes murine polyomavirus (Py), simian SV40, human JC virus (JCV), BK virus (BKV), KI virus, WU virus and Merkel cell polyomavirus (MCPyV). Murine polyomavirus induces tumors in mouse skin, gland, thymus, and other organs (Benjamin, 2001). SV40, a polyomavirus of the rhesus macaque, is oncogenic to rodents, and is also a potential oncogenic virus in human (Lee and Langhoff, 2006). BK virus and JC virus naturally infect humans, causing nephropathy and progressive multifocal leukoencephalopathy (Eash et al., 2006). KI (Allander et al., 2007), WU (Gaynor et al., 2007), Merkel cell (Feng et al., 2008) viruses were three new polyomaviruses recently isolated in humans, which further stimulate the studies of polyomaviruses as human pathogens.

Polyomaviruses are icosahedral particles with ~40 nm in diameter. They have three capsid proteins, VP1, VP2, and VP3 (Figure 1.1). Each virion contains 72 pentamers (360 copies) of the major capsid protein VP1, and 72 copies of internal structural protein VP2/VP3. Each VP1 pentamer is associated with an internal protein VP2 or VP3. The C-terminal arm of the VP1 molecule is extended to the adjacent pentamers to stabilize the interpentamer interaction (Liddington et al., 1991; Stehle et al., 1994). The virion also contains ~200 copies of histones, which is enclosed in the center of the viral particle. The genomes of polyomaviruses are ~5k bp in size. They encode T antigens that initiate viral DNA synthesis. Assessing the expression of large T antigens is an efficient way to

determine whether the virus infection is successful. All these capsids, histones and T antigens contain nuclear location sequence (NLS), which is not exposed in the intact virion (Benjamin, 2001).

Polyomaviruses hijack cellular machineries to cause diseases (Figure 1.2). Upon binding to their receptors on the plasma membrane, polyomaviruses are first endocytosed into the cell, and retrograde transported to the ER. Then they penetrate the ER membrane to enter the cytosol. From the cytosol, they are transported to the nucleus to replicate and transcribe the DNA, which leads to lytic infection or cell transformation (Whittaker, 2003). As the ER membrane is continuous with the nuclear membrane, it remains possible that polyomaviruses can enter the nucleus directly from the ER by penetrating the inner nuclear membrane. However, at least for SV40, reaching the cytosol is important because virus infection is inhibited by introducing an antibody against VP1 or VP3 to the cytoplasm (Nakanishi et al., 1996).

Murine polyomaviruses (Py) is the first isolated polyomavirus (Gross, 1953). They cause multiple tumors in different organs of mouse (Benjamin, 2001). Even though Py may not relate to human diseases directly, it is considered a good model to study the cellular machineries that guide the infection process generally. Additionally, findings based on Py should also lead to a better understanding of human polyomavirus infection. To initiate infection, Py first binds to ganglioside GD1a, which is the functional receptor for Py, on the plasma membrane (Tsai et al., 2003). The entry pathway of Py seems to be cell dependent. In mouse NIH 3T3 cells or primary baby mouse kidney (BMK) cells, Py enters cells through a clathrin independent and caveolin-1 independent pathway (Gilbert and Benjamin, 2000). By contrast, in rat glioma C6 cells, Py enters cells via a caveolin-1 dependent pathway (Gilbert and Benjamin, 2004). After entry, Py has been reported to be transported through the early endosomes, and the acidic environment in the endosomes is critical for Py infection, since neutralization of pH in the endosomes by NH_4Cl treatment blocks

Py infection (Liebl et al., 2006). However, there is another report demonstrating that Py does not need to traffic through an acidic compartment, and NH4Cl treatment does not affect Py infectivity (Gilbert and Benjamin, 2000). This discrepancy may be due to the differences in methodology. Regardless, Py does not appear to traffic through the Golgi complex en route to the ER (Gilbert and Benjamin, 2004).

After initial entry, Py must be transported to the ER and penetrate the ER membrane to reach the cytosol for productive infection. Brefeldin A (BFA), which inhibits retrograde β-COPI-dependent retrograde transport from the plasma membrane to the ER, blocks Py infection (Gilbert and Benjamin, 2004), consistent with the premise that ER targeting is required for virus infection.

In the ER, Py undergoes conformational changes that facilitate Py to breach the ER membrane to access the cytosol (Magnuson et al., 2005). As disulfide bonds and calcium ions stabilize the viral structure (Brady et al., 1978; Stehle et al., 1994; Stehle et al., 1996), ER-resident reductases and calcium binding proteins likely destabilizes Py in the ER and promotes the ER-to-cytosol penetration event. For example, Py infection is inhibited by knockdown of protein disulfide isomerase (PDI), an ER-resident protein that facilitates oxidation-reduction reactions, and restored by expression of PDI. Py could reach the ER but fail to exit the ER in cells with reduced PDI (Gilbert et al., 2006). ERp29, a member of the PDI family, plays a critical role in Py conformational change and initiates the ER membrane penetration of Py. Specifically, ERp29 unfolds the VP1 C-terminal arm, which normally functions to stabilize Py by interacting with the adjacent VP1 pentamer. The ERp29-dependent reaction results in formation of a hydrophobic viral particle that bind to and integrate into the ER membrane (Magnuson et al., 2005; Rainey-Barger et al., 2007), events that prime Py for penetration across the ER membrane. Derlin-2, an ER-resident protein that removes misfolded proteins from the ER to the cytosol for proteasomal degradation (Oda et al.,

2006), is required for Py infection, suggesting that Py penetrates the ER through a protein-conducting channel (Lilley et al., 2006).

Upon reaching the cytosol, Py is transported to the nucleus to replicate its DNA. Although all the capsid proteins and histones contain NLS, the NLS are not exposed in the intact virion (Benjamin, 2001). Since the size of nuclear pore complex (around 26 nm in diameter) (Otis et al., 2006; Yang et al., 2004) is smaller than the size of intact Py (about 40 nm in diameter) and that exposure of the NLS is required for nuclear entry, Py thus needs to undergo dramatic conformational changes and uncoating before entering the nucleus.

Other members of the polyomavirus family are also transported from the cell surface through the ER and the cytosol en route to the nucleus. However, they may bind to different receptors and take different endocytosis pathways. SV40 binds to ganglioside GM1 on the plasma membrane (Tsai et al., 2003; Low et al., 2004; Neu et al., 2008) and is endocytosed into cells via a caveolae-dependent pathway (Pelkmans et al., 2001). SV40 is then transported either to a pH-neutral compartment called caveosome for productive infection, or to the early endosome for non-productive infection (Pelkmans et al., 2004). It is also critical for SV40 to traffic to the ER, where it penetrates the ER membrane to the cytosol. The ER-resident protein PDI, ERp57 and ERp72 are reported to mediate the ER membrane penetration of SV40 (Schelhaas et al., 2007).

For human polyomaviruses, JC virus may also bind to gangliosides as receptors since the infectibility of JC virus coated with GT1b is inhibited (Komagome et al., 2002). JC virus is endocytosed into cells via a clathrin-dependent pathway and transported through the early endosomes (Pho et al., 2000; Querbes et al., 2004; Querbes et al., 2006). BK virus engages ganglioside GD1b and GT1b as functional receptors (Low et al., 2006) and enters cells via a caveolar-mediated pathway (Eash et al., 2004). Low pH is required for BK virus infection (Eash et

al., 2004). The ER-resident protein Derlin-1 interacts with BKV in the ER and facilitates infection (Jiang et al., 2008).

The observation that gangliosides are used by several members of the polyomavirus family for infection raises the possibility that these glycolipid receptors possess unique properties that facilitate the entry and intracellular sorting of the viruses along the infectious route. Ganglioside is a sialic acid-containing glycosphingolipid, consisting of a hydrophobic ceramide domain and a hydrophilic carbohydrate moiety (Kolter and Sandhoff, 2005; Schwarzmann, 2001). Gangliosides are biosynthesized on the ER and Golgi membranes, and then transported to the plasma membrane. On the plasma membrane, they are inserted into the outer leaflet via their hydrophobic ceramide residue, with their hydrophilic sugar portion protruding into the extracellular space. These lipids are normal components of plasma membranes, and usually concentrated in lipid rafts. Gangliosides on the cell surface undergo endocytosis into cells for catabolism. After internalization, these lipid molecules are transported through the early and late endosomes, finally reaching the lysosomes where they are hydrolyzed by lysosomal enzymes. If gangliosides are not properly degraded by the enzymes in the lysosome, it results in a disease called "Gangliosidosis“, which is a form of lipid storage disorder. From the endolysosomal system, gangliosides could be transported to the Golgi complex. However, their retrograde transport to the ER has not been observed (Schwarzmann, 2001).

Many research groups have documented that gangliosides act as functional receptors for polyomaviruses. Specifically, ganglioside GD1a and GT1b are the functional receptors for Py (Smith et al., 2003; Tsai et al., 2003); GM1 is the functional receptor for SV40 (Tsai et al., 2003; Low et al., 2004); GD1b and GT1b are the receptors for BKV (Low et al., 2006); GT1b is the receptor for the newly discovered Merkel Cell polyomavirus (Erickson et al., 2009). In addition, ganglioside GM1 also serves as the functional receptor for cholera toxin (Fujinaga et al., 2003). The virus-receptor interaction is based on the interaction

of the VP1 protein of the virus and the sialic acid-containing moiety of the receptor. Py binds to ganglioside GD1a / GT1b via the interaction of Py VP1 with the sialic acid-galactose moiety in GD1a / GT1b (Stehle et al., 1994; Stehle and Harrison, 1997; Tsai et al., 2003). Interaction of Py with the terminal sialic acid residues induces conformational change of the viral capsid, which may facilitate the viral entry step (Cavaldesi et al., 2004). SV40 also engages ganglioside GM1 via sialic acid binding (Neu et al., 2008). However, although the concept that gangliosides acting as polyomavirus receptors has been well established, whether gangliosides must engage polyomaviruses on the cell surface to serve as entry receptors, and how gangliosides regulate virus intracellular trafficking to promote infection, are still not clear.

In addition to Py's functional ganglioside receptors GD1a / GT1b, most glycoproteins on the cell surface also contain sialic acid-galactose moiety (Kornfeld and Kornfeld, 1985). Hence, glycoproteins in principle are able to serve as cell surface receptors for Py. Glycoprotein α4β1 integrin has been reported as the postattachment receptor of Py (Caruso et al., 2003). However, it remains unknown the general role of glycoprotein receptors in influencing Py infection. Whether glycoproteins act collaboratively with ganglioside to facilitate Py infection, or act as decoy receptors to compete with ganglioside for Py binding, is not understood well.

Studies in this thesis focus on the Py trafficking pathway from the plasma membrane to the ER, and the roles of ganglioside GD1a and glycoproteins in regulating Py trafficking and infection. With a combination of live cell imaging, cell infection and biochemical studies, we show that after internalization, Py is first transported through the endolysosomal compartments before reaching the ER. Trafficking through the endolysosomal system is part of the Py infectious pathway, as the low pH environment in the endolysosomes triggers a conformational change that promotes the subsequent ER-to-cytosol membrane penetration of Py (Chapter 2). Moreover we discovered that, after reaching the

endolysosomes, ganglioside GD1a plays a critical role in sorting Py from the endolysosomes to the ER (Chapter 2). That a glycolipid serves as an intracellular sorter for viral trafficking has not been reported.

Importantly, our studies unveiled that glycolipids (i.e. ganglioside GD1a) and glycoproteins act as two competitive receptors for Py binding on the cell surface (Chapter 3), guiding the virus down different intracellular pathways with opposite consequences on infection. In particular, we found that ganglioside GD1a acts as the functional entry receptor for Py: GD1a must bind to Py on the plasma membrane to promote Py infection. The GD1a-Py complex is internalized into cells and transported through the endolysosomes. GD1a next sorts Py from the endolysosomes to the ER, thus leading Py to the infectious pathway. GD1a binding is responsible for ER targeting, since an artificial particle designed to bind to GD1a also reaches the ER. In contrast, glycoproteins generally act as decoy receptors for Py to protect cells from virus infection. They compete with GD1a on the cell surface for Py binding, bringing the virus to the endolysosomes where Py becomes trapped and virus infection is restricted. Therefore, glycolipids and glycoproteins, two major constituents of the plasma membrane, act in opposing manners to regulate Py infection.

Figure 1.1. The general structure of polyomaviruses.
(a) The polyomavirus particle is composed of 72 pentamers (360 copies) of the major capsid protein VP1. (b) Each VP1 pentamer is associated with an internal protein VP2 or VP3.

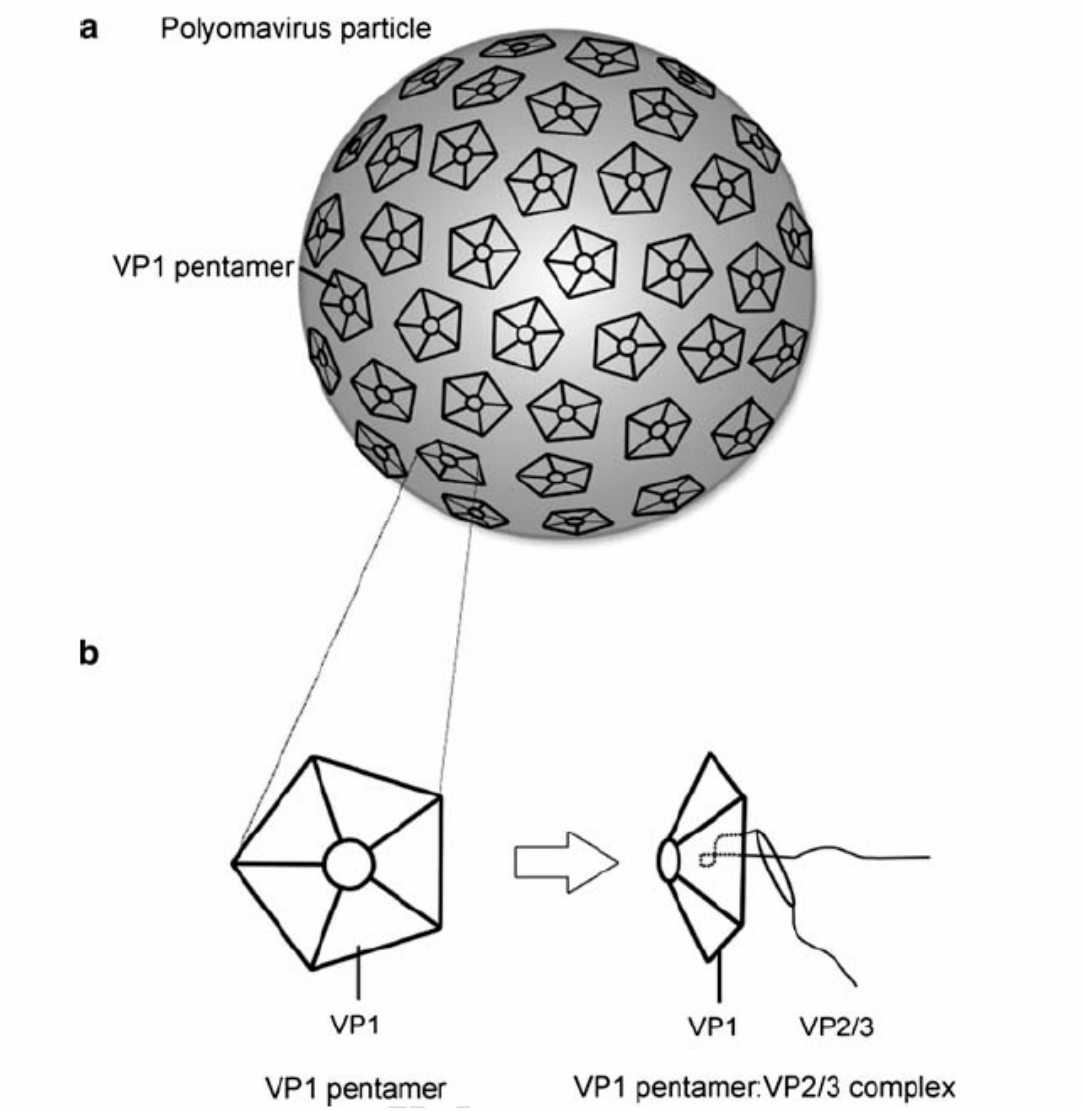

Figure 1.2. Intracellular trafficking of polyomaviruses.
Polyomavirus is transported from the plasma membrane to the nucleus to cause infection. It can be divided into four steps. Step 1, polyomavirus binds to the receptor on the host cell surface to initiate entry. Step 2, polyomavirus is transported from the plasma membrane to the ER. Step 3, polyomavirus penetrates the ER membrane to reach the cytosol. Step 4, polyomavirus is transported to the nucleus to cause infection. Since the ER membrane is contiguous with the nuclear membrane, it remains possible for polyomavirus to penetrate the inner nuclear membrane to reach the nucleus from the ER.

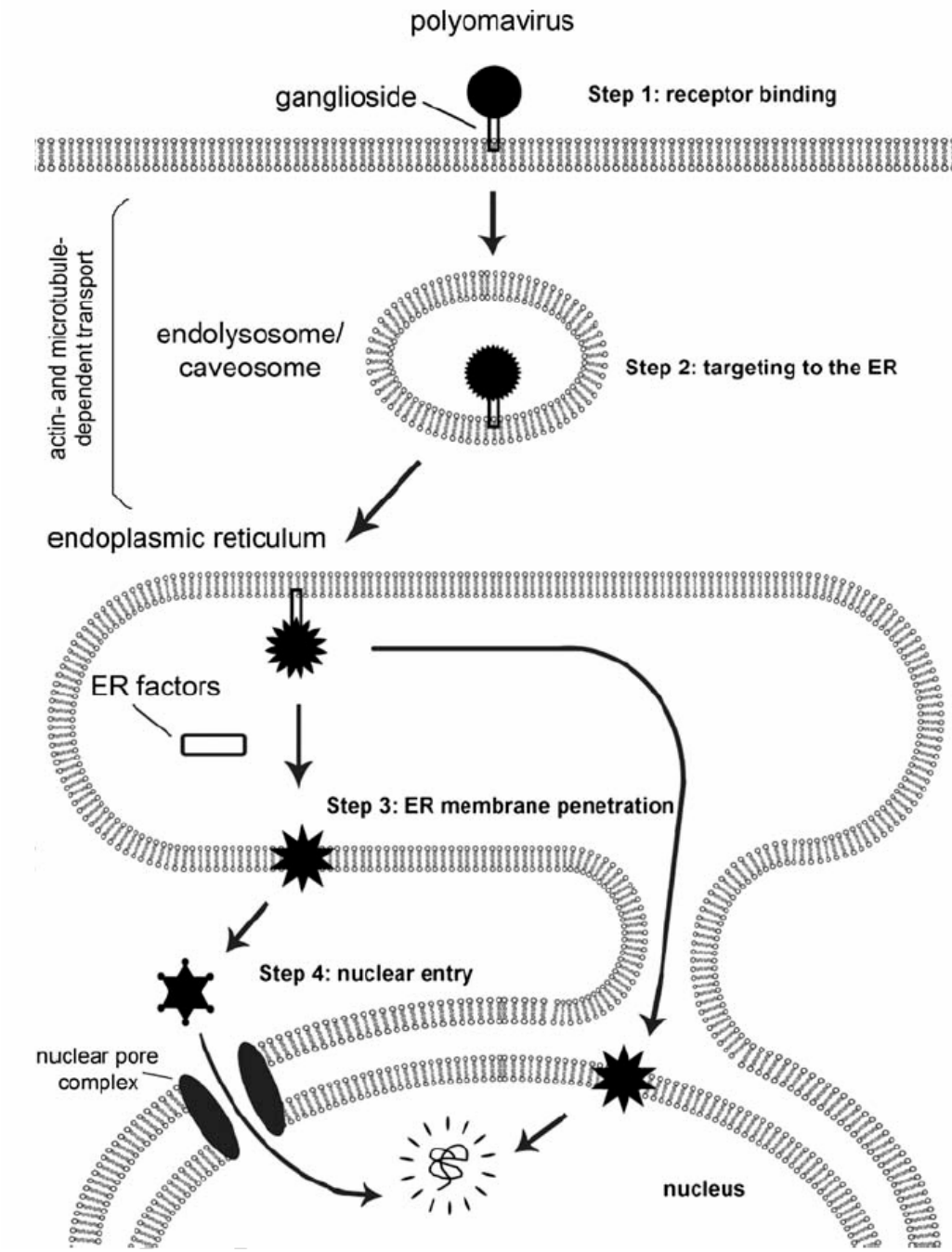

Chapter 2

A Lipid Receptor Sorts Polyomavirus from the Endolysosome to the Endoplasmic Reticulum to Cause Infection

Background and Introduction

Most nonenveloped viruses need to be endocytosed into cells and transport to the proper organelles to cause productive infection. Members of the polyomavirus family, including the murine polyomavirus (Py), SV40, and human BK, JC, KI, WU, Merkel Cell viruses, are non-enveloped DNA viruses (Tsai and Qian, 2010). They engage specific receptors on the plasma membrane, and are transported from the cell surface to the nucleus, where the DNA genomes are transcribed and replicated.

Py is composed of 72 pentamers of the outer structural protein VP1. Each VP1 pentamer encloses an internal structural protein VP2 or VP3. The DNA genome is encapsulated in the center of the viral particles (Stehle et al., 1994; Chen et al., 1998).

To initiate infection, Py interacts with the ganglioside receptor GD1a on the plasma membrane, and is transported from the cell surface to the lumen of the endoplasmic reticulum (ER) (Tsai et al., 2003). In the ER, Py interacts with ER-resident factors and undergoes conformational changes, facilitating the penetration of Py from the ER to the cytosol (Magnuson et al., 2005). Py finally reaches the nucleus to cause lytic infection or cell transformation. The successful arrival of one viral particle to the nucleus is sufficient to cause infection (Diacumakos and Gershey, 1977).

Ganglioside is sialic acid-containing glycosphingolipid, which consists of a hydrophobic ceramide domain that is inserted into the outer leaflet of the plasma membrane, and a hydrophilic carbohydrate moeity (Kolter and Sandhoff, 2005; Schwarzmann, 2001). After internalized into cells, ganglioside is transported to the early endosomes, the late endosomes and finally to the lysosomes where they are hydrolyzed by lysosomal enzymes. Although ganglioside could be transported to the Golgi (Schwarzmann, 2001), only a very low level could arrive in the ER. Ganglioside GD1a has been reported as the functional receptor for Py (Tsai et al., 2003), and supplementing GD1a in ganglioside deficient cell lines increase Py infection (Gelbert and Benjamin, 2004; Gilbert et al., 2005). The sialic acid-galactose moiety in GD1a interacts with the VP1 protein in Py. However, how GD1a promotes Py infection is poorly understood.

With a combination of live cell imaging, cell infection and biochemical studies, we show that Py is transported to the endolysosomal system after internalization. The low pH environment in the endosomes and lysosomes triggers structural alternations in Py, which is critical for its subsequent conformational change in the ER to initiate the ER-to-cytosol penetration process. Ganglioside GD1a then sorts Py from the endolysosome to the ER for productive infection. GD1a binding seems to be responsible for ER targeting, as an artificial particle coated with an antibody against GD1a is also targeted to the ER. Overall, our results demonstrate that the endolysosomal pathway is part of the Py infectious route, and identify a lipid-dependent mechanism that targets Py to the ER for productive infection.

Results

Live Cell Imaging of Polyomavirus Transport to the Endolysosome

First we investigated the Py internalization pathway in cells. Purified Py was labeled with Texas-Red or Alexa Fluor 594 dye, and imaged with wide field fluorescence microscopy. We showed that at 3 hrs post-infection, the fluorescence signal of the labeled Py overlapped significantly with the

fluorescence signal from immunofluorescence staining using an antibody against VP1 in NIH 3T3 cells (Figure 2.1A). This result indicates that most of the purified Py are labeled efficiently with Texas-Red or Alexa Fluor 594 dye, and the labeled dye still associates with Py after virus entry into cells. To test whether the labeling procedure affects Py infection, the expression of large T antigen was measured by immunofluorescence staining with an antibody against large T antigen. Both unlabeled Py and labeled Py infected cells with similar efficiency (Figure 2.1B), indicating that the labeling procedure did not affect Py infection. This finding is consistent with a previous observation (Gilbert and Benjamin., 2000). Therefore the labeled Py could be used to study the Py trafficking pathway inside the cells.

Intracellular trafficking of Py was studied using live cell imaging. Py infection was synchronized by incubating cells with Py at 4°C for 0.5 hr. Cells were washed to remove unbound Py and incubated in 37°C to allow Py to enter cells. To rule out any coincident co-localization, only those labeled Py that co-localizes with vesicles for more than 30 s were counted as real co-localization.

As GD1a is normally transported from the plasma membrane through the early and late endosome to the lysosome, we hypothesized that Py is also transported through this pathway after its initial entry. Co-localization of Py with the early endosome was investigated in cells transfected with cyan fluorescent protein (CFP)-Rab5, a marker of the early endosomes. It should be noted that when expressed at a moderate level, CFP-Rab5 did not alter the morphology or distribution of the early endosomes, which were stained with an antibody against EEA1 (Figure 2.8A). This result is consistent with a previous report that the low level expression of GFP-Rab5 did not affect the size of the early endosomes (Sonnichsen et al., 2000). An example of labeled Py (red) continuously co-localizing with the early endosome (blue) for 120 s is shown in Figure 2.1C. Py appears to be located on the endosome membrane, suggesting that the virus may still be attached to the receptors on the endosome membrane and not

released into the lumen of the endosome (Figure 2.1C). Quantification of the percentage of Py co-localizing with the early endosome at indicated post-infection time points is shown in Figure 2.1F (blue curve). Approximately 10% of the internalized Py co-localized with the early endosome after initial entry (0.5-2 hrs post-infection), and only about 5% of the internalized Py was located in the early endosomes at the later time points (after 4hrs post-infection). This finding is consistent with a previous report demonstrating that in fixed cells only a low percentage of Py was found in the Rab5-containing early endosomes (Mannova and Forstova., 2003).

Co-localization of Py with the late endosome was assessed in cells transfected with yellow fluorescent protein (YFP)-Rab7, a marker of the late endosomes (Rink et al., 2005). When expressed at a moderate level, YFP-Rab7 did not alter the morphology or distribution of the late endosomes / lysosomes, which were stained with an antibody against LAMP1 (Figure 2.8B). A typical image of labeled Py (red) continuously co-localizing with the Rab7-containing late endosome (green) for 80 s is shown in Figure 2.1D. The percentage of Py located in the late endosomes was quantified in Figure 2.1F (green curve). At the early time point (0.5-2 hrs post-infection), only a low percentage of Py (less than 20%) co-localized with the Rab7-containing late endosomes. However, unlike that found in the early endosomes, the percentage of Py in the late endosomes increased as the incubation time increased. More than 50% of Py were found in the late endosomes at 4-6 hrs post-infeciton, and the percentage of Py co-localizing with the late endosomes increased to about 70% at 16-17 hrs post-infection. This result suggests that Py gradually accumulates in the late endosomes.

Similarly, co-localization of Py with the endolysosomes was studied in cells expressing LAMP1-YFP, a marker of the late endosomes and the lysosomes. A representative image of labeled Py (red) continuously co-localizing with LAMP1-containing vesicles (cyan) for 45 s is shown in Figure 2.1E. Quantification analysis showed that the percentage of Py located in the LAMP1-containing

vesicles increased from about 12% at the early time point (0.5-2 hrs post-infection) to about 50% at the later time points (after 4 hrs post-infection) (Figure 2.1F, cyan curve), indicating that Py gradually accumulated in the LAMP1-containing vesicles. It should be noted that there is a significant overlap between the Rab7 and LAMP1 containing vesicles (Meresse et al., 1995). Thus the total percentage of Py located in the Rab7- and LAMP1-containing vesicles could exceed 100%, as observed in the green and cyan curves at the later time points (after 4 hrs post-infection) in Figure 2.1F. The result of the co-localization finding between Py and the Rab7- or LAMP1-containing vesicles is in contrast to a previous study (Mannova and Forstova, 2003) which showed that there was no co-localization between Py and Rab7- or LAMP2-containing vesicles. The conflicting result might be due to the differences in the detection methods (e.g., live cell imaging versus immunofluorescence staining in fixed cells) or the cell types used (NIH 3T3 cells used in our study versus 3T6 cells used in Mannova's paper).

In addition, by incubating NIH 3T3 cells expressing GFP-Caveolin-1 with Py at 4°C, we found that Py has very low co-localization with caveoline-1 containing vesicles (Figure 2.9), indicating that Py is internalized via a caveolin-1 independent pathway, consistent with a previous report (Gilbert and Benjamin, 2000). Overall, our results suggest that Py is transported through the endolysosomal compartments.

Effects of Expressing Rab5 and Rab7 mutants on Polyomavirus Infection

As Py is transported through the endolysosomal pathway, we sought to determine whether this endolysosomal pathway is part of the Py infectious or non-infectious pathway. It has been reported that Rab5 and Rab7 play an important role in regulating cargo transport in the endosomes and lysosomes (Zerial and McBride, 2001), and expression of dominant negative mutants of Rab5 or Rab7 block normal cargo transport in the endolysosomal system (Stenmark et al., 1994; Feng et al., 1995). Therefore, we asked whether Py

infection could be inhibited when cargo transport in the endolysosomes is blocked by expressing Rab5 or Rab7 dominant negative mutants. We first assessed Py infection in NIH 3T3 cells expressing wild type CFP-Rab5, and found that the virus infection was not affected by expression of CFP-Rab5 when compared to expression of CFP as a control. When virus infection in cells transfected with dominant negative CFP-Rab5 S34N (CFP-Rab5 DN) was tested, we found that expression of CFP-Rab5 DN decreased Py infection (Figure 2.2A). This result is consistent with a previous report that expression of a dominant negative Rab5 construct reduced Py infection (Liebl et al., 2006). In addition, expression of a constitutively active form of Rab5 (CFP-Rab5 Q79L, marked as CFP-Rab5 CA in Figure 2.2A) slightly increased Py infection. Therefore, trafficking through the early endosome is part of the Py infectious pathway.

Furthermore, we asked whether trafficking through the late endosome was also part of the Py infectious pathway by expressing dominant negative YFP-Rab7 N125I (YFP-Rab7 DN), which has been reported to block the transport of the vesicular stomatitis virus G protein from the early to the late endosome (Feng et al., 1995). As a control, we found that expression of YFP-Rab7 did not affect Py infection when compared to expression of YFP. However, expression of YFP-Rab7 DN inhibited Py infection (Figure 2.2B). These findings suggest that trafficking through the late endosome is also important for Py infection. Overall, we conclude that transport through the endolysosomal system is part of the Py infectious pathway.

A Role of the Endolysosomal Low pH in Py Infection and Conformational Change

We next asked why transport through the endolysosomal pathway is critical for Py infection. Does Py merely follow the ganglioside receptor GD1a trafficking pathway, or is the low pH environment in the endolysosomal system important for Py infection? We assessed whether the acidic environment in the endolysosomal system is important for Py infection by adjusting the endolysosomal environment

to a neutral pH. Bafilomycin A1 is a specific inhibitor of the vascular proton ATPase and blocks acidification of the endolysosomes. NIH 3T3 cells were incubated with bafilomycin A1 at different time points pre- or post-infection, and the effect on Py large T antigen expression was measured. We found that treatment with bafilomycin A1 at 2 hrs prior to infection or at infection significant inhibited Py infection, while treatment with bafilomycin A1 at 3 hrs after infection had no effect on Py infection (Figure 2.3A). Similarly, the effect of NH4Cl, which is a weak base that could adjust the pH in the endolysosomes to a neutral level (Maxfield, 1982), on Py infection was also assessed. We found that, similar to bafilomycin A1 treatment, treatment with NH4Cl at 2 hrs pre-infection or at infection blocked Py infection, while treatment with NH4Cl 3 hrs post-infection had no effect (Figure 2.13). It should be noted that one previous report showed that NH4Cl treatment inhibited Py infection (Liebl et al., 2006), while another finding showed that it did not (Gilbert and Benjamin, 2000). We concluded that the low pH environment in the endolysosomal system is essential for Py infection.

Elevating endolysosomal pH could affect Py infection in several ways. One possibility is that the acidic environment is critical for cargo transport from the early endosomes to the late endosomes (Clague et al., 1994). Thus perturbing the endolysosomal pH might block virus transport from the early to late endosomes, which would be important for Py to be delivered to the ER. To test this hypothesis, we studied whether treatment of bafilomycin A1 affects co-localization of Py with the late endosome or the ER using immunofluorescence staining. Cells expressing YFP-Rab7 were incubated with Py and bafilomycin A1 simultaneously, washed and fixed at 4.5 hrs post-infection, subjected to immunofluorescence staining with an antibody against Py VP1, followed by staining with a fluorescently tagged secondary antibody. We found that treatment with bafilomycin A1 did not affect co-localization of Py with the Rab7-containing late endosome (Figure 2.3B, top panel), indicating that Py trafficking to the late endosome is not affected by perturbation of the endolysosomal pH. Next, we assessed co-localization of Py with the ER using cells expressing the ER-

resident protein heme oxygenase-2 fused to CFP (CFP-HO2). We found that bafilomycin A1 did not block co-localization of Py with the ER as well (Figure 2.3B, bottom panel). Collectively, these results suggest that perturbation of endolysosomal pH does not block the delivery of Py to the late endosome or the ER. These findings suggest that the low pH environment in the endolysosomes might promote Py infection by acting directly on the viruses.

We therefore hypothesized that the low pH in the endolyosome induces Py conformational changes that facilitate the subsequent viral penetration, as reported in other viral systems (Skehel and Wiley, 2000). First we investigated whether there were any conformational changes induced on Py when the virus was exposed to a pH approximating the endolysosomal pH by using limited proteolysis. The pH in the early endosome is approximately 6.0, and pH in the late endosome / lysosome is approximately 5.0. Therefore Py was incubated at pH 7.5 (as a control), 6.0 (mimicking the pH in the early endosome), or 5.0 (mimicking the pH in the late endosome / lysosome) for 1 hr, neutralized to pH 7.5, and then treated with a low concentration of proteinase K (2.5 ng/ml). We found that pre-incubation with low pH generated discrete fragments of VP1 (Figure 2.3C, compare lanes 5 and 6 to lane 4). Similarly, Py was more sensitive to trypsin (1 mg/ml) digestion when Py was initially exposed to low pH (Figure 2.10, bottom panel, compare lanes 2 and 3 to lane 1). These results imply that low pH in the endolysosomal system could induce a conformational change to Py VP1.

We then asked why the low pH-triggered conformational change facilitates Py infection. We hypothesized that this low pH-triggered conformational change might be important to the subsequent conformational change the virus experiences in the ER, which has been shown to be essential for the ER-to-cytosol penetration process and infection (Magnuson et al., 2005). Our previous work established an in vitro trypsin digestion assay that measure the ER-dependent conformational change of Py (Magnuson et al., 2005; Rainey-Barger

et al., 2007). As disulfide bonds and calcium ions stabilize the viral structure (Brady et al., 1978; Stehle et al., 1994), Py was first incubated with the reducing agent DTT and the calcium chelating agent EGTA to destabilize the virus. When Py was incubated with the control protein bovine serum albumin (BSA), treatment with a low concentration of trypsin (0.25 mg/ml) generated a VP1-derived fragment called VP1a (Figure 2.3D, lane 2). In contrast, if Py was initially incubated with DTT, EGTA and ER luminal extract (an extract containing ER lumenal proteins), treatment with trypsin generated an additional cleavage product called VP1b (Figure 2.3D, lane 4); VP1b formation reflects a specific viral conformational change critical for its ER-to-cytosol penetration (Magnuson et al., 2005). It should be noted that in vivo Py might be destabilized by ER-resident PDI to reduce the disulfide bonds and by calcium-binding proteins calnexin / calreticulin to extract the calcium ions (Gilbert et al., 2006). Importantly we assessed whether there was more VP1b generated by this trypsin digestion assay if Py was initially exposed to low pH. We found pre-exposure to low pH did increase VP1b generation (Figure 2.3D, compare lane 8 to lane 6, and in duplicates, compare lane 12 to lane 10; quantified in right graph). Therefore, the low pH-triggered conformational change enhances the subsequent ER-dependent conformational change that facilitates the ER-to-cytosol penetration of Py.

Decreased Co-localization of Py with the Late Endosome and Lysosome in Cells Supplemented with GD1a

As our results suggest that Py trafficking through the acidic endolysosomal system is important for Py infection, and previous results showed that ganglioside GD1a is the receptor for Py and addition of GD1a in C6 cells promotes Py infection (Tsai et al., 2003; Gilbert and Benjamin, 2004), we asked whether GD1a stimulates Py infection by affecting Py trafficking through the endolysosomal system.

First we verified that supplementing GD1a in NIH 3T3 cells also promote Py infection as found in C6 cells (Tsai et al., 2003; Gilbert and Benjamin, 2004). NIH 3T3 cells were incubated with GD1a or a control ganglioside GM1 overnight, washed to remove unbound ganglioside, incubated with Py for 2 days, and then subjected to immunofluorescence staining with an antibody against large T antigen. We found that supplementing GD1a but not GM1 stimulated Py infection in NIH 3T3 cells (Figure 2.4A).

We then asked whether the increase in Py infection in GD1a-supplemented cells is due to enhanced Py binding to the plasma membrane. GD1a supplemented cells or control cells were incubated with Py at 4ºC for 1 hr, washed to remove the unbound Py, harvested, and the total cell lysate subjected to SDS-PAGE followed by immunoblotting with an antibody against VP1. We found that the VP1 level in GD1a-supplemented cells was similar to that in control cells (Figure 2.4B, compare lane 2 to lane 1). To confirm that the VP1 signal represents the Py on the cell surface, the proteinase K digestion assay was applied because cell surface bound Py should be sensitive to proteinase K digestion. As expected, we found that the VP1 signal disappeared completely after proteinase K treatment in both control and GD1a-supplemented cells (Figure 2.4B, lane 3 and lane 4). Our results indicate that supplementing GD1a did not stimulate cell surface binding of Py, consistent with a previous report in C6 cells (Gilbert and Benjamin, 2004). Since there are large amounts of endogenous sialic acid-galactose moiety containing gangliosides and glycoproteins that can bind to Py on the NIH 3T3 cell surface, it is not surprising that we did not detect any increase in Py binding in the GD1a-supplemented cells.

Next we asked whether the increase in Py infection in GD1a-supplemented cells is due to enhanced Py entry. Control or GD1a-supplemented cells were incubated with Py at 4 ºC and then shifted to 37ºC to allow Py entry into cells. Cells were harvested and treated with proteinase K to digest cell surface viruses. The remaining VP1 signal should represent the internalized Py since internalized

Py is resistant to proteinase K digestion. We found that supplementing GD1a did not stimulate Py entry into cells (Figure 2.4B, compare lane 8 to lane 7). Overall, we conclude that supplementing GD1a did not promote Py binding or entry in NIH 3T3 cells. Thus the addition of GD1a stimulates Py infection probably by regulating intracellular trafficking of the virus.

We asked whether supplementing GD1a stimulates more Py trafficking to the endolysosomal system. We found that supplementing GD1a in NIH 3T3 cells did not affect co-localization of Py with the Rab5-containing early endosomes in either early time points (0.5-2 hrs post-infection) or later time points (4-6 hrs post-infection) (Figure 2.4C). Also, supplementing GD1a did not affect co-localization of Py with the Rab7-containing late endosomes in the early time points (0.5-2 hrs post-infection) (Figure 2.4D). Surprisingly, GD1a addition significantly decreased co-localization of Py with the late endosomes in the later time points (4-6 hrs post-infection) in NIH 3T3 cells (Figure 2.4D). A similar decrease in co-localization of Py with the late endosomes was also observed in C6 cells at 1-2 hrs post-infection, a time point when about 70% of Py already localized in the late endosomes (Figure 2.4E). As C6 cells are ganglioside deficient cells, trafficking of Py to the late endosomes suggests that non-ganglioside receptors such as glycoproteins can also guide Py to the endolysosomal pathway. We also assessed co-localization of Py with the LAMP1-containing vesicles in control or GD1a-supplemented NIH 3T3 cells, and found that addition of GD1a also decreased co-localization of Py with the LAMP1-containing late endosomes / lysosomes at 4-6 hrs post-infection (Figure 2.4F). We conclude that supplementing GD1a decreases co-localization of Py and the late endosomes / lysosomes.

One possibility that supplementing GD1a decreases co-localization of Py with the late endosome and lysosome compartments is that GD1a creates a novel pathway for Py infection independent of the endolysosomal pathway. If this is the case, then expression of dominant negative Rab7 should not block Py infection in

GD1a-supplemented cells. However, we found that expression of YFP-Rab7 DN still inhibited Py infection in GD1a-supplemented cells (Figure 2.4G), indicating that the endolysosomal pathway remains part of the infectious pathway for Py in GD1a-supplemented cells.

Another possibility is that that GD1a supplement induces constriction of endolysosomes, which results in decrease of Py trafficking to the late endosomes and lysosomes. The sizes of CFP-Rab5, YFP-Rab7, or LAMP1-YFP vesicles were measured in control and GD1a-supplemented cells. No significant difference in vesicle sizes was detected between control and GD1a-supplemented cells (Figure 2.11 A-C), suggesting that GD1a supplement did not affect the size of the endolysosomal vesicles.

Taken together, we found that supplementing GD1a increased Py infection but decreased co-localization between Py and the late endosomes / lysosomes. These results suggest that GD1a addition sort Py out of the late endosomes / lysosomes to a specific organelles for productive infection.

GD1a Stimulates Transport of Py to the ER

What is Py's destination after it is sorted out of the endolysosomes? Trafficking of Py to the ER is a required step for infection. Thus we tested the level of Py in the ER in control and GD1a-supplemented cells. Control or GD1a-supplemented NIH 3T3 cells co-expressing CFP-HO2 and YFP-Rab7 were incubated with labeled Py for 4-6 hrs, and co-localization of Py with the ER was assessed using live cell imaging. As the ER tubules are highly convoluted, the ER images were filtered to ensure that the ER boundaries are clear (Figure 2.12). A representative image of continuous co-localization of labeled Py with the filtered ER for 60 s is shown in Figure 2.5A. We found that there were no co-localization between Py and the ER when cells were incubated with Py in 4ºC, a condition that prevents Py internalization into cells (Figure 2.5B). About 4% of Py co-localized with the ER when non-supplemented cells were incubated with Py at 37ºC for 4-6 hrs (Figure

2.5B). If BFA was added to the non-supplemented cells, the percentage of Py localized in the ER decreased to less than 1% (Figure 2.5B). These results indicate that the observed co-localization between Py and the ER represents the actual amount of Py in the ER, and not due to random co-localization. When cells were supplemented with GD1a, we found that the percentage of Py co-localizing with the ER increased to about 10% (Figure 2.5B). This result suggests that supplementing GD1a triggers more Py to be transported to the ER, consistent with a previous report in the ganglioside-deficient C6 cells (Gilbert and Benjamin, 2004). To further confirm this conclusion, we incubated cells with non-labeled Py followed by immunofluorescence staining. Similarly, we found that at 4-6 hrs post infection, the percentage of Py inside the ER increased in GD1a-supplemented cells when compared to that in non-supplemented cells (Figure 2.5C). Therefore, our data show that GD1a facilitates Py transport to the ER.

As the endolysosomal pathway is part of the infectious pathway, and ER trafficking is also required for infection, we hypothesized that the Py infectious pathway involves trafficking first to the endolysosomal system and then sorting to the ER. If this is the case, expression of dominant negative Rab7 should block Py's trafficking to the ER. We assessed co-localization of Py with the ER in cells transfected with wild type YFP-Rab7 or YFP-Rab7 DN construct. Indeed, we found that the trafficking of Py to the ER was inhibited in cells with YFP-Rab7 DN expressed (Figure 2.5D). As a control, we show that expression of YFP-Rab7 DN did not affect the trafficking of cholera toxin B subunit (CTB) to the ER (Figure 2.5E). It has been known that CTB does not require transport through the endolysosomal system to reach the ER (Fujinaga et al., 2003). In sum, our data indicate that Py is transported from the plasma membrane through the endolysosomal system to the ER as an infectious pathway, and that GD1a sorts Py from the endolysosomes to the ER for productive infeciton.

Transport of an Artificial Particle Coated with a GD1a Antibody to the ER

As we showed that supplementing GD1a facilitates Py transport to the ER, and that other polyomaviruses such as SV40, BKV and some bacterial toxins such as CT also bind to gangliosides to transport to the ER, we hypothesized that the ganglioside binding event might be sufficient to drive the ligands to the ER. To test this hypothesis, we asked whether an artificial particle that bind to GD1a can also be targeted to the ER.

Quantum-dot (Q-dot) is a fluorescent artificial particle that could be coated with an antibody against GD1a (Q-dot:GD1a Ab) and thus bind to GD1a. Q-dot is approximately 20 nm in diameter, thus mimicking the size of Py (about 45 nm in diameter). We employed the sucrose flotation assay, used previously to detect the Py-GD1a interaction (Tsai et al., 2003), to measure the interaction of Q-dot:GD1a Ab with GD1a. Q-dots coated with a high concentration of a GD1a antibody (10 mg/ml) were incubated with control or GD1a-contaning liposomes, and subjected to flotation in a sucrose gradient. We showed that the GD1a antibody heavy chain was floated to the top fraction in the sample with GD1a-containing liposomes, but not in the sample with liposomes only (Figure 2.6A). This result indicates that Q-dot:GD1a Ab particles can bind to GD1a.

We then assessed the level of Q-dot:GD1a Ab particles that bind to GD1a on the cell surface of NIH 3T3 cells. Q-dots were coated with either a low (0.1 mg/ml), middle (1 mg/ml) or high (10 mg/ml) concentration of antibody against GD1a, or with the control antibodies including an antibody against Myc (10 mg/ml, called Q-dot:Myc Ab high) and an antibody against transferrin receptor (TfR) (10 mg/ml, called Q-dot:TfR Ab high). GD1a-supplemented NIH 3T3 cells were incubated with these coated Q-dots at 4ºC for 30 min, and washed to remove the unbound Q-dots. As expected, there was a low level of Q-dot:Myc Ab but a higher level of Q-dot:TfR Ab particles binding to the plasma membrane per cell (Figure 2.6B), consistent with the fact that the cell surface contains TfR but not Myc. For Q-dots coated with GD1a antibody, the binding level increased in a GD1a antibody concentration-dependent manner. Specifically, about 500 Q-dot:GD1a Ab (low),

1000 Q-dot:GD1a Ab (middle) and 2200 Q-dot:GD1a Ab (high) bound to the plasma membrane per cell (Figure 2.6B). Therefore, Q-dots bind to the cell surface in a GD1a antibody concentration-dependent manner, suggesting that Q-dots coated with a higher concentration of GD1a antibody tend to have stronger interaction with GD1a on the cell surface.

We then asked whether Qdot:GD1a Ab particles can be targeted to the ER. We found that neither Qdot:Myc Ab or Qdot:TfR Ab can be transported to the ER, while Qdot:GD1a Ab particles were transported to the ER in a GD1a antibody concentration-dependent manner (Figure 2.6C, quantified in right graph). A representative image of Q-dot:GD1a Ab co-localizing with the ER for 40 s was shown in Figure 2.6C (left panel). To demonstrate that the co-localization observed is not random, we showed that the transport of Q-dot:GD1a Ab (high) was inhibited by addition of BFA, and very few Q-dot:GD1a Ab (high) were transported to the ER when cells were incubated at 4ºC to prevent endocytosis (Figure 2.6C, right graph). Therefore, we conclude that Q-dots coated with a higher concentration of GD1a antibody are more likely to be transported to the ER, indicating that GD1a binding contributes to the ER targeting of the ligands.

Discussion

To cause productive infection, Py must bind to receptors on the plasma membrane and be transported from cell surface to the ER. Here it breaches the ER membrane to enter the cytosol and finally to the nucleus. How Py reaches the ER is not clear. Our results demonstrate that after initial internalization, Py is transported through the endolysosome pathway to reach the ER. The low pH environment in the endolysosome system induces a conformational change in Py, which facilitates the subsequent ER-to-cytosol penetration process. Our results also indicate that GD1a sorts Py from the endolysosome to the ER, and that this lipid-dependent sorting event serves as a general ER targeting mechanism.

Transport to the Endolysosome

We found that the endolysosomal pathway was part of the infectious pathway for Py, as expression of dominant negative Rab5 or Rab7 inhibited Py infection. The low pH environment in the endolysosomal system triggers a conformational change in Py, and this conformational change is directly related to the subsequent ER dependent conformational change that enables the virus to breach the ER membrane (Magnuson et al., 2005; Rainey-Barger et al., 2007). We used bafilomycin A1 and NH4Cl to elevate pH in the endolysosomes, and both treatments significantly inhibited Py infection. These results are consistent with one report which demonstrated that NH4Cl addition blocked Py infection (Liebl et al., 2006), while not consistent with another study which showed that NH4Cl treatment did not affect Py infection (Gilbert and Benjamin, 2000). The discrepancy may be due to the differences in methodology, and also it should be noted that in the Gilbert paper, the authors used a very high level of virus, which might result in the resistance of Py to NH4Cl treatment.

In the polyomavirus family, infection of human JC and BK viruses have also been reported to be dependent on the low pH in the endolysosomes (Ashok and Atwood, 2003; Eash and Atwood, 2005). In contrast, SV40 was reported to be transported to caveosome, which is a pH-neutral compartment, and infection of SV40 was shown to be pH independent (Pelkmans et al., 2001; Ashok and Atwook, 2003). Whether the ganglioside receptor GM1 (Tsai et al., 2003) also sorts SV40 out of the caveosome to the ER requires further investigation.

In our studies, co-localization of Py with the early endosome, late endosome and lysosome was assessed at different time points post infection using live cell imaging. This method allows a more accurate co-localization measurement because coincident co-localization, which often occurs with immunofluoresence in fixed cells, can be excluded. Our results showed that only a small fraction of Py (less than 10%) was observed in the early endosomes during the entire time course, and most Py accumulated in the late endosomes and lysosomes. It should be noted that about 5% of Py remained localized in the early endosomes

for a long time. As internalization of Py was synchronized by incubating cells with Py at 4ºC for 30min, followed with washing to remove the unbound viruses and shifting to 37ºC to allow entry, it is not likely that those Py remained in the early endosomes at late time points were newly endocytosed virus. That some Py was transported to the late endosomes while some Py was localized in the early endosomes for a long time may be due to the existence of two populations of early endosomes -- dynamic early endosomes and static early endosomes (Lakadamyali et al., 2006). Py trafficking to the dynamic early endosomes could be transported to the late endosomes and lysosomes, while Py in the static early endosomes might be trapped for a long period and cause no infection.

A Role of GD1a in the Endolysosome-to-ER Transport of Py

Our results indicate that ganglioside GD1a plays an essential role in Py trafficking through its infectious pathway. GD1a is normally transported from the plasma membrane to the lysosomes for degradation (Schwarzmann, 2001). However, the data analyzed thus far indicate that targeting Py to the endolysosomes is not the critical function of GD1a. Our result in Figure 2.4E showed that Py was transported to the late endosomes efficiently in ganglioside-deficient C6 cells, indicating that non-ganglioside receptors such as glycoproteins, which contain the sialic acid-galactose moiety, could also target Py to the endolysosomes. Instead, we found that supplementing GD1a decreased the extent of Py in the late endosomes and lysosomes, suggesting that Py was sorted out of the endolysosomes by GD1a. Furthermore we found that supplement of GD1a facilitates Py transport to the ER. Therefore, one crucial role of GD1a is to sort Py out of the endolysosomes to the ER for productive infection, while the role of non-ganglioside receptors might be to trap Py in the endolysosomes for an extended period without causing infection.

Whether GD1a sorts Py out of the early endosome or the late endosome / lysosome is not clear. Our studies showed that dominant negative Rab7 inhibited Py infection, suggesting that trafficking through the late endosome is also part of

the infectious pathway. We also showed that addition of GD1a decreased co-localization of Py with the late endosomes / lysosomes and increased co-localization of Py with the ER. Hence a simple explanation is that Py is sorted out of the late endosome / lysosome to the ER by GD1a. However, it is also possible that Py is sorted out of the early endosome to the ER, and expression of dominant negative Rab7 interfered with upstreaming sorting processes in the early endosome and thus blocked Py infection. Therefore, further studies are required to determine which compartment Py is sorted from to reach the ER.

It was reported that lipid rafts / caveolae are important in the infectious pathway of Py in the rat glioma C6 cells (Gilbert and Benjamin, 2004). In our studies, we did not observe significant co-localization of Py with caveolin-1 containing vesicles in mouse NIH 3T3 cells, consistent with a previous report (Gilbert and Benjamin, 2000). However, it is still possible that the caveolin-1 dependent pathway interact with the endolysosome pathway to facilitate Py infection, since it has been reported that there is a complex crosstalk system between these two pathways (Pelkmans et al., 2004, Querbes et al., 2006). Also, we did not detect any significant co-localization of Py with Golgi, consistent with a previous report (Gilbert and Benjamin, 2004). Finally, it remains unclear how fusion occurs between Py-containing vesicles budded out of the endolysosomal system and the ER membrane.

Ganglioside Binding as a General ER Targeting Mechanism

The molecular mechanism by which GD1a sorts Py from the endolysosome to the ER is not clear. One possibility is that clustering of GD1a around Py may be important for sorting and represents an ER targeting mechanism. One Py virion contains 360 copies of VP1, and each copy of VP1 provides one GD1a binding site. Thus each viral particle has the potential to bind to multiple GD1a on the cell surface. In addition, since GD1a is normally transported from the plasma membrane to the lysosome, Py may recruit even more GD1a during its trafficking through the endolysosomal pathway. Therefore, one viral particle may already

cluster multiple molecules of GD1a before Py reaches the ER. This clustering of ganglioside may be critical for the ER targeting reaction. This has been indicated in the case of CT (Wolf et al., 2008; Fujinaga et al., 2003), whose receptor-binding B subunit is also a pentamer and has the potential to bind to five ganglioside GM1 receptors for each toxin. The cholera toxin-induced clustering of ganglioside GM1 likely targets CT to the ER. We also used an artificial particle Q-dot coated with an antibody against GD1a to cluster GD1a, and found that these particles were transported to the ER in a GD1a-clustering dependent manner. Therefore, it appears that ganglioside binding and clustering are responsible for the ER-targeting mechanism.

There are two possible GD1a-triggered sorting mechanisms. First, GD1a clustering may induce the formation of a hydrophobic platform within the bilayer of the endosomal membrane, and stimulate transmembrane signaling via unidentified transmembrane proteins to recruit cytoplasmic factors. These cytoplasmic factors then facilitate the budding of Py-containing vesicles from the endosomal membrane. Alternatively, GD1a clustering might alter the physical properties of the endolysosomal membrane attached to the virus, inducing membrane invagination and budding of Py-containing vesicles from the endolysosome. This concept has been reported in shiga toxin, where its binding to the glycolipid GB3 receptor trigger membrane invaginations and facilitate its uptake into cells (Romer et al., 2007). Thus we propose that ganglioside clustering is an essential component of the mechanism by which Py is sorted from the endolysosomes to the ER.

Experimental Methods

Materials

Purified Py and antibodies against Py VP1 and large T were generous gifts from Tom Benjamin (Harvard Medical School). The CFP-Heme Oxygenase-2 construct was provided by Melissa Rolls (Penn State). The wild type CFP-Rab5a, dominant negative CPF-Rab5a S34N, constitutively active CFP-Rab5a Q79L,

wild type YFP-Rab7, dominant negative YFP-Rab7 N125I and wild type LAMP1-YFP constructs were provided by Joel Swanson (University of Michigan). A monoclonal antibody against GD1a was purchased from Millipore, purified GD1a and GM1 from Matreya, monoclonal Myc antibody, Quantum dots 655, Texas Red-X, and Alexa Fluor 594 from Invitrogen, and proteinase K, trypsin, and NH4Cl from Sigma.

Preparation of Texas Red or Alexa Fluor 594 labeled Py

Purified Py was labeled with Texas Red–X succinimidyl ester (1 mM) or Alexa Fluor 594 succinimidyl ester (1 mM) following the manufacturer's protocol (Invitrogen). The labeled Py was separated from excess labeling reagent using a Micro Bio-Spin 30 Column (Bio-Rad Lab).

Preparation of Quantum dot coated with a GD1a or Myc antibody

Quantum dot 655 (goat F (ab') 2 anti-mouse IgG conjugate) (1 uM) was incubated with a monoclonal antibody against GD1a (0.1, 1, or 10 mg/ml) or Myc (10 mg/ml) in 30 ul PBS at 4ºC for 16 hrs with mixing. Protein A agarose beads were added to the sample to precipitate the excess GD1a or Myc antibodies. GD1a- or Myc-coated Quantum dots were present in the resulting supernatant.

Infection assay

NIH 3T3 cells were transfected using Effectene (Qiagen) with constructs encoding wild-type and mutant CFP-Rab5, or wild-type and mutant YFP-Rab7. 24 hrs post-transfection, cells were incubated with Py (multiplicities of infections were approximately 100 PFU/cell), washed after 24 hrs, and incubated for an additional 24 hrs. Cells were then fixed and subjected to immunofluorescence (IF) with an antibody against the virus-encoded large T antigen. Phase and IF images were collected with a Nikon TE2000-E microscope using the Plan Fluor Ph2 40X/Na 0.75 objective. Only those cells expressing the transfected protein were analyzed. Where indicated, GD1a (180 uM) or GM1 (180 uM) were incubated for 24 hrs prior to infection. For characterizing the effect of bafilomycin A1 and

NH4Cl on Py infection, cells were treated with bafilomycin A1 (0.2 uM) or NH4Cl (50 mM) 2 hrs pre-infection, simultaneously with infection, or 3 hrs post-infection. Cells were then infected with crude Py for 3 hrs and the unbounded virus was removed by washing. Cells were incubated at 37ºC for additional 48 hrs, fixed and subjected to T antigen expression analysis.

Time-lapse live fluorescence microscopy and image analysis

NIH 3T3 cells were transfected using Effectene (Qiagen) with the indicated constructs for 1 to 2 days, and where indicated, GD1a was added 24 hrs pre-infection. Cells were incubated with labeled Py (or Q-dot) at 4ºC for 0.5 hr and the unbounded virus (or Q-dot) was removed by washing. Cells were incubated at 37ºC for the indicated time, and observed with a Nikon TE2000-E microscope equipped with 100x objective. Images were acquired at 5 s or 10 s intervals.

For co-localization of Py (or Q-dot) and endolysosomal markers (CFP or YFP), different color images were taken sequentially with Nikon filter cubes for Texas Red (96313), CFP (96341) and YFP (96345). For co-localization of Py with ER (CFP-HO2), the ECFP/DsRed filter set (51018, Chroma) was used to simultaneously image the two colors. The dual-color image was split to two channels by Dual-View image splitter (Optical Insight) and projected to the two halves of a CCD camera (CoolSnap EZ2, Photometrics). To correct the imaging mis-alignment between different channels, Py or Q-dot images were registered to the other channels by bilinear transformation. To define the boundaries of the ER clearly, the ER images were subjected to filtering with the Fast Fourier Transform Bandpass Filter embedded in Image J (NIH). Co-localization was defined as overlapping of the objects of interest in the two channels for at least 30 s in a movie.

Immunofluorescence staining

Cells were fixed with formaldehyde (3%), permeabilized with Triton X-100 (0.2%), and incubated with either an antibody against Py large T antigen or VP1. Cells

were then washed, and incubated with a fluorescently tagged secondary antibody (rhodamine labeled donkey anti-rat for large T or anti-rabbit for VP1).

Cell surface binding and entry

Control or GD1a-supplemented cells were incubated at 4ºC, infected with Py, and either continued to be incubated at 4ºC for 1 hr or incubated at 37ºC for 1 hr to allow entry. Cells were harvested and treated with proteinase K (30 ug/ml) where indicated. Proteinase K was heat-inactivated, and the lysate was subjected to SDS-PAGE followed by immunoblotting with a VP1 antibody.

Low pH-induced Py conformational change

Py was initially incubated in phosphate buffered saline (PBS) at pH 7.5, 6.0, 5.0, or 4.0 for 60 min at 37ºC. Virus incubated at pH 6.0, 5.0, and 4.0 were then neutralized to pH 7.5 by addition of PBS (pH 10.0). The virus was subsequently incubated with a high concentration of the general protease trypsin (1 mg/ml) for 30 min at 4ºC, and subjected to SDS-PAGE followed by immunoblotting with a VP1 antibody.

ER-dependent conformational change

Py incubated at pH 7.5, or pretreated at pH 6, 5, or 4 and neutralized to pH 7.5, were analyzed as described in Magnuson et al., 2005.

Sucrose flotation of Q-dot

Sucrose flotation analysis is described in Tsai et al., 2003, except that Q-dot coated with a GD1a antibody was used instead of Py, and a monoclonal secondary antibody fused to HRP was used during immunoblotting.

Figure 2.1. Time-dependent transport of Py through the endolysosome.
(A) NIH 3T3 cells were incubated with Texas-Red-labeled purified Py for 3 hrs at 37ºC, washed, and subjected to immunofluorescence using a VP1 antibody followed by FITC-labeled secondary antibody. White line, edge of cell. Scale bar, 5 um. (B) Cells were incubated with labeled or non-labeled Py for 48 hrs, and the extent of infection assessed by immunofluorescence using a Py large T antigen antibody. Cells stained with large T antigen in the nucleus were scored as positive for infection. Scale bars, 30 um. (C-E) Live cell imaging of labeled Py in cells expressing (C) CFP-Rab5, (D) YFP-Rab7, or (E) LAMP1-YFP. C and E are images taken at the 4-6 hrs post-infection time point, and D is images taken at the 16-17 hrs post-infection time point. Yellow lines, edge of cells. Scale bars, 10 um (whole cell) and 1 um (inset). (F) Quantification of the extent of co-localization between labeled Py and the respective markers at the indicated post-infection time points. For each time point, at least 90 viral particles were analyzed from 3 cells. Data are the mean +/- SD.

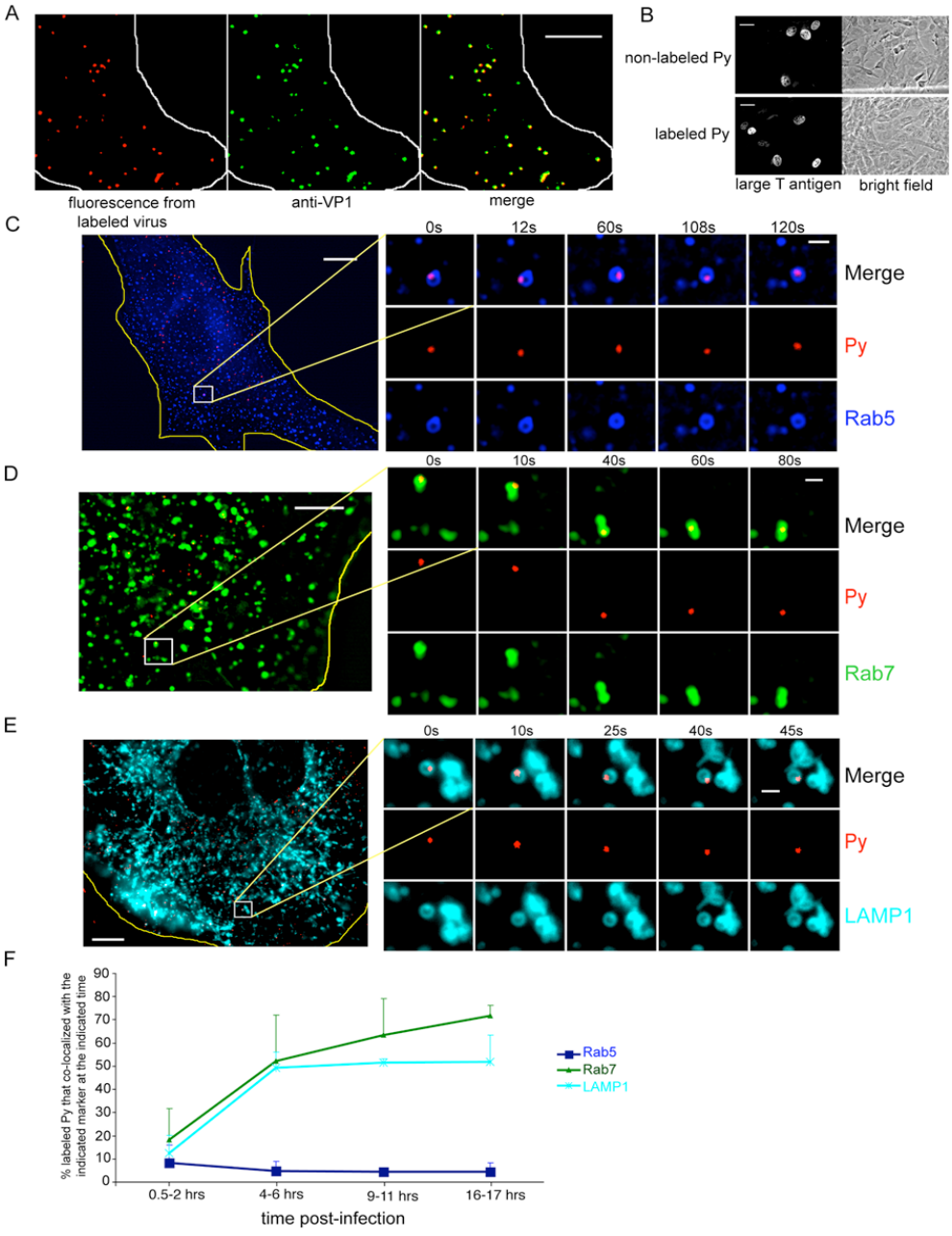

Figure 2.2. Expression of Rab5- and Rab7-interfering mutants affects Py infection
NIH 3T3 cells expressing (A) CFP control, wild-type CFP-Rab5, dominant-negative CFP-Rab5 (DN), or constitutively active CFP-Rab5 (CA) or (B) YFP control, wild-type YFP-Rab7, or dominant-negative Rab7 (DN) were incubated with Py. 48 hrs later, the extent of infection in transfected cells was assayed as in Figure 2.1B. Data represent the mean +/- SD of at least four independent experiments. At least 220 transfected cells were analyzed for each construct.

A

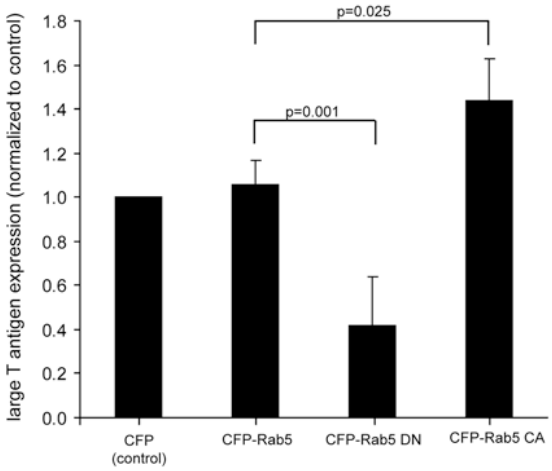

B

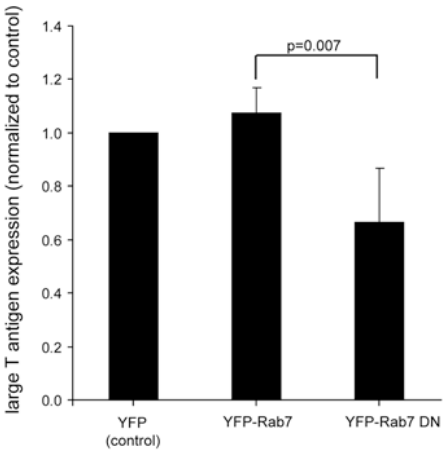

Figure 2.3. Effect of low pH on Py infection and conformational change.
(A) NIH 3T3 cells were treated with bafilomycin A1 2 hrs before, at the same time, or 3 hrs after infection with non-labeled Py, and washed to remove the drug. 48 hrs later, the extent of large T antigen expression was determined as in Figure 2.1B. Infection efficiency was normalized to the control cells. Data are the mean +/- SD. (B) Cells expressing YFP-Rab7 (top) or CFP-HO2 (bottom) were infected with non-labeled Py and treated with bafilomycin A1 simultaneously. 4.5 hrs post-infection, cells were fixed and stained with an antibody against Py VP1, followed by addition of a fluorescently tagged secondary antibody; the extent of co-localization between this fluorescent signal and the fluorescence from YFP-Rab7 or CFP-HO2 were assessed. Data are the mean +/- SD. (C) Py was incubated at pH 7.5, 6.0, or 5.0, neutralized to pH 7.5, and then treated with a low concentration of proteinase K (2.5 ng/ml). The samples were immunoblotted with an antibody against VP1. (D) Py pretreated at pH 7.5 (top and bottom panels) or at pH 5 (bottom panel) was incubated with DTT, EGTA, and either BSA or an ER lumenal extract, and then treated with a low trypsin (0.25 mg/ml) concentration. Appearance of the ER-induced VP1b fragment was analyzed by immunoblotting with an antibody against VP1. Graph on the right represents quantification of the relative VP1b level generated from Py pretreated at pH 7.5 or 5. A two-tailed t test was used. Data are the mean+/2SD.

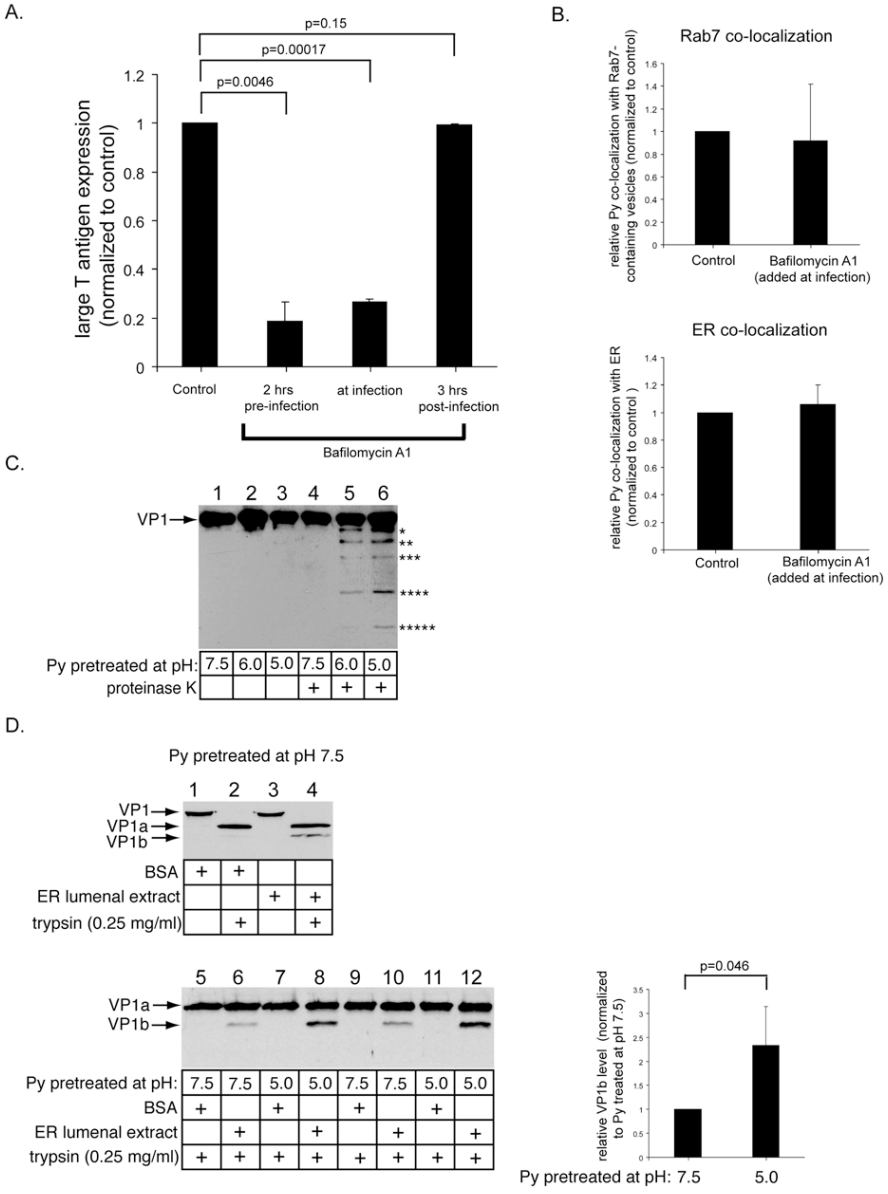

Figure 2.4. Decreased co-localization of Py with the late endosome and lysosome in GD1a-supplemented cells.
(A) NIH 3T3 cells were incubated with purified GM1 or GD1a, washed, infected with Py, and the extent of infection was assessed as in Figure 2.1B. Results were normalized to non-supplemented cells (control cells). (B) Untreated (control) or GD1a-supplemented NIH 3T3 cells were incubated with Py at 4ºC to allow viral binding and then treated with proteinase K where indicated (top panel) or incubated at 37ºC for 1 hr before proteinase K treatment to determine viral entry (bottom panel). (C, D) The extent of co-localization of labeled Py with (C) Rab5-containing vesicles or (D) Rab7-containing vesicles at the early (0.5-2 hrs) and late (4-6 hrs) time points in both control and GD1a-supplemented NIH 3T3 cells. (E) Co-localization of labeled Py with Rab7-containing vesicles at 1-2 hrs post-infection in the ganglioside-deficient C6 cells. (F) Co-localization of labeled Py with LAMP1-containing vesicles 4-6 hrs post-infection in NIH 3T3 cells. (G) The extent of Py infection in GD1a-supplemented cells expressing wild type YFP-Rab7 or dominant negative YFP-Rab7 (DN). At least 220 transfected cells were analyzed from three independent experiments. All data are the mean +/- SD.

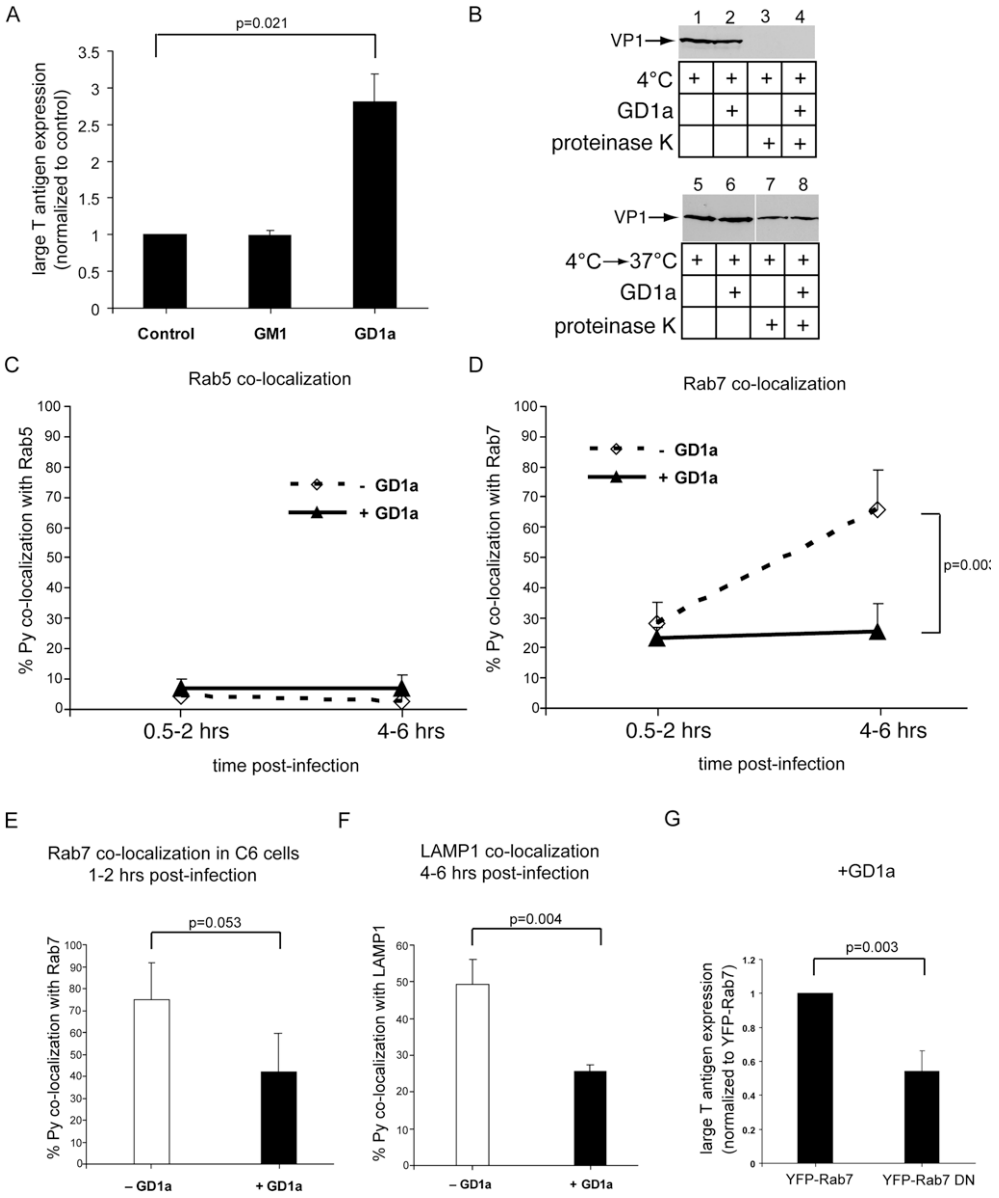

Figure 2.5. Increased co-localization of Py with the ER in GD1a-supplemented cells. (A) Live cell imaging of labeled Py co-localization with the ER. NIH 3T3 cells co-expressing CFP-HO2 and YFP-Rab7 were infected with labeled Py and the extent of co-localization of Py with the ER was analyzed 4–6 hrs post-infection. The images of the ER were subjected to filtering (see Figure 2.12) to more clearly define the ER tubule boundaries. Scale bar, 1 um. (B) Quantification of Py and ER co-localization in GD1a (4ºC, 37ºC, BFA+37ºC) and GD1a-supplemented cells. More than 300 viral particles were analyzed from at least 5 different cells. (C) Py and ER co-localization in control and GD1a-supplemented cells using immunofluorescence staining. Scale bar, 2 um. (below) Quantification of the extent of co-localization, normalized to control cells. Arrowhead, Py that co-localized with the ER. Arrow, Py that did not co-localize with the ER. (D) Quantification of Py and ER co-localization in cells expressing either wild-type YFP-Rab7 (WT) or dominant-negative YFP-Rab7 (DN) using live cell tracking, as in A. The extent of co-localization was normalized to wildtype Rab7 expressing cells. (E) Quantification of CTB and ER co-localization in cells expressing either wild-type YFP-Rab7 or dominant-negative YFPRab7. Data are the mean+/-SD. A two-tailed t test was used.

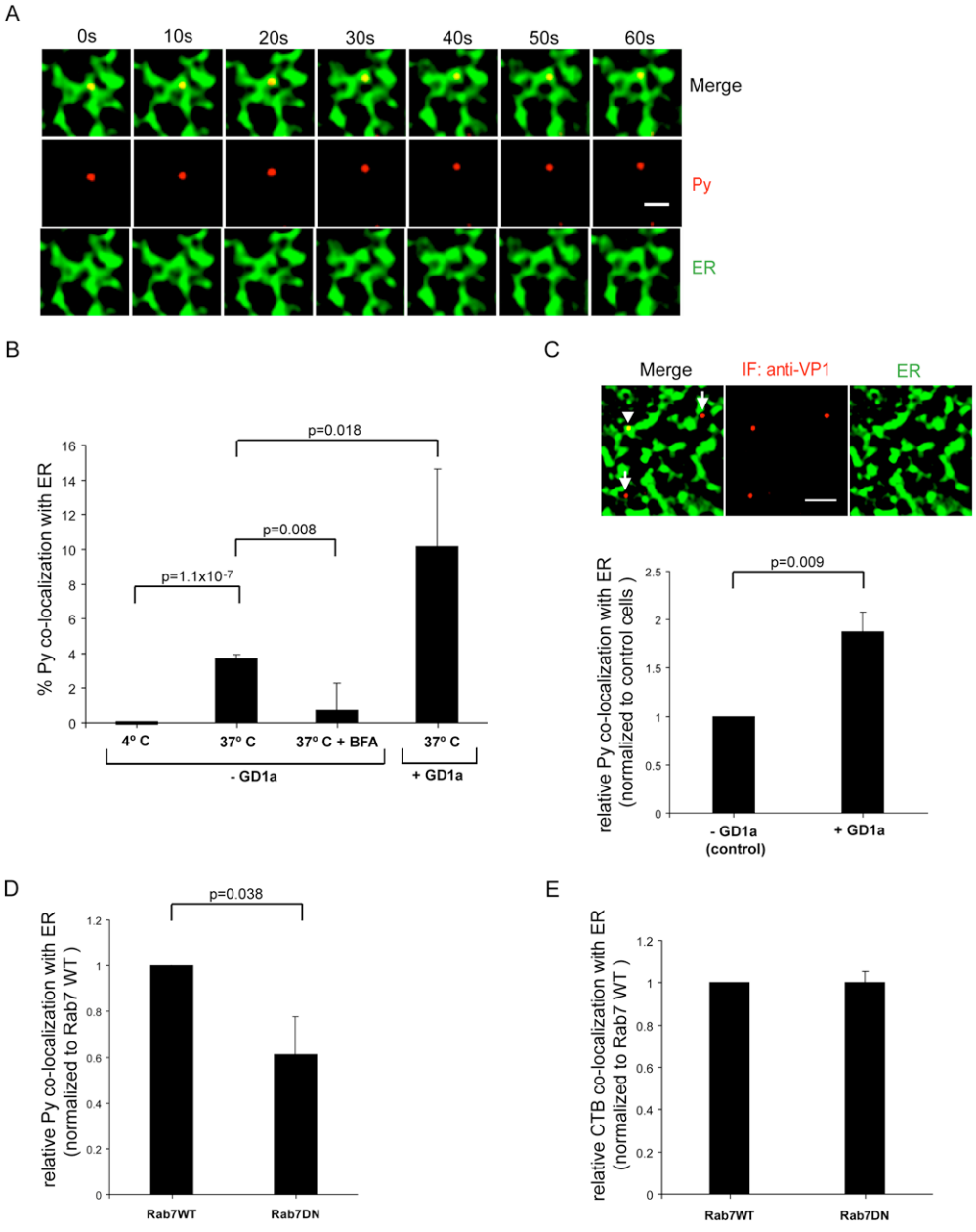

Figure 2.6. Quantum-dot coated with a GD1a antibody is transported to the ER.
(A) Q-dot GD1a Ab (high) was incubated with liposomes or liposomes containing GD1a. Samples were floated in a sucrose gradient, fractionated, subjected to SDS-PAGE, and immunoblotted for the GD1a antibody heavy chain. (B) Q-dot:Myc Ab (high), Q-dot:TfR Ab (high), Q-dot:GD1a Ab (low), Q-dot:GD1a Ab (middle), and Q-dot:GD1a Ab (high) were incubated with GD1a-supplemented cells at 4ºC, washed to remove unbound Q-dots, and imaged. Left panels, representative images. Yellow lines, edge of cells. Scale bars, 10 um for bright field image, and 2 um for Q-dot image. Right panel, quantification of the indicated Q-dot binding to the plasma membrane from at least 3 cells. Data are mean+/-SD. (C) Co-localization of Q-dot:GD1a Ab (high) with CFP-HO2 in GD1a-supplemented NIH 3T3 cells. Left panel, representative images (ER image processed as in Figure 2.5A). Scale bar, 2 um. Right panel, quantification of the indicated Q-dot co-localizing with the ER at various conditions from at least 3 different cells. Data are the mean+/-SD. A two-tailed t test was used.

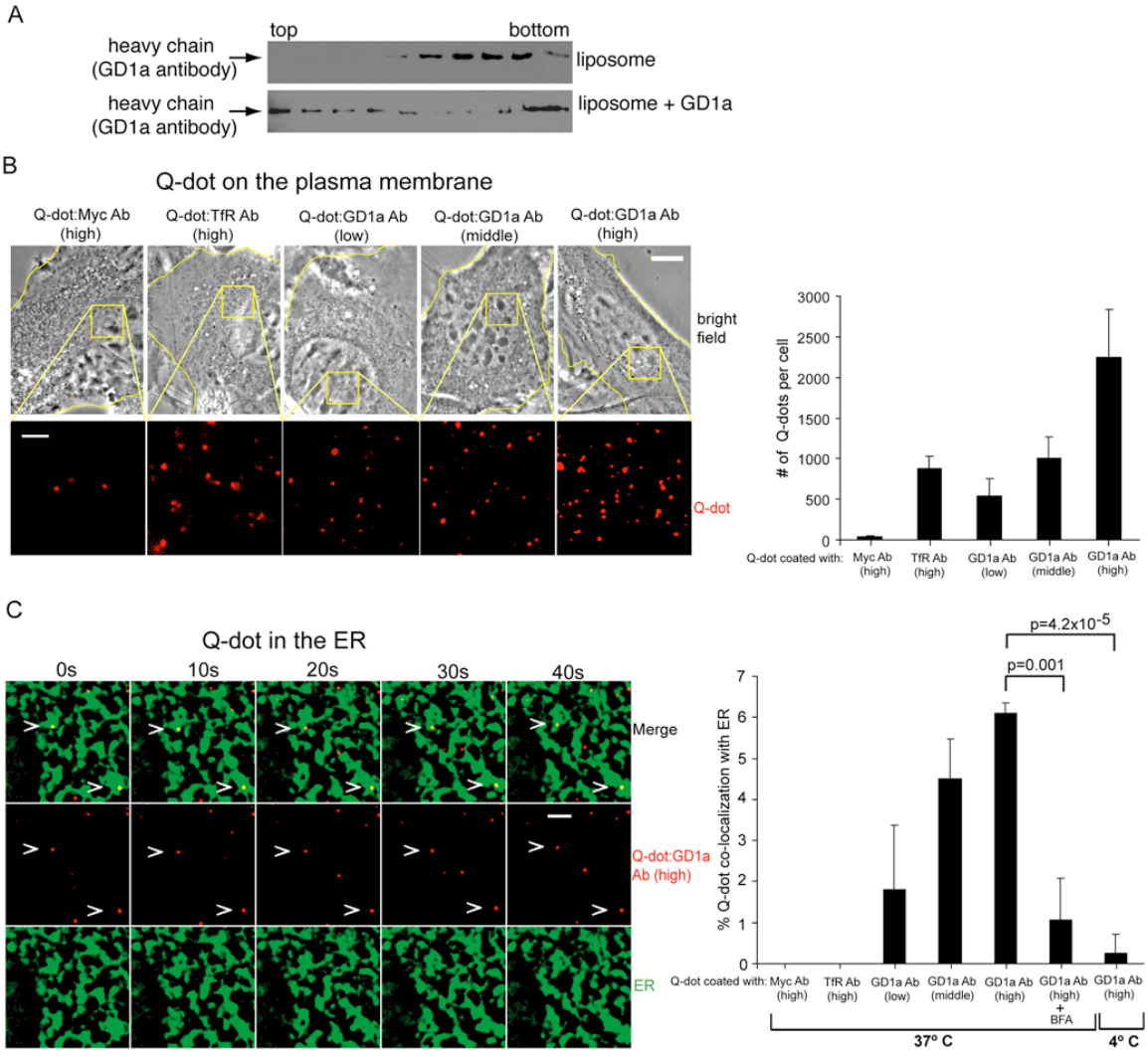

Figure 2.7. Model for sorting of Py from the plasma membrane to the ER.
Model for sorting of Py from the plasma membrane to the ER. Polyomavirus binds to ganglioside GD1a or non-ganglioside receptors at the plasma membrane and is transport to the endolysosome. The low pH in this environment induces a conformational change on the virus that facilitates its subsequent structural alteration in the ER. Py that is bound to GD1a in the endolyosome is sorted to the ER where it undergoes an ERp29-dependent structural change that initiates viral penetration across the ER membrane.

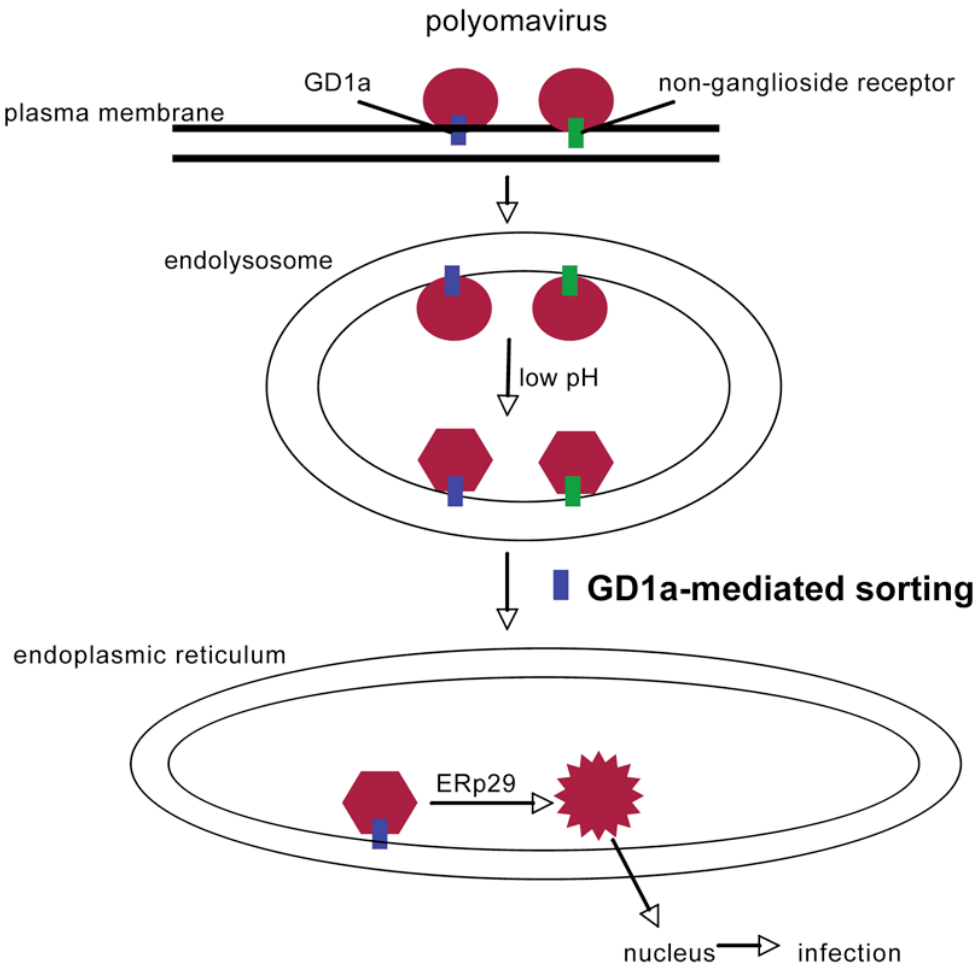

Figure 2.8. Morphology and distribution of early endosomes in CFP-Rab5 expressing cells, and of the late endosomes/lysosomes in YFP-Rab7 expressing cells.
(A) A non-transfected cell (arrow head) and a cell expressing CFP-Rab5 (arrow) were fixed and stained with an antibody against the early endosomal marker EEA1, followed by addition of a fluorescently tagged secondary antibody. The fluorescent signal from this antibody and CFP-Rab5 are shown. (B) As in A, except cells are expressing YFP-Rab7 and an antibody against the late endosomal/lysosomal marker LAMP1 was used. Scale bar, 10 μm.

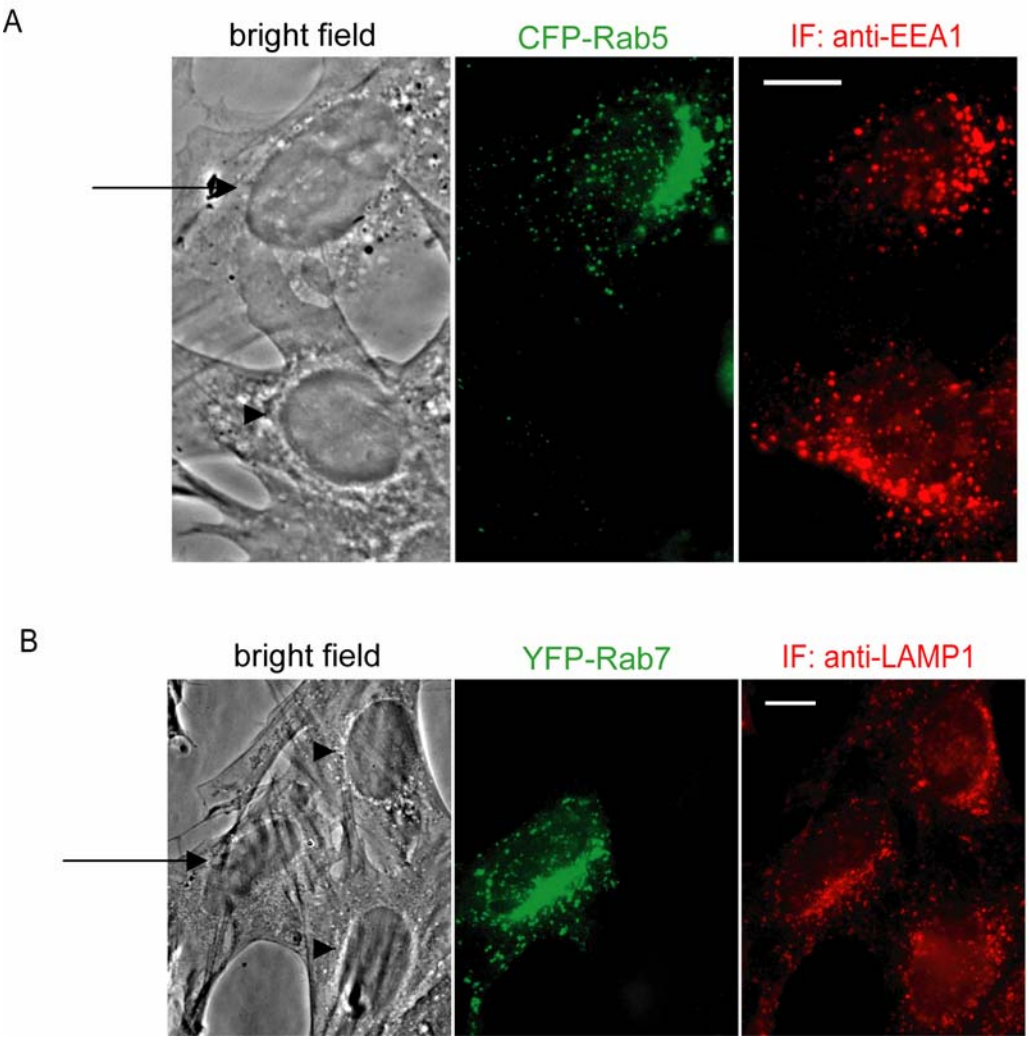

Figure 2.9. Lack of Py and caveolin-1 co-localization in NIH 3T3 cells.
Cells expressing caveolin-1-mCitrine were incubated with Py for 20 min, fixed and stained with an antibody against Py VP1. Caveolin-1-mCitrine in green and Py in red.

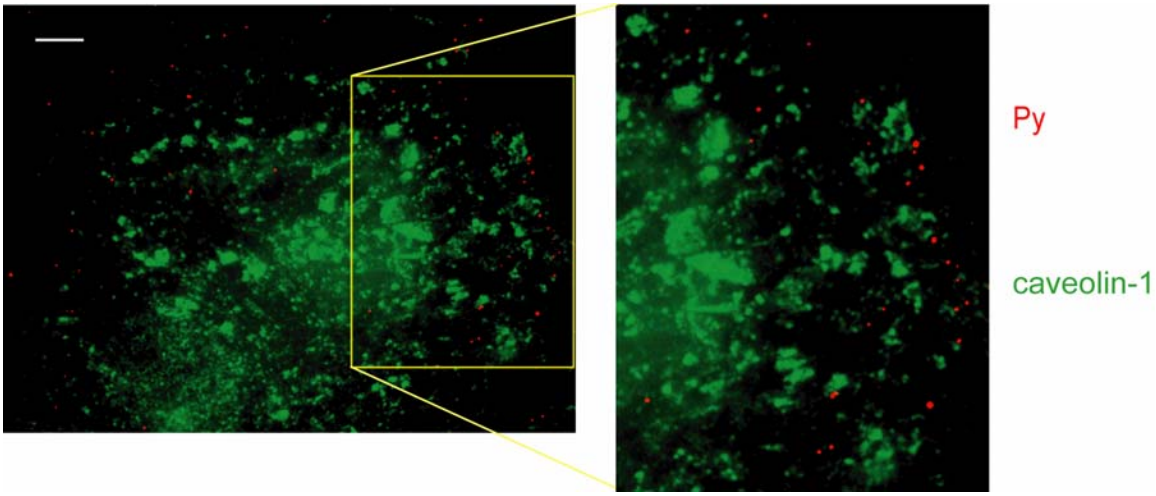

Figure 2.10. Effect of low pH on polyomavirus conformational change.
Py incubated with the indicated pH were neutralized and incubated with a high trypsin (1 mg/ml) concentration (bottom panel) or untreated (top panel). The samples were immunoblotted with an antibody against VP1.

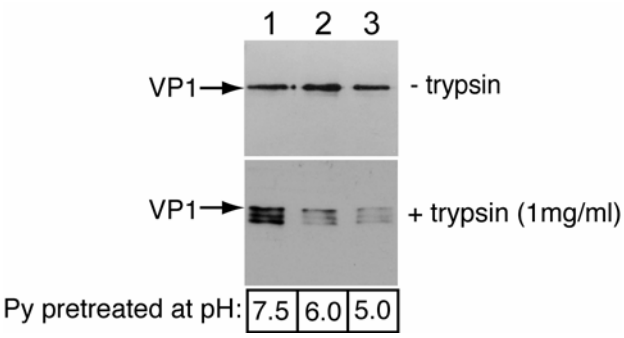

Figure 2.11. GD1a does not alter the size of endolysosomal vesicles.
(A) The diameters of vesicles containing CFP-Rab5 in control and GD1a-supplemented cells were measured using an automated image analysis algorithm written for Image J (NIH). The fraction of total Rab5 vesicles within indicated vesicle sizes is shown. (B) As in A, except the diameter of vesicles containing YFP-Rab7 was analyzed. (C) As in A, except the diameter of vesicles containing LAMP1-YFP was analyzed. Data are the mean+/−SD. More than 400 vesicles were analyzed from 3 cells.

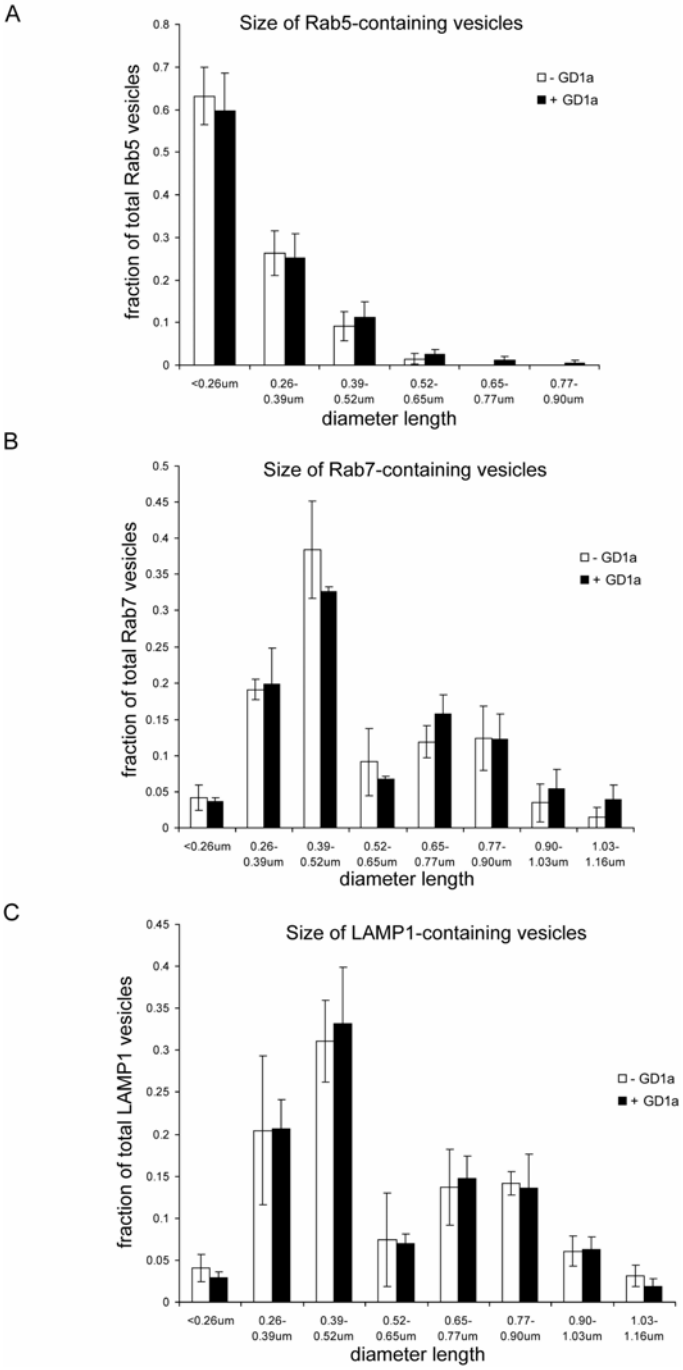

Figure 2.12. Image filtering of the ER image.
A raw image of the ER (i.e. expressing CFP-HO2) was subjected to filtering with the Fast Fourier Transform Bandpass Filter embedded in Image J (NIH), and pseudocolored. Yellow square, area used for live cell tracking in Figure 5A. Scale bar, 2 μm.

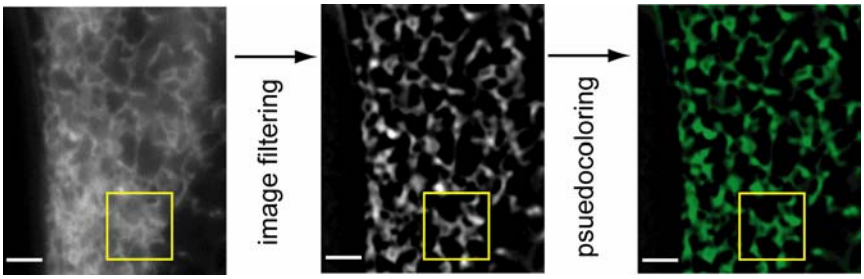

Figure 2.13. Effect of NH4Cl on Py infection.
NIH 3T3 cells were treated with NH4Cl 2 hrs before, at the same time, or 3 hrs after infection with non-labeled Py, and washed to remove the drug. 48 hrs later, the extent of large T antigen expression was determined as in Figure 2.1B. Infection efficiency was normalized to the control cells. Data are the mean +/- SD.

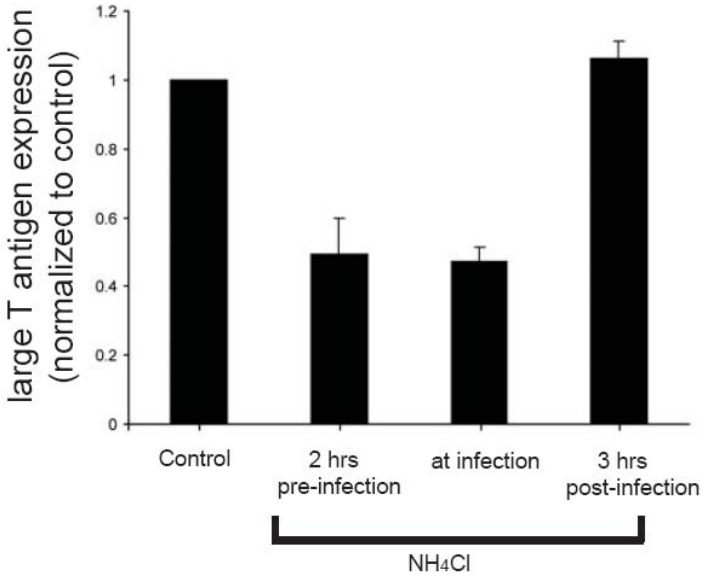

Chapter 3

Lipids and Proteins Act in Opposing Manners to Regulate Polyomavirus Infection

Background and Introduction

To initiate infection, viruses bind to receptors on the plasma membrane to enter cells. Previous works indicated that polyomaviruses engage multiple receptors on the plasma membrane, such as gangliosides and glycoproteins (Tsai and Qian, 2010). However, how these different receptors function together to regulate virus infection is still poorly understood.

Gangliosides have been shown to be receptors for many members in the polyomavirus family, such as the murine polyomavirus (Py), SV40, BK virus (BKV) and Merkel Cell Polyomavirus (MCPyV). Gangliosides are synthesized in the ER and Golgi, and then transported to the plasma membrane. These lipids can be recycled to the endolysosomal compartment through endocytosis. Gangliosides in the lysosomes are then degraded by exohydratases which remove saccharide units. Defects in ganglioside degradation in the lysosomes will cause lysosomal storage disorders (Schwarzmann, 2001; Jeyakumar et al., 2005). Although gangliosides can be transported from the plasma membrane to the Golgi complex, only a very low level are transported back to the ER (Schwarzmann, 2001).

Py engages ganglioside GD1a as its functional receptor. Structurally, Py is a non-enveloped virus that is composed of 360 copies (72 pentamers) of the major capsid protein VP1 and 72 copies of the minor capsid protein VP2 / VP3 (Stehle et al., 1994; Chen et al., 1998). Py binds to GD1a through interaction of VP1 with

the sialic acid-galactose moiety in GD1a. After engaging the receptor on the plasma membrane, Py is endocytosed and transported through the early endosomes, late endosomes and lysosomes (Liebl et al., 2006; Qian et al., 2009). GD1a then sorts Py out of the endolysosomes to the ER (Qian et al., 2009) where the virus penetrates the ER membrane to reach the cytosol (Magnuson et al., 2005). Py subsequently enters the nucleus to cause infection. However, whether GD1a acts as an entry receptor for Py or only as an intracellular sorter still remains unknown.

In addition to ganglioside GD1a, many glycoproteins also contain the sialic acid-galactose moiety (Kornfeld and Kornfeld, 1985), a motif sufficient to bind to Py on the cell surface (Stehle and Harrison, 1996; Stehle et al., 1994; Tsai et al., 2003). In this case, it is also unclear what role the glycoprotein receptors play in regulating Py infeciton.

Using a combination of microscopy, cell infection and biochemical studies, we clarified that GD1a acts as the functional entry receptor for Py. GD1a must engage Py on the plasma membrane, and the ensuing GD1a-Py complex is transported through the endolysosomes to the ER to cause infeciton. In addition, we show that retrograde transport of gangliosides to the ER is induced by ligand-binding. Importantly, we found that removal of glycoproteins stimulated Py infection, while over-expression of model glycoproteins blocked infection. These results indicate that glycoproteins generally act as decoy receptors that drive Py away from the ER to the non-infectious pathway, thus attenuating infection. Our results demonstrate that glycolipid and glycoprotein receptors function in opposing manners to regulate Py infection.

Results

GD1a Addition to a Cell Line Lacking Functional Receptors Stimulates Py Binding, Entry, ER Transport, and Infection

Previous work indicates that GD1a is the functional receptor for Py infection (Tsai et al., 2003). To determine how GD1a functions at different stages of Py infection, we used the A1-1 cell line, a murine mammary tumor-derived cell line that is devoid of gangliosides including GD1a (Gilbert et al., 2005). To test whether addition of GD1a to A1-1 cells stimulates Py cell surface binding, cells supplemented with or without GD1a or GM1 were incubated with Py at 4ºC for 1 hr to prevent endocytosis, and then washed to remove the unbound virus. Cells were fixed and subjected to immunofluorescence with an antibody against VP1. We found that the amount of cell surface virus increased in the GD1a-supplemented cells when compared to that in non-supplemented cells or GM1-supplemented cells (Figure 3.1A), indicating that GD1a interacts with Py on the cell surface. Py entry was investigated by incubating A1-1 cells with Py at 37ºC for 4 hrs. The entry of Py into cells also increased in GD1a-supplemented cells (Figure 3.1B). These results indicate that the functional receptor GD1a interacts with Py on the plasma membrane, and promotes Py binding and internalization.

After entry, Py is transported to the ER and undergoes conformational changes in the ER, a reaction important for subsequent ER-to-cytosol penetration and infection (Gilbert and Benjamin, 2004; Magnuson et al., 2005; Qian et al., 2009). To test whether GD1a stimulates transport of Py to the ER, A1-1 cells were transfected with the ER marker CFP-Heme Oxygenase-2 (CFP-HO2). ER images were subjected to filtering with the Fast Fourier Transform Bandpass Filter embedded in Image J (Qian et al., 2009) to define the ER boundaries clearly. This method ensures that co-localization of Py with the ER can be analyzed more accurately. An example of the Py-ER co-localization after filtering is shown in Figure 3.1C (top panel). By examining co-localization of Py with the ER in A1-1 cells at 4.5 hrs post-infection, we found that the less than 1% of Py co-localized with the ER in non-supplemented cells, and that about 4.7% of Py co-localized with the ER in GD1a-supplemented cells (Figure 3.1C, see quantification in graph below). Thus supplementing GD1a increased the transport of Py to the ER. Furthermore, Py infection was measured by the percentage of

cells expressing virally-encoded large T antigen in the nucleus. Consistent with Gilbert's report (Gilbert et al., 2005), A1-1 cells without GD1a supplement displayed a very low Py infection, while supplementing GD1a increased Py infection significantly (Figure 3.1D). Together, these results show that ganglioside GD1a promotes the binding, entry, ER transport and infection of Py.

Py Co-localizes with GD1a on the Plasma Membrane, the Late Endosomes, and the ER

To ask whether GD1a remains complexed with Py after viral entry, guiding the virus through the endolysosomes en route to the ER, we used BODIPY-GD1a to assess co-localization of Py with GD1a in A1-1 cells. BODIPY-GD1a is a modified form of GD1a in which the BODIPY fluorophore is conjugated to the ceramide domain of GD1a (Boldyrev et al., 2007; Kalinin et al., 2001). When A1-1 cells were incubated with BODIPY-GD1a at 4ºC for 20 min, the majority of BODIPY-GD1a was localized on the plasma membrane (Figure 3.2A, top panels). When A1-1 cells were incubated with BODIPY-GD1a at 37ºC for 30 min, most of BODIPY-GD1a was internalized into cells and localized to vesicular structures, indicating that BODIPY-GD1a are internalized into cells efficiently (Figure 3.2A, bottom panels).

Purified Py labeled with Alexa Fluor 594 dye (AF594-Py) was used to study co-localization of Py with BODIPY-GD1a. The labeling procedure was previously shown to be efficient and do not affect Py infection (Qian et al., 2009). To show co-localization of Py with BODIPY-GD1a on the plasma membrane, A1-1 cells were incubated with BODIPY-GD1a at 4ºC for 15 min, washed to remove the unbound BODIPY-GD1a, and then incubated with labeled Py at 4ºC for 30 min. A representative image of labeled Py (red) co-localizing with BODIPY-GD1a (green) is shown in Figure 3.2B. The percentage of Py co-localizing with BODIPY-GD1a was quantified, and only approximately 12% of Py co-localized with BODIPY-GD1a on the plasma membrane (Figure 3.2E). The low percentage of Py co-localizing with GD1a on cell surface is not surprising because non-ganglioside

receptors such as glycoproteins compete with GD1a for Py binding on the plasma membrane.

To visualize co-localization of Py with GD1a in the endolysosomal system, A1-1 cells were transfected with CFP-Rab7, a marker of the late endosomes. A1-1 cells expressing CFP-Rab7 were incubated with BODIPY-GD1a at 4ºC for 15 min, washed, and then incubated with labeled Py at 37ºC for 3 hrs to allow Py to enter the late endosomes. A typical image of labeled Py (red) co-localizing with BODIPY-GD1a (blue) in the Rab7-containing late endosome (green) is shown in Figure 3.2C. We found that approximately 43% of Py in the late endosomes co-localized with BODIPY-GD1a (Figure 3.2E), indicating that a higher percentage of Py co-localizes with GD1a in the late endosomes when compared to that on the cell surface.

To assess the extent of co-localization of Py with BODIPY-GD1a in the ER, A1-1 cells expressing CFP-HO2 were incubated with BODIPY-GD1a at 4ºC for 15 min, washed, and then incubated with labeled Py at 37ºC for 4.5 hrs to allow Py to enter the ER. A typical image of labeled Py (red) co-localizing with BODIPY-GD1a (blue) in the ER (green) is shown in Figure 3.2D. Quantification analysis showed that approximately 67% of Py in the ER co-localized with BODIPY-GD1a (Figure 3.2E), indicating that an even higher extent of Py co-localized with GD1a in the ER when compared to that in the late endosomes.

These results suggest that GD1a binds to Py on the plasma membrane and remains complexed with Py when they are transported to the late endosomes and the ER. The increasing percentage of Py-GD1a co-localization, starting from 12% on the plasma membrane to 43% in the late endosomes and then to 67% in the ER, suggests that those Py that bind to GD1a on the plasma membrane is preferentially targeted to the ER. This is consistent with our previous finding demonstrating that GD1a sorts Py to the ER (Qian et al., 2009).

Ligand-Induced Retrograde Transport of Gangliosides to the ER

As addition of GD1a to A1-1 cells stimulates the transport of Py to the ER (Figure 3.1C), and that more than half of Py in the ER co-localizes with GD1a (Figure 3.2D, 3.2E), we want to test whether addition of Py to cells stimulates transport of GD1a to the ER. A1-1 cells expressing CFP-HO2 were incubated with BODIPY-GD1a at 4^{o} C for 15 min, washed, and then incubated with or without Py at 37ºC for 4.5 hrs. A typical image depicting a punctated BODIPY-GD1a (red) co-localizing with the ER (green) is shown in Figure 3.3A (left panel). We found that the amount of punctated BODIPY-GD1a co-localizing with the ER significantly increased in Py-supplemented cells when compared to that in non-supplemented cells (Figure 3.3A, see quantification on the left graph). As a control, the amount of BODIPY-GD1a in the ER did not increase when cells were incubated with cholera toxin B subunit (CTB), which binds to ganglioside GM1 (Figure 3.3A, see quantification on the right graph). These findings indicate that Py is transported together with GD1a to the ER, thus increasing the amount of GD1a in the ER. We conclude that Py binding promotes the retrograde transport of ganglioside GD1a to the ER.

In order to understand whether ligand-triggered retrograde transport of gangliosides to the ER is a common mechanism, we studied whether CTB triggers the transport of its receptor GM1 to the ER. Ganglioside GM1 normally binds to cholera toxin (CT) on the plasma membrane, and guides the toxin to the ER to cause intoxication of intestinal epithelial cells (Lencer and Tsai, 2003). NIH 3T3 cells were incubated with BODIPY-GM1 at 4ºC for 30 min, washed to remove unbound BODIPY-GM1, and then incubated with or without CTB at 37ºC for 1 hr. A representative image showing co-localization of a punctated BODIPY-GM1 (red) with the ER (green) is shown in Figure 3.3B (left panel). We found that the amount of punctated BODIPY-GM1 co-localizing with the ER significantly increased in CTB-supplemented cells when compared to that in non-supplemented cells (Figure 3.3B, see quantification on the left graph). Co-localization between BODIPY-GM1 and the ER did not increase in Py-

supplemented cells (Figure 3.3B, see quantification on the right graph). These data indicate that the interaction of CTB with its receptor GM1 facilitates the retrograde transport of BODIPY-GM1 to the ER.

Our results imply a general mechanism of the ligand-induced retrograde transport of gangliosides to the ER. They also indicate that gangliosides remains complexed with their ligands from the plasma membrane to the ER, and are not released from the ligands immediately after entry into the ER. It is interesting to note that both Py VP1 capsid and CTB are pentamers when assembled into their native structures (Lencer and Tsai, 2003; Stehle et al., 1994), indicating that a multivalent ligand-ganglioside interaction might be important for the ligand-ganglioside complex to be transported to the ER.

GD1a Must be Added Before, but not After, Incubation of Cells with Py to Stimulate Infection

As Figure 3.1 shows, supplementing GD1a to A1-1 cells stimulated Py binding and entry, indicating that GD1a is the entry receptor. We want to further confirm that GD1a is the entry receptor by asking whether addition of GD1a after Py entry also stimulates Py infection. Should addition of GD1a after Py entry promotes Py infection, Py does not need to engage GD1a on the cell surface. For example, it is possible that cell surface glycoproteins, which contain sialic acid-galactose moiety, bind to Py on the plasma membrane and guide the virus to the endolysosomes. In this compartment, Py may be released from the glycoprotein receptor, re-bind to GD1a and cause productive infection. In this situation, GD1a does not act as the entry receptor. By contrast, if addition of GD1a after Py entry fails to stimulate Py infection, Py most engage GD1a on the plasma membrane, suggesting that GD1a functions as the entry receptor.

To answer this question, A1-1 cells were incubated with GD1a at 2 hrs pre-infection, 1 hr post-infection or 3 hrs post-infection. We found that supplementing GD1a prior to infection stimulated Py infection significantly, while supplementing

GD1a after virus incubation did not affect Py infection (Figure 3.4A). To exclude the possibility that GD1a added after virus entry failed to reach the endolysosomal system efficiently, we assessed co-localization of Py with BODIPY-GD1a in the late endosomes in cells supplemented with BODIPY-GD1a before or after virus entry. We found that the extent of Py co-localizing with BODIPY-GD1a in the late endosomes was similar regardless of whether cells were treated with BODIPY-GD1a before or after virus entry (Figure 3.4B; see also Figure 3.2E). Therefore, that addition of GD1a after virus incubation does not stimulate Py infection is not due to the failure of GD1a to reach the endolysosomes containing Py. In NIH 3T3 cells we found that addition of GD1a prior to but not after Py incubation stimulated Py infection (Figure 3.4C), similar to results in the A1-1 cells. We conclude that GD1a only stimulated Py infection when it was added before Py incubation, suggesting that GD1a must engage Py on the plasma membrane to initiate infection. These results further confirm that GD1a is the entry receptor for Py.

Removing Plasma Membrane Glycoproteins Stimulates Py Infection and ER Transport

Since many glycoproteins also contain sialic acid-galactose moiety and could bind to Py on the cell surface (Kornfeld nad Kornfeld, 1985; Stehle and Harrison, 1996; Stehle et al., 1994; Tsai et al., 2003), we want to understand the role of glycoprotein receptors in Py infection. We approached this problem by measuring Py infection in NIH 3T3 cells in which the plasma membrane glycoproteins were removed.

First we verified the efficiency of removal of the cell surface glycoproteins by proteinase K. NIH 3T3 cells were treated with or without proteinase K at 4ºC for 1 hr, and the contents of the media from these cells were precipitated and subjected to SDS-PAGE followed by Coomassie staining. We found that there were more degraded proteins of various molecular weights in the media derived from the proteinase K-treated cells when compared to that from non-treated cells

(Figure 3.5A, compare lane 2 to lane 1). Therefore, proteins could be efficiently removed by proteinase K. Furthermore, we asked whether the proteinase K only removed the proteins on the cell surface but not proteins inside the cells. Cell lysates from NIH 3T3 cells treated with or without proteinase K were subjected to SDS-PAGE followed by immunoblotting with antibodies against specific proteins on the plasma membrane or inside the cells. We found that the cell surface EGF receptor (EGFR) and transferrin receptor (TfR) were degraded completely by proteinase K treatment, while the ER membrane protein Derlin-1 was not affected (Figure 3.5B, compare lane 2 to lane 1). These results suggested that proteinase K treatment removed proteins on the plasma membrane effectively, without affecting the internal proteins.

Next we studied virus binding and infection in the proteinase K-treated and non-treated cells. We found that removing proteins from the plasma membrane by proteinase K decreased the number of viral particles bound to cell surface (Figure 3.5C). This result indicates that Py binds to glycoproteins on the cell surface, as suggested by our previous report (Qian et al., 2009). Importantly, we found that NIH 3T3 cells treated with proteinase K showed enhanced susceptibility to Py infection (Figure 3.5D). Moreover, we assessed the extent of co-localization between Py and the ER, and found that the percentage of Py transported to the ER also increased in the proteinase K-treated cells when compared to non-treated cells (Figure 3.5G). Our results showed that removing proteins from the cell surface enhanced Py infection.

Why does removing cell surface proteins increase Py trafficking to the ER and infection? One possibility is that this condition stimulates GD1a expression on the plasma membrane. To test this possibility, we measured the GD1a level on the cell surface using a quantum dot coated with an antibody against GD1a (Q-dot:GD1a Ab) that was shown previously to bind to GD1a (Qian et al., 2009). We found that cell surface binding of Q-dot:GD1a Ab particles did not increase in cells treated with proteinase K (Figure 3.5E), suggesting that the GD1a level

remained constant regardless of whether cell surface proteins were removed or not.

Hence it is likely that that cell surface proteins normally act to attenuate Py infection, and removal of cell surface proteins results in more Py binding to GD1a, thereby promoting infection. We asked whether the extent of labeled Py binding to BODIPY-GD1a increased in the A1-1 cells treated with or without proteinase K. A1-1 cells were used here because they do not contain endogenous GD1a on the plasma membrane. We found that proteinase K treatment stimulated co-localization of labeled Py with BODIPY-GD1a on the plasma membrane (Figure 3.5F). This result suggests that the increased infection in cells treated with proteinase K is due to increased interaction between Py and GD1a on the cell surface.

To confirm that glycoproteins compete with GD1a, NIH 3T3 cells were treated with PNGase F, a glycosidase that removes carbohydrate residues from glycoproteins but not glycolipids, at 37ºC for 1 hr (PNGase F has very low activity at 4ºC). When cell lysates were subjected to immunoblotting, we found that the carbohydrate residues of the cell surface glycoprotein EGFR were removed by PNGase F, while the ER membrane glycoprotein Ribophorin I (Ribo I) was not affected (Figure 3.5H, compare lane 2 to lane 1). These findings indicate that PNGase F only acts on glycoproteins on the cell surface but not internal glycoproteins. When infection was assessed, we found that it was stimulated when cells were treated with PNGase F (Figure 3.5I). We conclude that glycoproteins normally act in an opposing manner to GD1a in regulating Py infection, likely by engaging Py on the cell surface and targeting the virus along the non-infectious pathway.

Over-expression of the model glycoprotein EGFR decreases Py infection and ER transport.

As removing glycoproteins stimulates Py infection, we asked whether over-expression of a model glycoprotein on the cell surface would decrease virus infection. The plasma membrane protein EGFR, which contains terminal sialic acid-galactose residues, was used for this experiment. First we showed that the EGFR interacted with Py using a co-immunoprecipitation approach. NIH 3T3 cells were incubated with Py at 4ºC for 1hr, washed to remove the unbound Py, and the cell pellets were harvested and incubated with the crosslinker dithiobis succinimidyl propionate (DSP) at 4ºC for 1hr. The resulting cell lysates were subjected to immunoprecipitation with an antibody against Ribo I or an antibody against EGFR. The precipitated samples were then subjected to SDS-PAGE followed by immunoblotting with an antibody against VP1 or EGFR. We found that the EGFR interacted with Py, while the ER-resident glycoprotein Ribo I did not (Figure 3.6A, top panel, compare lane 2 to lane 1).

Next we showed the extent of EGFR over-expression in NIH 3T3 cells transfected with an EGFR construct. NIH 3T3 cells were transfected with the control GFP construct only or co-transfected with GFP and EGFR, and the total cell lysates were subjected to immunoblotting with an antibody against EGFR. We found that the EGFR level significantly increased in cells transfected with both GFP and EGFR when compared to cells transfected with GFP only (Figure 3.6B).

To assess the level of Py binding in cells transfected with or without EGFR, NIH 3T3 cells transfected with GFP only or co-transfected with GFP and EGFR were incubated with Py at 4ºC for 1hr, washed to remove the unbound viruses, and subjected to immunofluorescence with an antibody against VP1. Only cells with GFP fluorescent signal were analyzed. We found that more Py bound to cells transfected with both GFP and EGFR when compared to cells transfected with GFP only (Figure 3.6C), indicating that EGFR over-expression promotes Py binding to the cell surface.

To detect the infection efficiency, NIH 3T3 cells transfected with GFP only or co-transfected with GFP and EGFR were infected with Py, and only those GFP positive cells were analyzed. We found that cells co-transfected with GFP and EGFR displayed decreased infection when compared to cells transfected with GFP only (Figure 3.6D), suggesting that the excess EGFR competes with GD1a receptor for Py binding and leads the virus to the non-infectious pathway. Furthermore, we assessed the Py-ER co-localization in cells transfected with CFP-HO2 only and cells co-transfected with CFP-HO2 and EGFR. We found that the extent of Py transported to the ER was also blocked by EGFR over-expression (Figure 3.6F). In addition, in A1-1 cells, we found that the extent of co-localization between labeled Py and BODIPY-GD1a was inhibited in cells co-expressing CFP and EGFR when compared to cells expressing CFP only (Figure 3.6E), indicating that excess EGFR competed with GD1a for Py binding. Together, these results demonstrate that over-expression of EGFR blocked Py transport to the ER and infection, suggesting that the cell surface glycoproteins, such as EGFR, compete with GD1a, leading Py to the non-infectious pathway. In this way, glycoproteins protect cells from Py infection.

Where are the virus when bound to glycoproteins? Using cells transfected with YFP-Rab7 only or co-transfected with YFP-Rab7 and EGFR, we found that the extent of Py co-localizing with the Rab7-containing late endosomes increased in cells overexpressing the EGFR (Figure 3.6G). Therefore Py that bound to glycoprotein receptors such as the EGFR might be trapped in the late endosomes and unable to be further sorted to the ER to cause productive infection.

To exclude the possibility that overexpression of EGFR may induce signaling events that perturbs the Py infectious pathway, we studied Py infection in NIH 3T3 cells stably expressing the IGF-1 receptor (IGF-1R), which is another glycoprotein on the cell surface. Again we found that Py infection was inhibited in cells with IGF-1R stably expressed when compared to control cells (Figure 3.6I).

Since IGF-1R expression induce different signaling properties than EGFR (Tong et al., 2000), the decrease in Py infection is more likely due to competition between glycoproteins and GD1a for Py binding, rather than signaling events.

In conclusion, we found that over-expression of model glycoproteins on the cell surface inhibited Py infection and trapped Py in the late endosomes. These data indicate that glycoproteins normally function to compete with ganglioside receptor on the plasma membrane, and guides Py to the non-infectious pathway to restrict Py infection. Therefore, ganglioside and glycoprotein receptors act in opposing manners to regulate Py infection.

Discussion

It is not uncommon for viruses to bind to multiple receptors on the cell surface during their entry process (Baranowski et al., 2001; Dimitrov, 2004). These multiple receptors could be redundant, where several receptors independently mediate the entry of viruses. For example, the entry of alphaherpesviruses could be mediated by nectins, herpesvirus entry mediator (HVEM) and heparin sulfate, and these receptors bind to the virus independently without acting as co-receptors (Heldwein and Krummenacher, 2008; Shieh et al., 1992).

Alternatively, multiple receptors could also function sequentially. For example, the DC-SIGN functions as an attachment receptor that concentrates the dengue virus on the plasma membrane, allowing the dengue virus to interact efficiently with an unidentified receptor that is responsible for the entry of the virus (Lozach et al., 2005). Additionally, HIV initially binds to its primary receptor CD4, and then interacts with one of the chemokine receptors, either CCR5 or CXCR4, for entry (Kuritzkes, 2009).

Py could use both gangliosides and glycoproteins as receptors, but it was not clear what roles these two receptors played during viral infection. In our studies, we found that once Py binds to the glycoprotein receptors, it can not be

transported to GD1a even when it is exposed to a high concentration of GD1a inside cells, indicating that glycoproteins and gangliosides do not act as sequential receptors. More importantly, we found that removal of glycoproteins increased Py infection, while over-expression of the model glycoprotein EGFR on the cell surface inhibited Py infection, suggesting that gangliosides and glycoproteins function as competitive receptors, opposing each other to regulate Py infection. Therefore, our results clearly demonstrate that gangliosides and glycoproteins play opposite roles in Py infection. We will discuss in detail the roles of gangliioside and glycoprotein receptors in Py infection.

Glycolipid Ganglioside GD1a as the Functional Entry Receptor

It is known that ganglioside GD1a is the functional receptor for Py (Gilbert and Benjamin., 2004; Gilbert et al., 2005; Qian et al., 2009; Smith et al., 2003; Tsai et al., 2003). This conclusion is mainly based on the following three evidences. First, direct interaction between Py and GD1a was detected by using sucrose flotation experiments, which used liposomes containing GD1a or control gangliosides to study the interaction between Py and gangliosides (Tsai et al., 2003). This interaction is presumably mediated by the termimal sialic acid-galactose moiety in GD1a and VP1 in Py (Stehle et al., 1994; Tsai et al., 2003). Second, addition of GD1a to NIH 3T3 cells or ganglioside deficient cells, such as rat glioma C6 and mouse A1-1 cells, promoted Py infection (Gilbert and Benjamin, 2004; Gilbert et al., 2005; Qian et al., 2009; Tsai et al., 2003). Third, supplementing GD1a facilitated transport of Py to the ER, a step required for productive infection (Gilbert and Benjamin, 2004; Qian et al., 2009; Tsai et al., 2003; Gilbert et al., 2006; Lilley et al., 2006; Magnuson et al., 2005).

However, there was no direct evidence that GD1a is an entry receptor for Py. It is still possible that Py enters cells by interacting with non-ganglioside receptors, and when after entry Py is transferred to GD1a in the endolysosomes where gangliosides accumulate. Interaction of Py with GD1a in the endolysosomes may also result in sorting of Py to the ER to cause productive infection. In this case,

GD1a might only act as an intracellular sorter for Py (Qian et al., 2009), and not as an entry receptor. In this paper, we identify GD1a as an entry receptor for Py based on the following findings.

First, using a murine A1-1 cell line that lacks of gangliosides (Gilbert et al., 2005), we found that supplementing GD1a stimulated Py binding, entry, transport to the ER and infection. Second, using a fluorescently-labeled GD1a (BODIPY-GD1a), we directly detected co-localization of Py with GD1a on the plasma membrane, in the late endosome, and in the ER. Quantitative analysis showed that the percentage of Py co-localizing with GD1a increases when Py is transported from the plasma membrane through the late endosome to the ER, indicating that GD1a binding preferentially targets Py to the ER. Third, we showed that GD1a stimulated Py infection only when GD1a was added before, but not after, incubation of cells with Py. Also we found that GD1a could still reach the endolysosomes efficiently when GD1a was added after Py incubation, excluding the possibility that the inability of GD1a to stimulate infection when supplemented after virus incubation is due to failure of GD1a to reach the endolysosomes that harbor the virus. Therefore, our data demonstrate that GD1a is required to interact with Py on the cell surface to stimulate virus infection, and thus GD1a plays the role of the functional entry receptor for Py.

Consistent with the finding that Py-GD1a complex was preferentially targeted to the ER, we found that the extent of GD1a in the ER was stimulated by incubation of cells with Py. Similarly, we found that the level of GM1 in the ER was also stimulated by incubation of cells with CTB. These results suggest a general mechanism that ligand binding triggers the transport of ganglioside receptors from the plasma membrane to the ER. It should be noted that, although gangliosides are biosynthesized in the ER and Golgi and transported forward to the plasma membrane, the retrograde transport of gangliosides from the plasma membrane to the ER is a very inefficient process. Most gangliosides are transported to the lysosomes for degradation, and only a small fraction are

transported to the Golgi complex, and an even smaller fraction might be transported to the ER (Schwarzmann, 2001).

The molecular mechanism by which the ligand-triggered retrograde transport of gangliosides to the ER is not clear. One possibility is that the clustering of gangliosides around the ligand may generate a hydrophobic platform that is responsible for the ER targeting. For Py, one virion contains 360 copies of VP1 and each copy of VP1 provides one GD1a binding site. Thus each viral particle has the potential to accumulate multiple GD1a around it. For cholera toxin, CTB is a pentamer and each CTB has the potential to bind to five GM1 molecules. Ganglioside clustering around the ligand may induce the formation of a hydrophobic platform within the bilayer of the membrane, and stimulate transmembrane signaling to recruit cytoplasmic factors. These cytoplasmic factors may be able to facilitate budding of the ganglioside-containing vesicles and transport of these vesicles to the ER. In addition, ganglioside clustering might alter the physical properties of the membrane, inducing membrane curvature. This concept has been reported for SV40, where interaction of SV40 with ganglioside GM1 receptor is sufficient to trigger membrane invagination in giant unilamellar vesicles (Ewers et al., 2010). Therefore, clustering of gangliosides might be the essential mechanism of retrograde transport of gangliosides to the ER.

Glycoproteins as Decoy Receptor

To enter cells and cause infection, Py needs to bind to the sialic acid-galactose containing GD1a on the cell surface. Most glycoproteins on the plasma membrane also contain the sialic acid-galactose moiety, and thus have the ability to bind to Py and act as Py receptors. In our studies, we found that removing glycoproteins stimulated Py infection, while over-expression of two model glycoproteins inhibited Py infection. These results show that glycoproteins act as the “decoy” receptors for Py. “Decoy” receptors can bind to Py, and guide the virus to the endolysosomes, as Py was found in the endolysosomes in

ganglioside-deficient C6 cell (Qian et al., 2009). However, Py that engages glycoprotein receptors seems to be trapped in the endolysosomes and can not be sorted to the ER for infection.

As there are a large amount of different glycoproteins on the plasma membrane, glycoproteins act as strong competitors against GD1a to engage Py on the cell surface and lead Py to the non-infectious pathway. However, one viral particle that successfully arrives in the nucleus is sufficient to cause infection (Diacumakos and Gershey, 1977). Therefore, even though NIH 3T3 cells probably contain much more glycoprotein receptors than GD1a receptors, and have different defensive systems inside the cells to block Py infection, Py can nonetheless cause productive infection. In the ganglioside deficient A1-1 cells, the infection efficiency of Py is significantly reduced, but there is still a very low level of infection (below 0.1%). This might be due to the remaining gangliosides on the cell surface, or Py can occasionally escape the non-infectious pathway guided by the glycoprotein and enter the nucleus for infection.

Our results show that over-expression of either EGFR or IGF-1R decreases Py infection, indicating that this effect is not likely due to specific signaling events. It is possible that over-expression of the model glycoprotein overwhelms GD1a on the plasma membrane**,** allowing the glycoprotein to bind to more Py than GD1a. This scenario explains why infection is decreased when excess glycoproteins are expressed.

A previous finding showed that the glycoprotein integrin acts as a postattachment receptor for Py (Caruso et al., 2003). We analyzed the level of integrin in NIH 3T3 cells treated with proteinase K, and found that proteinase K treatment did not degrade integrin efficiently (Figure 3.8). Therefore, it remains possible that some specific glycoproteins such as integrin stimulates Py infection, for example, by acting together with GD1a as sequential receptors. Nonetheless, our data

suggest that glycoproteins in general work as “decoy” receptors to deceive Py to the non-infectious pathway.

In conclusion, our findings showed two competitive receptors for Py, ganglioside GD1a as the functional entry receptor and glycoproteins as decoy receptors. To cause infection, Py develops a direct interaction with the sialic acid-galactose moiety in GD1a to maximize its infection efficiency. However, the presence of sialic acid-galactose moiety in most glycoproteins in turn inhibits Py infection efficiency and protects cells from virus infection.

Experimental Methods

Reagents.

Antibodies against VP1 and large T antigen, and purified Py were provided by Tom Benjamin (Harvard Medical School). The CFP-Heme Oxygenase-2 construct was a gift from Melissa Rolls (Penn State). The CFP-Rab7 and YFP-Rab7 plasmids were from Joel Swanson (University of Michigan). The FLAG-tagged human EGFR construct was from John Kuriyan (University of California, Berkeley). Purified GM1 and GD1a were purchased from Matreya, Alexa Fluor 594 and BODIPY FL C5-ganglioside GM1 from Invitrogen, dithiobis succinimidyl propionate (DSP) from Thermo Scientific , proteinase K from Sigma, and PNGase F from New England BioLabs. BODIPY-GD1a was provided kindly from Julian Molotkovsky (Russian Academy of Sciences). NIH 3T3 cells stably over-expressing the IGF-1R is from Peter Arvan’s lab (University of Michigan).

Preparation of Alexa Fluor 594 labeled Py.

Purified Py (RA strain) was labeled with Alexa Fluor 594 succinimidyl ester (1 mM) following the manufacturer’s protocol (Invitrogen). Labeled Py was separated from excess labeling reagent using a Micro Bio-Spin 30 Column (Bio-Rad Lab).

Infection assay.

NIH 3T3 cells or A1-1 cells were incubated with Py (about 100 PFU/cell or 1×10^4 particles/cell) for 1 hr, washed and incubated for 48 hrs at 37°C. Cells were fixed with 3.6% formaldehyde, permeabilized with 0.2% Triton X-100, and subjected to immunofluorescence (IF) with an antibody against the large T antigen. Bright phase and fluorescence images were taken under Nikon Eclipse TE2000-E microscopy with 40X objective. For the GD1a time course experiments, NIH 3T3 cells or A1-1 cells were treated with GD1a (80 uM) at the indicated time pre- or post-infection for at least 2 hrs. For the proteinase K or PNGase F experiments, cells were treated with 4 ug/ml proteinase K for 1 hr at 4°C, or with 10,000 units of PNGase F with the G7 buffer in 1 ml medium for 1 hr at 37°C. For the EGFR over-expression experiments, cells were transfected using Effectene (Qiagen) with either the control GFP construct or with a combination of GFP and EGFR constructs for 2 days prior to infection.

Immunofluorescence staining.

Cells were fixed with formaldehyde (3.6%) and permeabilized with Triton X-100 (0.2%). The cells were then incubated with an antibody against Py large T antigen or an antibody against Py VP1 protein for 1-2 hrs at room temperature, washed, and incubated with a fluorescently tagged secondary antibody (rhodamine labeled donkey anti-rat antibody for large T antigen or a rhodamine labeled donkey anti-rabbit antibody for VP1).

Image analysis.

Different color images were taken with Nikon filter cubes for Texas Red (96313), YFP (96345) and CFP (96341). The images for co-localization experiments were taken with a 100X objective in a Nikon TE2000-E microscope. The ECFP/DsRed filter set (51018, Chroma) was used to take the images with two fluorescence simultaneously. The dual-color image was split to two channels by Dual-View image splitter (Optical Insight) and projected to the two halves of a CCD camera (CoolSnap EZ2, Photometric). Bilinear transformation calculation was used to correct the imaging mis-alignment between different channels. The Fast Fourier

Transform Bandpass Filter in Image J (NIH) was used to define the boundaries of the ER clearly. The filtering settings were set as filtering large structures down to 15 pixels and filtering small structures up to 3 pixels, and a tolerance of direction of 5%.

Py-EGFR binding studies.

NIH 3T3 cells were incubated with Py at 4°C for 1 hr, the unbound virus removed by washing, and the resulting cell pellet incubated with the crosslinker dithiobis succinimidyl propionate (DSP) at 4°C for 1 hr. Cells were lysed with a buffer containing 150 mM KOAc, 50 mM HEPES (pH 7.4), 2 mM Mg(OAc)2, 250 mM sucrose, and 1% Triton X-100, and the resulting lysate subjected to immunoprecipitation using either a control Ribo I or an EGFR-specific antibody. The precipitated sample was subjected to SDS-PAGE followed by immunoblotting with antibodies against Py VP1 and EGFR.

FACS assay

NIH 3T3 cells were seeded at 1.5 x10^6 cells/ 60 mm plate. The next day, cells were either mock treated or treated with 4ug/ml PK for 1h at 4°C. Cells were treated with Accutase, spun at 13000 x g for 5m, and resuspended in 1 ml PBSA. Cells were split evenly between 3 FACS tubes (mock, secondary Ab alone, and CD51 + secondary Ab). Cells were spun again and resuspended in "residual" liquid. Fcblock was then added and cells incubated on ice for 5 min, except for the mock treated which remained in ice. Anti-CD51 primary Ab was added to sample, vortexed, and incubated on ice for 30 min. Cells were washed with 1 ml PBSA and then resuspended in "residual" liquid. Anti Rat PE was added to samples and incubated on ice for 20 min. Cells were washed with PBSA and then resuspended in "residual" liquid. All cells were fixed with 2% formaldehyde and stored overnight at 4°C. Samples were ran on the FACS and examined for level of PE.

Figure 3.1. GD1a addition to a murine cell line lacking functional receptors stimulates Py binding, entry, ER transport, and infection.
(A-B) Control, GM1-supplemented (only in A), and GD1a-supplemented A1-1 cells were incubated with Py at 4°C for 1 hr (A) or at 37°C for 4 hrs (B), washed to remove the unbound virus, and subjected to immunofluorescence with an antibody against VP1. Top panel, representative images. Scale bar, 10 um for bright field image, and 2 um (A) or 1 um (B) for the Py images. Bottom panel, quantification of the Py binding to the plasma membrane from at least 3 cells. Data are the mean +/- SD. A two-tailed t test was used. (C) Control and GD1a-supplemented A1-1 cells expressing CFP-HO2 were incubated with Py at 4°C for 40 min, washed to remove the unbound Py, and then incubated at 37°C for 4.5 hrs. Cells were subjected to immunofluorescence with an antibody against VP1. Top panel, representative image. Arrow, Py that co-localized with the ER. Scale bar, 1 um. Bottom panel, quantification of the Py co-localizing with the ER from at least 3 cells. Data are the mean +/- SD. (D) Control and GD1a-supplemented A1-1 cells were incubated with Py at 37°C for 48 hrs, and subjected to immunofluorescence with an antibody against large T antigen. Data represent the mean +/- SD of at least 2 independent experiments. 3/4004 cells expressed T antigen in the control cells.

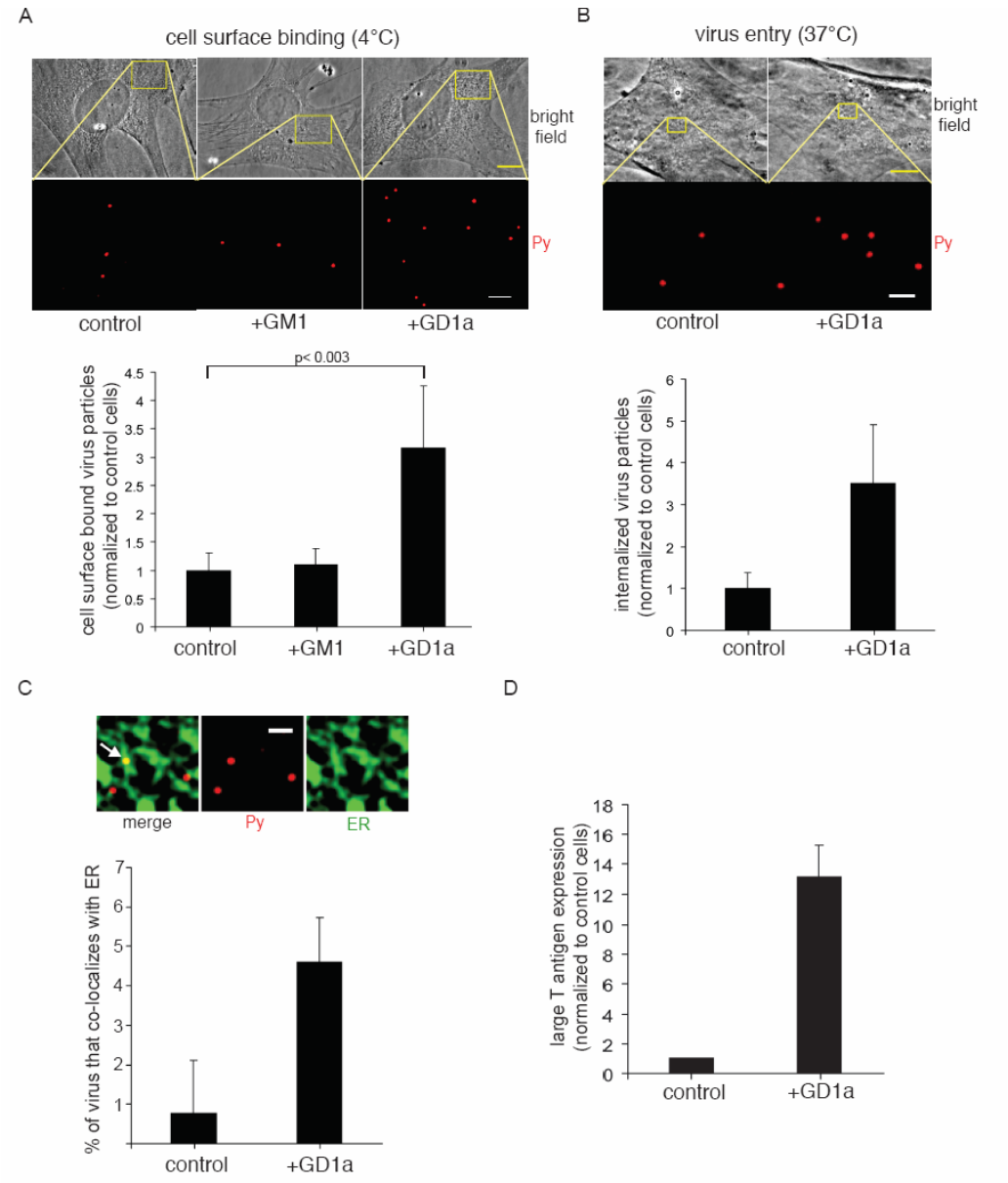

Figure 3.2. Py co-localizes with GD1a on the plasma membrane, the late endosomes, and the ER.
(A) A1-1 cells were incubated with BODIPY-GD1a at 4°C for 20 min (top panels) or at 37°C for 30 min (bottom panels). (B) Cells were incubated first with BODIPY-GD1a at 4°C for 15 min and then with labeled Py at 4°C for 30 min. Arrow, Py that co-localized with BODIPY-GD1a on the plasma membrane. Scale bar, 1 um. (C) Cells expressing CFP-Rab7 were incubated first with BODIPY-GD1a at 4°C for 15 min and then with labeled Py at 37°C for 3 hrs. A representative image of Py co-localizing with BODIPY-GD1a in the Rab7-containing vesicle is shown. Scale bar, 1 um. (D) Cells expressing CFP-HO2 were incubated first with BODIPY-GD1a at 4°C for 15 min and then with labeled Py at 37°C for 4.5 hrs. A representative image of Py co-localizing with BODIPY-GD1a in the ER is shown. Scale bar, 1 um. (E) Quantification of the extent of co-localization between labeled Py and BODIPY-GD1a in the indicated membrane from at least 3 cells. Data are the mean +/- SD.

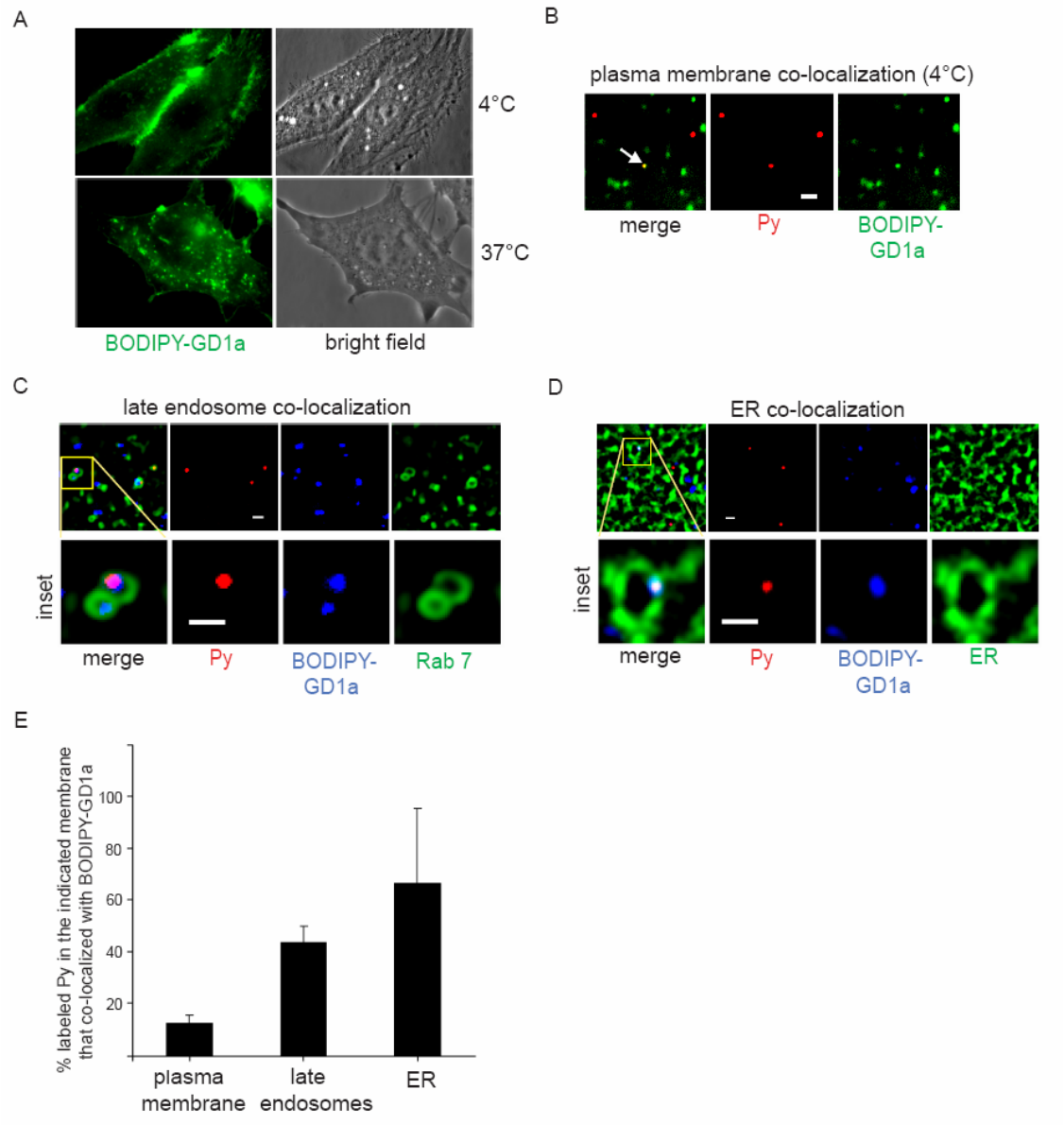

Figure 3.3. Ligand-induced retrograde transport of gangliosides to the ER.
(A) A1-1 cells expressing CFP-HO2 were incubated first with BODIPY-GD1a at 4°C for 15 min and then either with or without Py at 37°C for 4.5 hrs, or with or without CTB at 37°C for 1 hrs. The picture shown is a representative image of BODIPY-GD1a co-localizing with the ER. Scale bar, 1 um. Left graph, quantification of the extent of co-localization between BODIPY-GD1a and the ER from at least 3 control or Py-supplemented cells. Right graph, quantification of the extent of co-localization between BODIPY-GD1a and the ER from at least 3 control or CTB-supplemented cells. Data are the mean +/- SD. (B) NIH 3T3 cells expressing CFP-HO2 were incubated first with BODIPY-GM1 at 4°C for 15 min and then either with or without CTB at 37°C for 1 hr, or with or without Py at 37°C for 4.5 hr. The picture shown is a representative image of BODIPY-GM1 co-localizing with the ER. Scale bar, 1 um. Left graph, quantification of the extent of co-localization between BODIPY-GM1 and the ER from at least 3 control or CTB-supplemented cells. Right graph, quantification of the extent of co-localization between BODIPY-GM1 and the ER from at least 3 control or Py-supplemented cells. Data are the mean +/- SD.

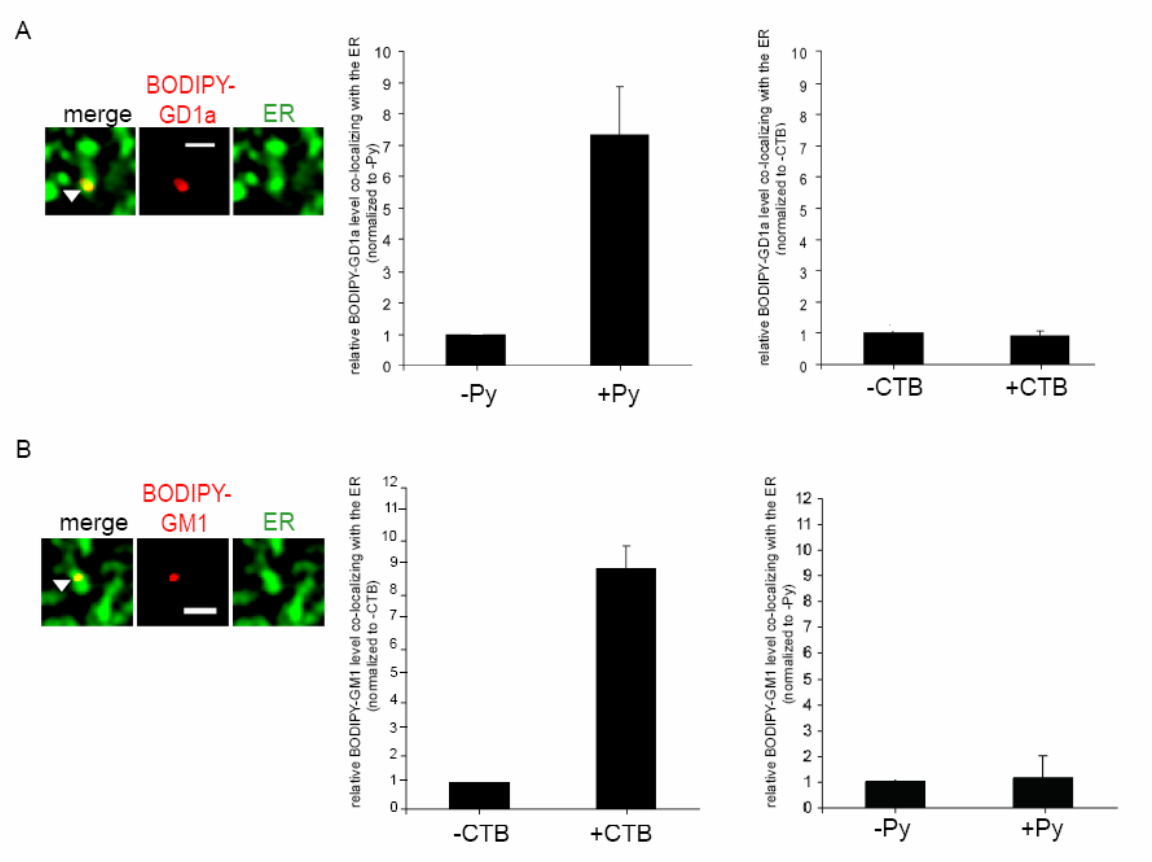

Figure 3.4. GD1a must be added before, but not after, incubation of cells with Py to stimulate infection.
(A) A1-1 cells were treated with 80 uM GD1a at the indicated time points with respect to addition of cells with Py. 48 hrs after incubation of cells with Py, cells were subjected to immunofluorescence with an antibody against the large T antigen. Data represent the mean +/- SD for at least 2 independent experiments. 3/4004 cells expressed T antigen in the control cells. (B) A1-1 cells expressing CFP-Rab7 were incubated first with BODIPY-GD1a at 4°C for 15 min and then with labeled Py at 37°C for 3 hrs. 80 uM GD1a was added pre- or post-infection. The extent of co-localization between labeled Py and BODIPY-GD1a in the CFP-Rab7 late endosomes was quantified from at least 3 cells. Data are the mean +/- SD. (C) As in (A) except NIH 3T3 cells were used. 78/1006 cells expressed T antigen in the control cells.

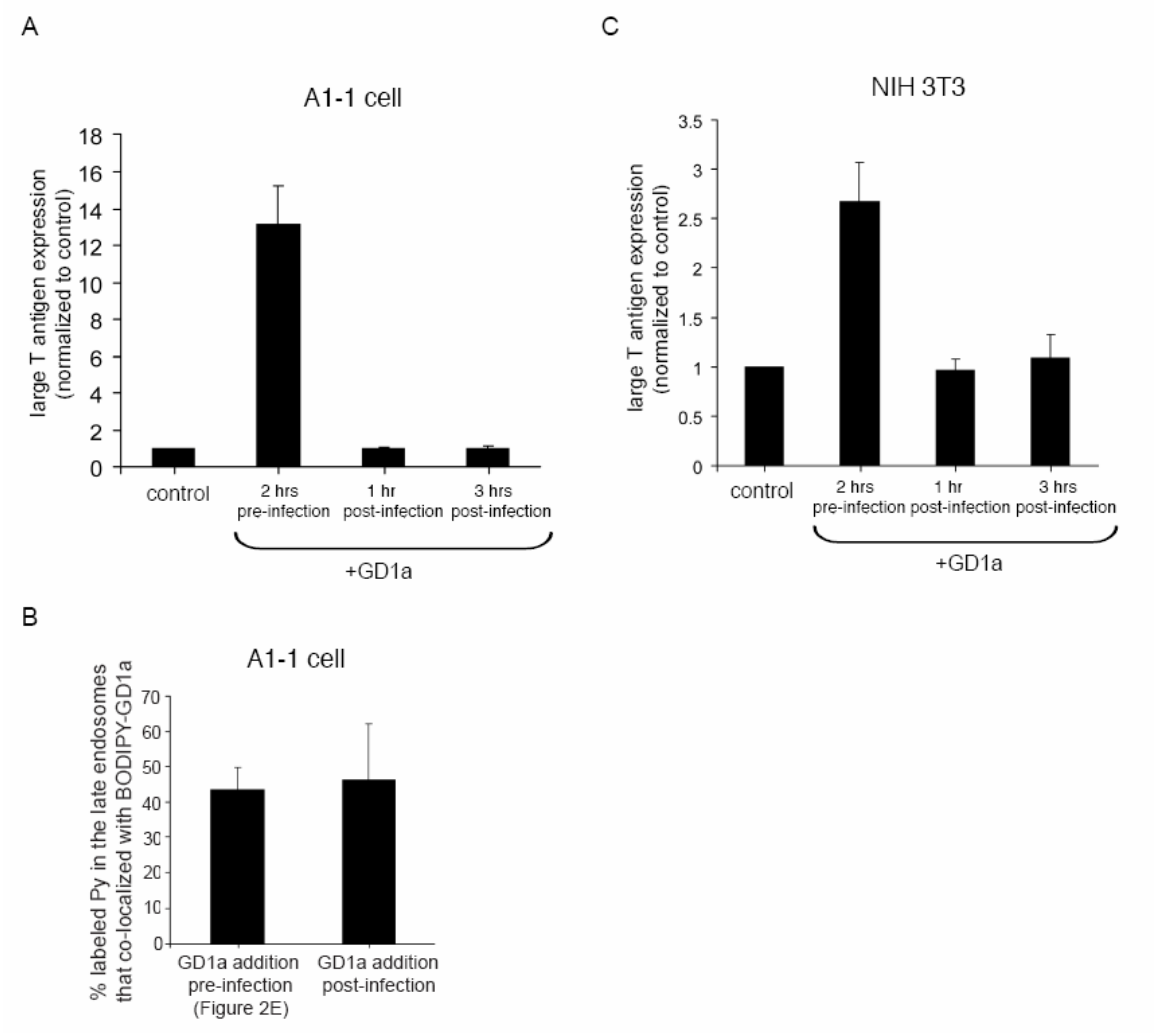

Figure 3.5. Removing plasma membrane glycoproteins stimulates Py infection and ER transport.
(A) NIH 3T3 cells were treated with or without 4 ug/ml proteinase K at 4°C for 1 hr. Contents in the media from these cells were precipitated and subjected to SDS-PAGE analysis followed by Coomassie staining. (B) Cells were treated with or without 4 ug/ml proteinase K at 4°C for 1 hr. Cell lysates were subjected to SDS-PAGE followed by immunblotting with antibodies against the EGFR, TfR, and Derlin-1. (C) Quantification of the number of Py particles bound to the plasma membrane in control and proteinase K treated cells. At least 3 cells in each group were analyzed. Data are the mean +/- SD. (D) Large T antigen expression in control and proteinase K treated cells were analyzed as in Figure 3.1D. Data represent the mean +/- SD from at least 3 independent experiments. 81/5404 cells expressed large T antigen in control cells. (E) Quantification of the number of Q-dot (GD1a Ab) bound to the cell surface of control and proteinase K-treated cells. (F) Quantification of Py and BODIPY-GD1a co-localization on the plasma membrane of control and proteinase K-treated A1-1 cells. Data were analyzed as in FIG 3.2. (G) Py-ER co-localization in control and proteinase K treated cells were analyzed by immunofluorescence staining. Top panel, representative images. Arrowhead, Py that co-localized with the ER. Arrow, Py that did not co-localize with the ER. Scale bar, 1 um. Bottom panel, quantification of Py co-localizing with the ER from at least 3 cells. Data are the mean +/- SD. (H) Cells were treated with or without PNGase F at 37°C for 1 hr. Cell lysates were subjected to SDS-PAGE followed by immunblotting with antibodies against the EGFR and Ribo I. (I) Large T antigen expression in control and PNGase F treated cells were analyzed as in FIG 3.1D. Data represent the mean +/- SD from at least 2 independent experiments. 27/1232 cells expressed large T antigen in control cells.

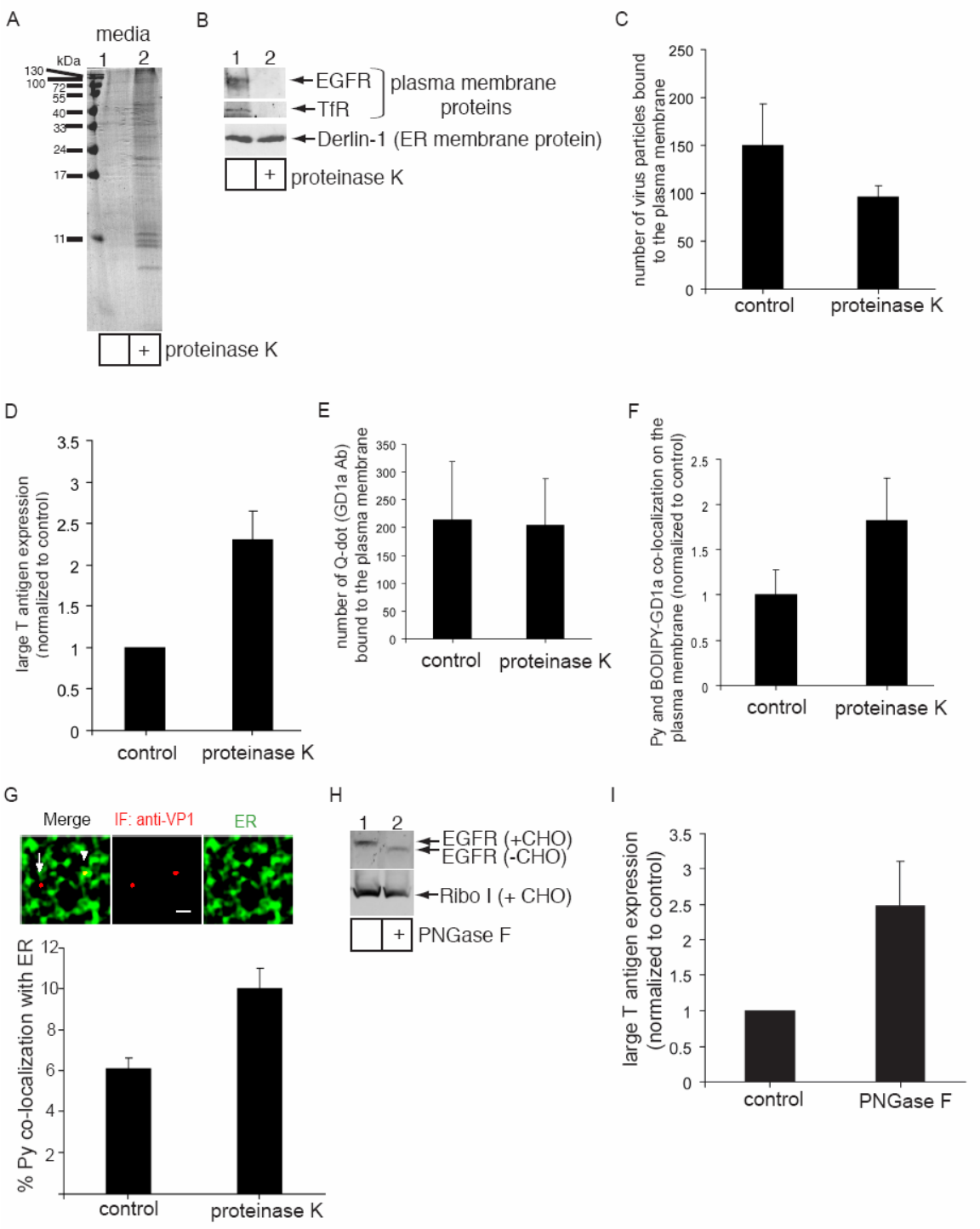
A
media
kDa
1
2
130
100
72
55
40
33
24
17
11
+
proteinase K
B
1
2
EGFR
TfR
plasma membrane proteins
Derlin-1 (ER membrane protein)
+
proteinase K
C
number of virus particles bound to the plasma membrane
250
200
150
100
50
0
control
proteinase K
D
large T antigen expression (normalized to control)
3.5
3
2.5
2
1.5
1
0.5
0
control
proteinase K
E
number of Q-dot (GD1a Ab) bound to the plasma membrane
350
300
250
200
150
100
50
0
control
proteinase K
F
Py and BODIPY-GD1a co-localization on the plasma membrane (normalized to control)
2.5
2
1.5
1
0.5
0
control
proteinase K
G
Merge
IF: anti-VP1
ER
% Py co-localization with ER
12
10
8
6
4
2
control
proteinase K
H
1
2
EGFR (+CHO)
EGFR (-CHO)
Ribo I (+ CHO)
+
PNGase F
I
large T antigen expression (normalized to control)
3.5
3
2.5
2
1.5
1
0.5
0
control
PNGase F

Figure 3.6. Over-expression of the model glycoprotein EGFR decreases Py infection and ER transport.
(A) NIH 3T3 cells were incubated with Py at 4°C for 1 hr, washed to remove the unbound virus, and the resulting cell pellet was incubated with the crosslinker DSP at 4°C for 1 hr. Cells were lysed and the resulting lysate was subjected to immunoprecipitation using either a control Ribo I or EGFR-specific antibody. The precipitated sample was subjected to SDS-PAGE followed by immunoblotting with antibodies against Py VP1 and EGFR. (B) Cells were transfected with either the control GFP construct or with a combination of GFP and EGFR constructs. Cell lysates were subjected to SDS-PAGE followed by immunblotting with antibodies against the EGFR and Ribo I. (C) Quantification of the number of Py particles bound to the plasma membrane in cells transfected with either the control GFP construct or with a combination of GFP and EGFR constructs. At least 3 cells that expressed GFP in each group were analyzed. Data are the mean +/- SD. (D) Large T antigen expression in cells transfected with either the control GFP construct or with a combination of GFP and EGFR constructs were analyzed as in FIG 3.1D. Only those cells that expressed GFP were counted. Data represent the mean +/- SD for at least 3 independent experiments. 23/342 cells expressed large T antigen in control cells. (E) Quantification of Py and BODIPY-GD1a co-localization on the plasma membrane of A1-1 cells transfected with CFP or with a combination of CFP and EGFR. Only those cells expressing CFP were counted. Data were analyzed as in FIG 3.2. (F) Quantification of the Py-ER co-localization in cells transfected with either the control CFP-HO2 construct or with a combination of CFP-HO2 and EGFR constructs. At least 3 cells in each group were analyzed. Data are the mean +/- SD. (G) Quantification of Py-late endosome co-localization in cells transfected with either the control YFP-Rab7 construct or with a combination of YFP-Rab7 and EGFR constructs. At least 3 cells in each group were analyzed. Data are the mean +/- SD. (H) Large T antigen expression in control NIH 3T3 cells or NIH 3T3 cells stably over-expressing the IGF-1R were analyzed as in FIG 3.1D.

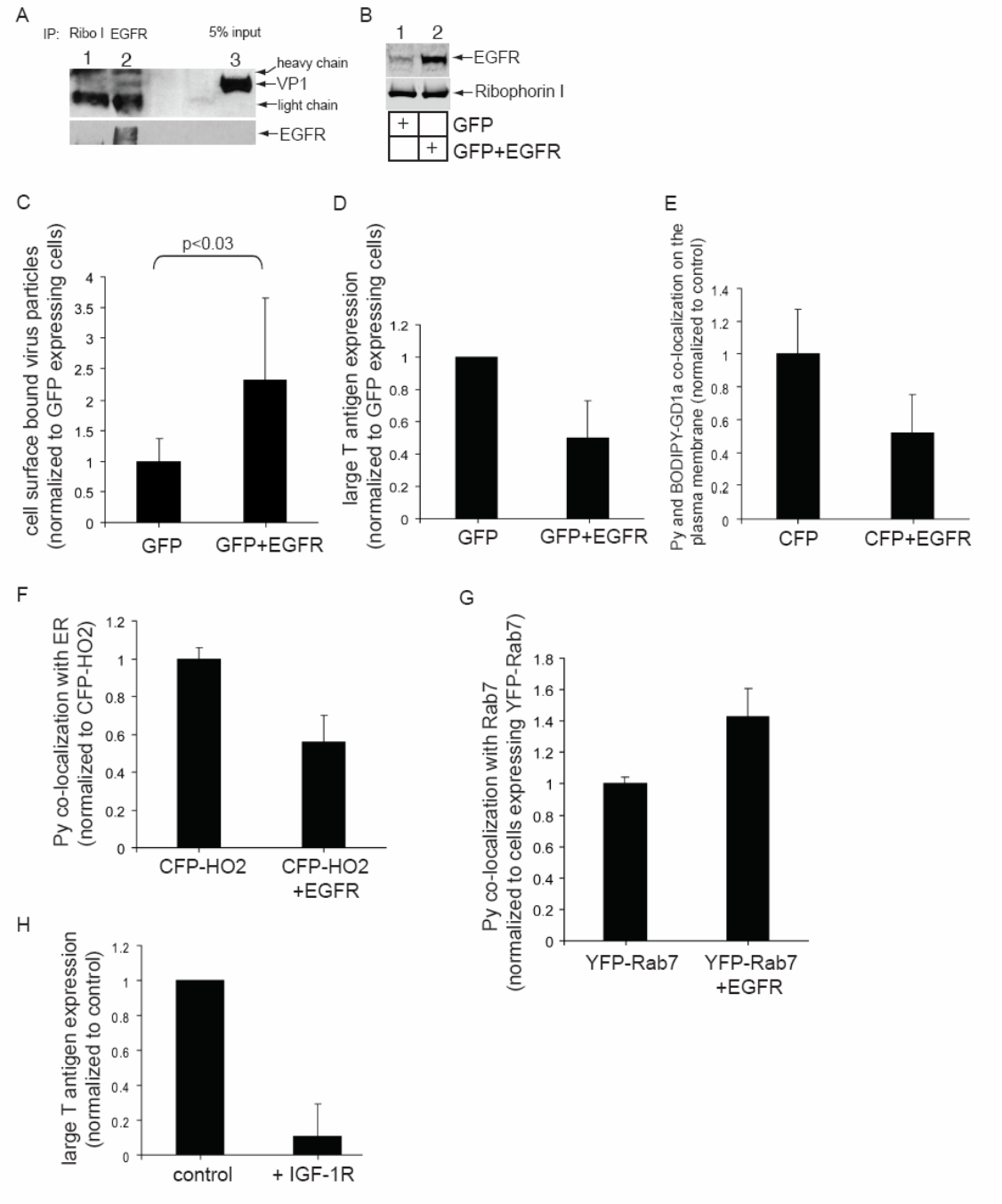
A
IP: Ribo I EGFR
5% input
1 2 3
heavy chain
VP1
light chain
EGFR
B
1 2
EGFR
Ribophorin I
+
GFP
+
GFP+EGFR
C
cell surface bound virus particles (normalized to GFP expressing cells)
p<0.03
GFP
GFP+EGFR
D
large T antigen expression (normalized to GFP expressing cells)
GFP
GFP+EGFR
E
Py and BODIPY-GD1a co-localization on the plasma membrane (normalized to control)
CFP
CFP+EGFR
F
Py co-localization with ER (normalized to CFP-HO2)
CFP-HO2
CFP-HO2 +EGFR
G
Py co-localization with Rab7 (normalized to cells expressing YFP-Rab7)
YFP-Rab7
YFP-Rab7 +EGFR
H
large T antigen expression (normalized to control)
control
+ IGF-1R

Figure 3.7. Lipids and proteins play opposing roles in mediating murine polyomavirus infection.
Py that binds to the glycolipid ganglioside receptors are targeted down the infectious route. In this pathway, gangliosides first target Py to the endolysosomes, and then sort the virus to the ER where the virus then penetrates the ER membrane to reach the cytosol. From the cytosol, Py is transported further to the nucleus to initiate infection. By contrast, Py that interacts with glycoproteins such as the EGFR commits to a non-productive route. After engaging glycoproteins, the virus is taken up to endolysosomes and sequestered in this compartment. Because these viruses do not bind to glycolipids, they are not sorted to the ER and consequently do not cause infection.

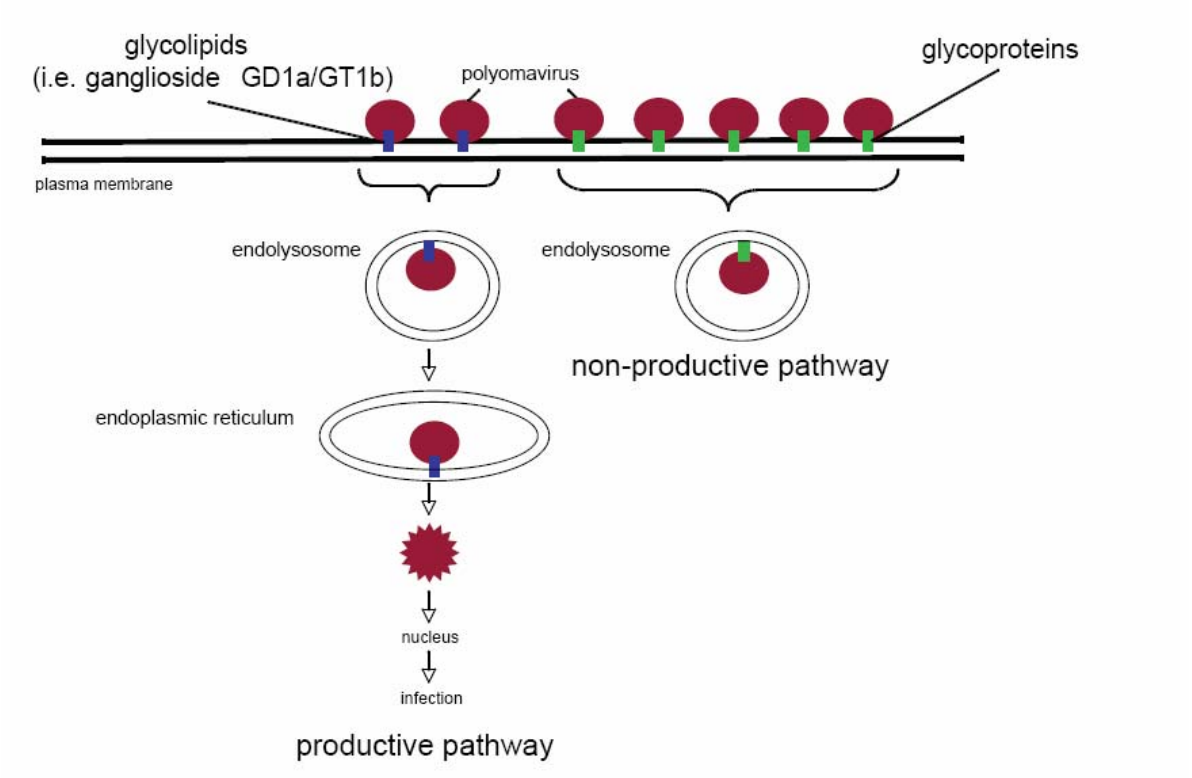

Figure 3.8. Proteinase K treatment does not degrade integrin efficiently.
NIH 3T3 cells were treated with or without 4ug/ml proteinase K at 4°C for 1hr, and washed to remove proteinase K. The amount of alphaV integrin on the cell surface was assessed by Fluorescence-Activated Cell Sorting (FACS).

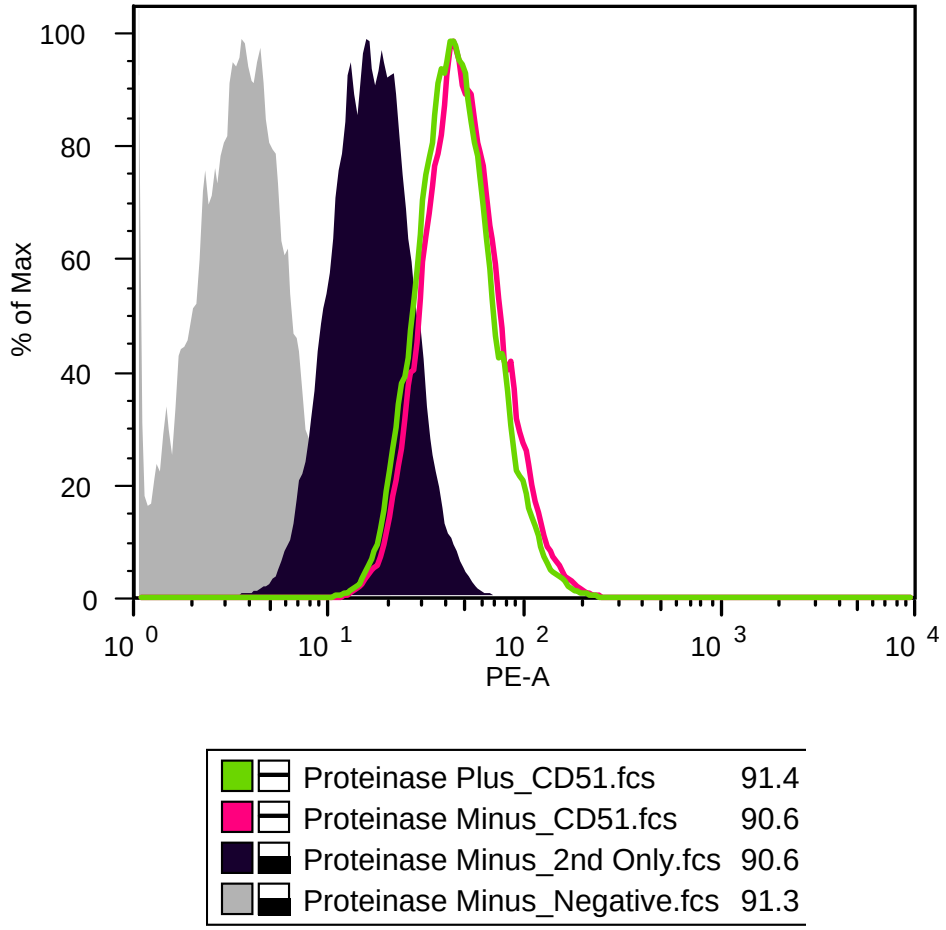

Chapter 4

Conclusion

Polyomaviruses, as non-enveloped DNA tumor viruses, invade host cells and hijack cellular machineries to cause different diseases, such as human skin cancer (Feng et al., 2008; Tsai and Qian, 2010). They bind to cell surface receptors to enter cells, and hijack cellular machineries to cause lytic infection or cell transformation. Therefore, assessing the relationship between polyomaviruses and their host cells will lead to a better understanding of the cellular machineries mediating the infection process and human diseases.

Cellular entry of polyomaviruses

In general viruses need to transport their genomes to the cytosol or nucleus of host cells to cause infection. Different strategies and cellular pathways are used by viruses to deliver their genomes into the host. The cellular entry and membrane penetration mechanism of enveloped viruses have been studied for a long time. For these viruses, fusion of viral and cellular membranes allows the nucleoprotein complex to be delivered across the cellular membrane to the cytosol or nucleus. For example, the influenza virus is endocytosed and transported to the endosomes, where the low pH triggers a conformational change that initiate the fusion of viral and endosomal membranes. As a consequence, the viral nucleocapsid is delivered to the cytosol (Skehel and Wiley, 2000). However, membrane penetration of non-enveloped viruses is a more complicated and less understood process. As a non-enveloped virus, polyomavirus has been reported to be transported to the ER where it penetrates the ER membrane to enter the cytosol. Multiple ER-resident proteins and viral conformational changes are involved in this membrane penetration event (Tsai

and Qian, 2010). Transport of polyomaviruses to the ER is an essential step for virus infection. My thesis is focused on studying how Py is transported from the plasma membrane to the ER.

Viruses enter cells through different endocytosis mechanisms, such as clathrin-mediated endocytosis, macropinocytosis, and caveolar/raft-mediated internalization (Mercer et al., 2010). SV40 and BK virus are endocytosed into cells via a caveolar/raft-mediated pathway (Pelkmans et al., 2004; Eash et al., 2004), while JC virus is encodytosed into cells via a clathrin-dependent pathway (Pho et al., 2000). The endocytosis pathway of Py is not clearly understood, and it appears to be cell dependent. For example, Py enters mouse NIH 3T3 cells or BMK cells via a clathrin independent and caveolin-1 independent pathway (Gilbert and Benjamin, 2000), but it enters rat glioma C6 cells via a caveolin-1 dependent pathway (Gilbert and Benjamin, 2004). In our study, we did not detect significant co-localization between Py and caveolin-1 in NIH 3T3 cells (Figure 2.9), consistent with a previous report (Gilbert and Benjamin, 2000). It is not clear why polyomaviruses use different endocytic pathways to enter cells. As different endocytic pathways may crosstalk with each other inside cells, it remains possible that polyomaviruses are able to take multiple endocytic pathways to enter cells initially, and then hijack intracellular transport systems to reach the ER to cause productive infection.

Regardless of the endocytic pathways, many members of the polyomavirus family are transported through the acidic endolysosomal system. It has been reported that low pH is required for BK virus infection (Eash et al., 2004), and JC virus is transported through the endosomes (Querbes et al., 2006). Although SV40 has been originally reported to traffic to a pH-neutral compartment called the caveosome (Pelkmans et al., 2004), a recent report indicates that in most cell types the caveosomes correspond to modified late endosomes or endolysosomes (Mercer et al., 2010). Py has been reported to be transported via the early endosomes (Liebl et al., 2006). However, there is a discrepancy

regarding whether the low pH environment of the endolysosomes regulates Py infection (Liebl et al., 2006; Gilbert and Benjamin, 2000). Although the reason for this discrepancy is not clear, the very high infection level might render Py resistance to NH4Cl treatment in Gilbert's paper. In our study, we found that Py is transported via the endolysosomal system, and elevating pH in the endolysosomes with either bafilomycin A1 or NH4Cl treatment significantly inhibited Py infection (Chapter 2). Hence we conclude that Py is transported through the acidic endolysosomal system.

The endolysosomal pathway seems to be a common pathway used by members of the polyomavirus family. It is interesting to ask why these polyomaviruses prefer to take this pathway. In the case of Py, our data demonstrate that the low pH environment in the endolysosomes triggers a conformational change in Py (Figure 2.3), facilitating the subsequent conformational change the virus experiences in the ER that initiates ER-to-cytosol penetration (Magnuson et al., 2005). Therefore, the low pH environment in the endolysosomes seems to destabilize Py, and primes the virus for further conformational change in the ER. Whether this is a common mechanism for other polyomaviruses requires further studies.

Several steps of conformational changes have been reported during Py entry and intracellular trafficking. The conformational changes of Py VP1 proteins can take place on the plasma membrane when the virus binds to a sialic acid (Cavaldesi et al., 2004), in the endolysosome when Py encounters the low pH environment (Qian et al., 2009), and in the ER when Py interacts with ER-resident factors such as ERp29 (Magnuson et al., 2005). Given that Py with its relatively big size (approximately 40~50 nm in diameter) must penetrate the ER membrane and likely the nuclear pore complex (NPC, only approximately 26 nm in diameter) (Otis et al., 2006; Yang et al., 2004) to cause infection, it is not surprising that the viral particle undergoes dramatic conformational changes. The timing of the series of conformational changes may also be important for infection. For

instance, these sequential remodeling reactions may prevent Py from targeting to specific organelles prematurely or be detected by cellular defense mechanisms. A systematic study of the conformational changes experienced by Py inside the cells will provide critical insights into how Py successfully transport its DNA into the nucleus for infection. For example, proteinase K or trypsin digestion assay could be applied to Py extracted from different organelles at different time points post infection to assess the conformational changes of Py. Structure analysis (such as electron microscopy or X-ray crystallography) of Py capsid proteins at different stages of infection will also help to access the series of Py conformational changes.

Roles of lipid and protein receptors

Viruses usually need to engage specific receptors on the plasma membrane to initiate infection. The studies of the roles of cell surface receptors are critical for understanding how viruses invade host cells, as well as how they protect host from virus infection.

Ganglioside GD1a was identified as Py's functional receptor (Tsai et al., 2003; Smith et al., 2003; Gilbert and Benjamin, 2004). However, the mechanism by which GD1a stimulates Py infection is not clear during these initial reports. Our data demonstrate that GD1a functions as Py's entry receptor -- this lipid receptor must engage Py on the cell surface to promote Py infection (Chapter 3). The timing of interacting between Py and GD1a is critical, and dictates Py's ability to cause infection. If Py does not interact with GD1a on the cell surface, it may be endocytosed by binding to other receptors. However, once inside the cells, Py can not bind to GD1a even though the concentration of ganglioside is high in the endolysosomes. This observation indicates that the initial binding event on the cell surface is essential for Py infection. Whether other factors such as integrin on the cell surface help Py to engage GD1a requires further studies.

Our findings demonstrate that GD1a engages Py on the cell surface and traffics with Py as a complex from the plasma membrane to the ER (Figure 3.2). In this role, GD1a is able to guide intracellular trafficking of Py and lead the virus to the infectious pathway. It is not clear when GD1a is released from Py. A better live cell tracking system and fluorophores that are more resistant to photobleaching will help to answer this question. For example, if co-localization of labeled Py and GD1a can be tracked for a longer time, Py release from GD1a might be observed in a specific organelle such as in the ER, cytosol, or nucleus using live cell imaging. The resolution of microscopy is also important for the live cell tracking technique. Recently several super-resolution imaging approaches such as stochastic optical reconstruction microscopy (STORM) or photoactivation localization microscopy (PALM) have been developed (Zhuang, 2009), allowing live cell imaging to be performed with higher resolution.

In addition to acting as the entry receptor (Chapter 3), our data also show that GD1a behaves as an intracellular sorter, guiding Py from the endolysosomes to the ER (Chapter 2). Since a single Py virion is able to cluster multiple GD1a, GD1a clustering is likely to be the mechanism of targeting Py to the ER (Figure 2.5, 2.6). There are two possibilities to explain how the clustering of ganglisodes sorts its ligand to the ER. One possibility is that clustering of gangliosides induces a hydrophobic platform in the endolysosomal membrane and stimulates transmembrane signaling to recruit cytoplasmic factors. These cytoplasmic factors may be able to facilitate the budding of Py-containing vesicles from the endolysosomal membrane. Alternatively, GD1a clustering might alter the physical properties of the endolysosomal membrane attached to the virus, inducing membrane invagination and budding of Py-containing vesicles from the endolysosomes. This concept has been reported in the case of shiga toxin, where its binding to the glycolipid GB3 receptor promotes membrane invaginations and stimulates its uptake into cells (Romer et al., 2007). In addition, the interaction of SV40 with ganglioside GM1 receptor also induces membrane invagination in giant unilamellar vesicles (Ewers et al., 2010). To elucidate

whether ganglisode clustering is a general mechanism for ER targeting, an experiment assessing whether GM1 could target SV40 or Q-dot coated with GM1 antibody to the ER will help. Future studies are required to delineate these two possibilities, and to identify the cytoplasmic factors involved in this sorting event.

ER targeting of ligands via ganglioside binding is not virus specific, as an artificial particle that binds to GD1a can also be targeted to the ER. During the normal fate of gangliosides, these lipids are endocytosed into cells and transported through the endolysosomes to the lysosomes for degradation. If gangliosides are not properly degraded by enzymes in the lysosome, it results in lipid storage diseases. Although gangliosides can be transported back to the Golgi complex (Schwarzmann, 2010), their retrograde transport to the ER is not a common pathway. Our studies show that ligand interaction induces the retrograde transport of gangliosides to the ER (Figure 3.3), indicating that clustering gangliosides by ligand binding can induce their transport to the ER. In addition, it has been reported that lipid storage diseases may involve ER stress (Vitner et al., 2010; Brunetti-Pierri and Scaglia, 2008). Therefore, it is possible that this endolysosome-to-ER trafficking pathway for gangliosides normally exists at a low efficiency, but is increased by ganglioside clustering.

The previously unappreciated transport pathway between the endolysosome and the ER has been recently described in several papers. For example, under pathological conditions where gangliosides accumulate in the lysosomes as these lipids can not be degraded, a fraction of the gangliosides can be targeted to the ER (Tessitore et al., 2004). ER-to-endolysosome transport pathway, the reverse of the endolysosome-to-ER pathway used by Py, was observed in toll-like receptors (Kim et al., 2008). These examples further demonstrate the existence of a communication route between the endolysosome and the ER.

The observation that a receptor mediates virus entry and undergoes intracellular trafficking as a complex with virus is not without precedent. For example, the

entry of Moloney murine leukemia virus (MoMuLV) is mediated by its receptor murine cationic amino acid transporter (MCAT-1), and this virus remains in contact with the receptor when trafficking inside the cell for an extended time (Lee et al., 1999). However, to our best knowledge, GD1a-mediated sorting of Py to the ER is the first report that a cell surface receptor functions as an intracellular sorter to regulate the intracellular trafficking of a virus. Future studies of intracellular transport of other virus-receptor complex may reveal more cases of receptor-mediated intracellular virus trafficking. Receptor-mediated intracellular sorting may also regulate toxin trafficking, such as in the case of GM1's potential role in targeting CT to the ER (Fujinaga et al, 2003).

Ganglioside GD1a is not the only receptor that Py binds to on the cell surface. Glycoproteins, which contain sialic acid-galactose motif, can also bind to Py and serve as cell surface receptors. Our finding shows that glycoprotein receptors normally act as decoy receptors, which compete with the functional receptor GD1a for Py binding (Chapter 3). Therefore, although Py develops the simple strategy of interacting with the sialic acid-galactose moiety in GD1a to gain entry into cells to cause infection, the fact that a large number of glycoproteins also contain sialic acid-galactose moiety in turn limits Py's infection as a trade-off. Because one Py that arrives in the nucleus successfully is sufficient to cause infection (Diacumakos and Gershey, 1977), Py seems to choose simplicity rather than specificity for receptor binding strategy. The binding efficiency of Py to GD1a versus glycoproteins requires further studies. In addition, not all glycoproteins serve as decoy receptors for Py. For example, α4β1 serves as a postattachment receptor for Py and facilitates virus infection (Caruso et al., 2003). Therefore, future studies should focus on pinpointing the unique features of α4β1 that enables it to promote Py infection.

In sum, our data demonstrate the opposite manners by which lipids and proteins regulate Py infection (Figure 4.1). The glycolipid ganglioside GD1a plays a role as the functional entry receptor. It must engage Py on the cell surface, and guide

the virus down the infectious pathway by sorting Py out of the endolysosomes to the ER. In contrast, glycoproteins in general function as decoy receptors. They compete with GD1a on the cell surface for Py binding. In turn, Py that bind to glycoproteins are trapped in the endolysosomes, and as a consequence, targeted down the non-infectious pathway. Although our data show that transport through the endolysosomes is part of the Py infectious pathway, Py in this compartment must be sorted out of the endolysosomes and into the ER. Otherwise, it would become trapped in this compartment, effectively blocking infection. In conclusion, our findings demonstrate the trafficking pathway of Py from the plasma membrane to the ER, and the opposing roles of two types of cell surface receptors in regulating Py infection.

Figure 4.1. Roles of glycolipids and glycoproteins in regulating polyomavirus infection. In step 1, glycolipid GD1a acts as the entry receptor for Py, while glycoproteins compete with glycolipids for virus binding. Upon entry, Py is initially targeted to the endolysosomes, regardless of the nature of the receptor that engages the virus on the cell surface. However, Py is only sorted out of the endolysosomes en route to the ER if it engages glycolipids (step 2). Transport to the ER constitute the infectious route. By contrast, if Py is transported to the endolysosomes by glycoproteins, it fails to sort further to the ER and remains trapped in the endolysosomes. This pathway represents the non-productive route.

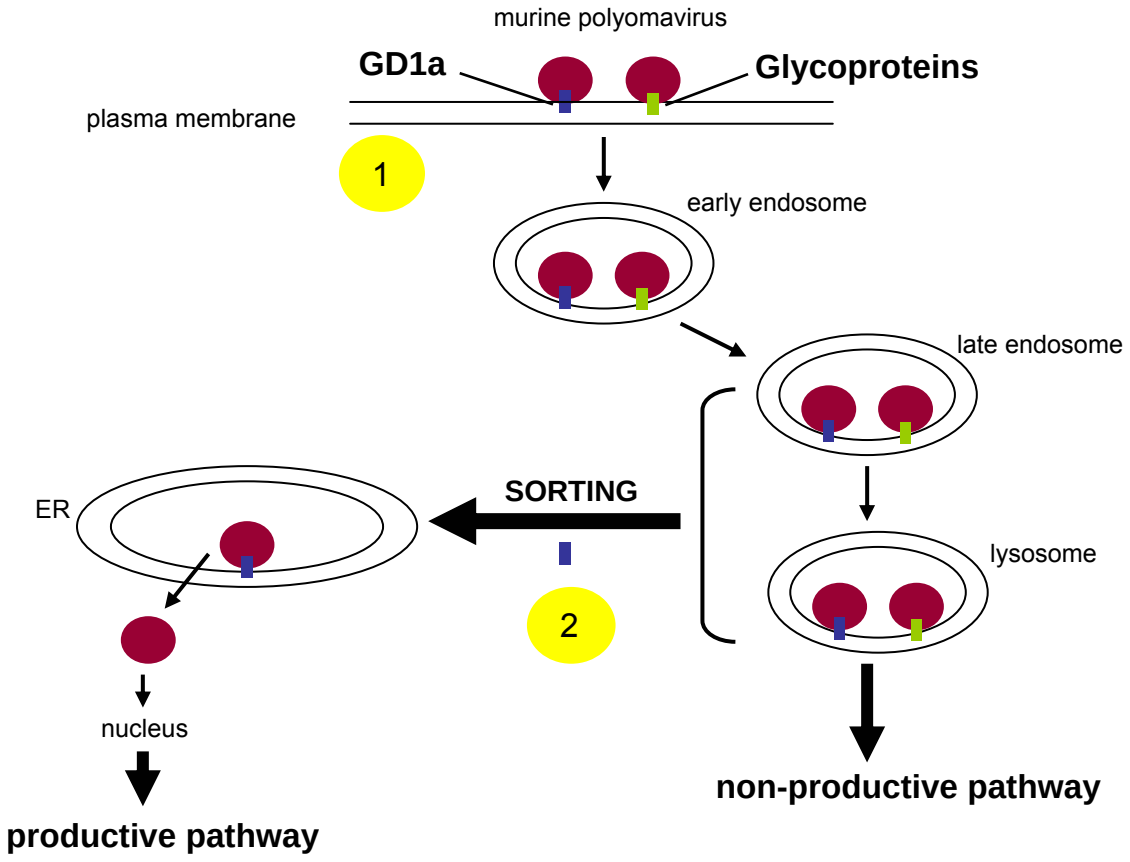

References

Allander, T., Andreasson, K., Gupta, S., Bjerkner, A., Bogdanovic, G., Persson, M.A., Dalianis, T., Ramqvist, T., and Andersson, B. (2007). Identification of a third human polyomavirus. Journal of virology 81, 4130-4136.

Ashok, A., and Atwood, W.J. (2003). Contrasting roles of endosomal pH and the cytoskeleton in infection of human glial cells by JC virus and simian virus 40. Journal of virology 77, 1347-1356.

Baranowski, E., Ruiz-Jarabo, C.M., and Domingo, E. (2001). Evolution of cell recognition by viruses. Science (New York, NY 292, 1102-1105.

Baranowski, E., Ruiz-Jarabo, C.M., Pariente, N., Verdaguer, N., and Domingo, E. (2003). Evolution of cell recognition by viruses: a source of biological novelty with medical implications. Advances in virus research 62, 19-111.

Bauer, P.H., Cui, C., Liu, W.R., Stehle, T., Harrison, S.C., DeCaprio, J.A., and Benjamin, T.L. (1999). Discrimination between sialic acid-containing receptors and pseudoreceptors regulates polyomavirus spread in the mouse. Journal of virology 73, 5826-5832.

Benjamin, T.L. (2001). Polyoma virus: old findings and new challenges. Virology 289, 167-173.

Boldyrev, I.A., Zhai, X., Momsen, M.M., Brockman, H.L., Brown, R.E., and Molotkovsky, J.G. (2007). New BODIPY lipid probes for fluorescence studies of membranes. Journal of lipid research 48, 1518-1532.

Brady, J.N., Winston, V.D., and Consigli, R.A. (1978). Characterization of a DNA-protein complex and capsomere subunits derived from polyoma virus by treatment with ethyleneglycol-bis-N,N'-tetraacetic acid and dithiothreitol. Journal of virology 27, 193-204.

Brown, M.S., Anderson, R.G., Basu, S.K., and Goldstein, J.L. (1982). Recycling of cell-surface receptors: observations from the LDL receptor system. Cold Spring Harbor symposia on quantitative biology 46 Pt 2, 713-721.

Brunetti-Pierri, N., Scaglia, F. (2008). GM1 gangliosidosis: review of clinical, molecular, and therapeutic aspects. Mol Genet Metab 94(4):391-6.

Cahan, L.D., Singh, R., and Paulson, J.C. (1983). Sialyloligosaccharide receptors of binding variants of polyoma virus. Virology 130, 281-289.

Campanero-Rhodes, M.A., Smith, A., Chai, W., Sonnino, S., Mauri, L., Childs, R.A., Zhang, Y., Ewers, H., Helenius, A., Imberty, A., et al. (2007). N-glycolyl GM1 ganglioside as a receptor for simian virus 40. Journal of virology 81, 12846-12858.

Caruso, M., Belloni, L., Sthandier, O., Amati, P., and Garcia, M.I. (2003). Alpha4beta1 integrin acts as a cell receptor for murine polyomavirus at the postattachment level. Journal of virology 77, 3913-3921.

Cavaldesi, M., Caruso, M., Sthandier, O., Amati, P., and Garcia, M.I. (2004). Conformational changes of murine polyomavirus capsid proteins induced by sialic acid binding. The Journal of biological chemistry 279, 41573-41579.

Chen, M.H., and Benjamin, T. (1997). Roles of N-glycans with alpha2,6 as well as alpha2,3 linked sialic acid in infection by polyoma virus. Virology 233, 440-442.

Chen, X.S., Stehle, T., and Harrison, S.C. (1998). Interaction of polyomavirus internal protein VP2 with the major capsid protein VP1 and implications for participation of VP2 in viral entry. The EMBO journal 17, 3233-3240.

Ciechanover, A., Schwartz, A.L., Dautry-Varsat, A., and Lodish, H.F. (1983). Kinetics of internalization and recycling of transferrin and the transferrin receptor in a human hepatoma cell line. Effect of lysosomotropic agents. The Journal of biological chemistry 258, 9681-9689.

Clague, M.J., Urbe, S., Aniento, F., and Gruenberg, J. (1994). Vacuolar ATPase activity is required for endosomal carrier vesicle formation. The Journal of biological chemistry 269, 21-24.

Cummings, R.D., Soderquist, A.M., and Carpenter, G. (1985). The oligosaccharide moieties of the epidermal growth factor receptor in A-431 cells. Presence of complex-type N-linked chains that contain terminal N-acetylgalactosamine residues. The Journal of biological chemistry 260, 11944-11952.

Diacumakos, E.G., and Gershey, E.L. (1977). Uncoating and gene expression of simian virus 40 in CV-1 cell nuclei inoculated by microinjection. Journal of virology 24, 903-906.

Dimitrov, D.S. (2004). Virus entry: molecular mechanisms and biomedical applications. Nat Rev Microbiol 2, 109-122.

Eash, S., and Atwood, W.J. (2005). Involvement of cytoskeletal components in BK virus infectious entry. Journal of virology 79, 11734-11741.

Eash, S., Manley, K., Gasparovic, M., Querbes, W., and Atwood, W.J. (2006). The human polyomaviruses. Cell Mol Life Sci 63, 865-876.

Eash, S., Querbes, W., and Atwood, W.J. (2004). Infection of vero cells by BK virus is dependent on caveolae. Journal of virology 78, 11583-11590.

Erickson, K.D., Garcea, R.L., and Tsai, B. (2009). Ganglioside GT1b is a putative host cell receptor for the Merkel cell polyomavirus. Journal of virology 83, 10275-10279.

Ewers, H., Romer, W., Smith, A.E., Bacia, K., Dmitrieff, S., Chai, W., Mancini, R., Kartenbeck, J., Chambon, V., Berland, L., et al. GM1 structure determines SV40-induced membrane invagination and infection. Nature cell biology 12, 11-18; sup pp 11-12.

Ewers, H., Smith, A.E., Sbalzarini, I.F., Lilie, H., Koumoutsakos, P., and Helenius, A. (2005). Single-particle tracking of murine polyoma virus-like particles on live cells and artificial membranes. Proceedings of the National Academy of Sciences of the United States of America 102, 15110-15115.

Fanidi, A., Hancock, D.C., and Littlewood, T.D. (1998). Suppression of c-Myc-induced apoptosis by the Epstein-Barr virus gene product BHRF1. Journal of virology 72, 8392-8395.

Feng, H., Shuda, M., Chang, Y., and Moore, P.S. (2008). Clonal integration of a polyomavirus in human Merkel cell carcinoma. Science (New York, NY 319, 1096-1100.

Feng, Y., Press, B., and Wandinger-Ness, A. (1995). Rab 7: an important regulator of late endocytic membrane traffic. The Journal of cell biology 131, 1435-1452.

Fried, H., Cahan, L.D., and Paulson, J.C. (1981). Polyoma virus recognizes specific sialyligosaccharide receptors on host cells. Virology 109, 188-192.

Fujinaga, Y., Wolf, A.A., Rodighiero, C., Wheeler, H., Tsai, B., Allen, L., Jobling, M.G., Rapoport, T., Holmes, R.K., and Lencer, W.I. (2003). Gangliosides that associate with lipid rafts mediate transport of cholera and related toxins from the plasma membrane to endoplasmic reticulm. Molecular biology of the cell 14, 4783-4793.

Gaynor, A.M., Nissen, M.D., Whiley, D.M., Mackay, I.M., Lambert, S.B., Wu, G., Brennan, D.C., Storch, G.A., Sloots, T.P., and Wang, D. (2007). Identification of a novel polyomavirus from patients with acute respiratory tract infections. PLoS pathogens 3, e64.

Geraghty, R.J., Krummenacher, C., Cohen, G.H., Eisenberg, R.J., and Spear, P.G. (1998). Entry of alphaherpesviruses mediated by poliovirus receptor-related protein 1 and poliovirus receptor. Science (New York, NY 280, 1618-1620.

Gilbert, J., and Benjamin, T. (2004). Uptake pathway of polyomavirus via ganglioside GD1a. Journal of virology 78, 12259-12267.

Gilbert, J., Dahl, J., Riney, C., You, J., Cui, C., Holmes, R., Lencer, W., and Benjamin, T. (2005). Ganglioside GD1a restores infectibility to mouse cells lacking functional receptors for polyomavirus. Journal of virology 79, 615-618.

Gilbert, J., Ou, W., Silver, J., and Benjamin, T. (2006). Downregulation of protein disulfide isomerase inhibits infection by the mouse polyomavirus. Journal of virology 80, 10868-10870.

Gilbert, J.M., and Benjamin, T.L. (2000). Early steps of polyomavirus entry into cells. Journal of virology 74, 8582-8588.

Greber, U.F., and Fassati, A. (2003). Nuclear import of viral DNA genomes. Traffic (Copenhagen, Denmark) 4, 136-143.

Gross, L. (1953). A filterable agent, recovered from Ak leukemic extracts, causing salivary gland carcinomas in C3H mice. Proceedings of the Society for Experimental Biology and Medicine Society for Experimental Biology and Medicine (New York, NY 83, 414-421.

Heldwein, E.E., and Krummenacher, C. (2008). Entry of herpesviruses into mammalian cells. Cell Mol Life Sci 65, 1653-1668.

Henderson, S., Huen, D., Rowe, M., Dawson, C., Johnson, G., and Rickinson, A. (1993). Epstein-Barr virus-coded BHRF1 protein, a viral homologue of Bcl-2, protects human B cells from programmed cell death. Proceedings of the National Academy of Sciences of the United States of America 90, 8479-8483.

Jeyakumar, M., Dwek, R.A., Butters, T.D., and Platt, F.M. (2005). Storage solutions: treating lysosomal disorders of the brain. Nature reviews 6, 713-725.

Jiang, M., Abend, J.R., Johnson, S.F., and Imperiale, M.J. (2009). The role of polyomaviruses in human disease. Virology 384, 266-273.

Jiang, M., Abend, J.R., Tsai, B., and Imperiale, M.J. (2008). Early Events during BK Virus Entry and Disassembly. Journal of virology.

Kalia, M., and Jameel, S. (2009). Virus entry paradigms. Amino acids.

Kalinin, S.V., and Molotkovsky, J.G. (2001). Anion binding to lipid bilayers: a study using fluorescent lipid probes. Membrane & cell biology 14, 831-846.

Kim, Y.M., Brinkmann, M.M., Paquet, M.E., and Ploegh, H.L. (2008). UNC93B1 delivers nucleotide-sensing toll-like receptors to endolysosomes. Nature 452, 234-238.

Kolter, T., and Sandhoff, K. (2005). Principles of lysosomal membrane digestion: stimulation of sphingolipid degradation by sphingolipid activator proteins and anionic lysosomal lipids. Annual review of cell and developmental biology 21, 81-103.

Komagome, R., Sawa, H., Suzuki, T., Suzuki, Y., Tanaka, S., Atwood, W.J., and Nagashima, K. (2002). Oligosaccharides as receptors for JC virus. Journal of virology 76, 12992-13000.

Kornfeld, R., and Kornfeld, S. (1985). Assembly of asparagine-linked oligosaccharides. Annual review of biochemistry 54, 631-664.

Kuritzkes, D.R. (2009). HIV-1 entry inhibitors: an overview. Current opinion in HIV and AIDS 4, 82-87.

Lakadamyali, M., Rust, M.J., and Zhuang, X. (2006). Ligands for clathrin-mediated endocytosis are differentially sorted into distinct populations of early endosomes. Cell 124, 997-1009.

Lee, S., Zhao, Y., Anderson, WF. (1999). Receptor-mediated Moloney murine leukemia virus entry can occur independently of the clathrin-coated-pit-mediated endocytic pathway. J Virol 73 (7):5994-6005.

Lee, W., and Langhoff, E. (2006). Polyomavirus in human cancer development. Advances in experimental medicine and biology 577, 310-318.

Lencer, W.I., and Tsai, B. (2003). The intracellular voyage of cholera toxin: going retro. Trends in biochemical sciences 28, 639-645.

Liddington, R.C., Yan, Y., Moulai, J., Sahli, R., Benjamin, T.L., and Harrison, S.C. (1991). Structure of simian virus 40 at 3.8-A resolution. Nature 354, 278-284.

Liebl, D., Difato, F., Hornikova, L., Mannova, P., Stokrova, J., and Forstova, J. (2006). Mouse polyomavirus enters early endosomes, requires their acidic pH for productive infection, and meets transferrin cargo in Rab11-positive endosomes. Journal of virology 80, 4610-4622.

Lilley, B.N., Gilbert, J.M., Ploegh, H.L., and Benjamin, T.L. (2006). Murine polyomavirus requires the endoplasmic reticulum protein Derlin-2 to initiate infection. Journal of virology 80, 8739-8744.

Low, J., Humes, H.D., Szczypka, M., and Imperiale, M. (2004). BKV and SV40 infection of human kidney tubular epithelial cells in vitro. Virology 323, 182-188.

Low, J.A., Magnuson, B., Tsai, B., and Imperiale, M.J. (2006). Identification of gangliosides GD1b and GT1b as receptors for BK virus. Journal of virology 80, 1361-1366.

Lozach, P.Y., Burleigh, L., Staropoli, I., Navarro-Sanchez, E., Harriague, J., Virelizier, J.L., Rey, F.A., Despres, P., Arenzana-Seisdedos, F., and Amara, A. (2005). Dendritic cell-specific intercellular adhesion molecule 3-grabbing non-integrin (DC-SIGN)-mediated enhancement of dengue virus infection is independent of DC-SIGN internalization signals. The Journal of biological chemistry 280, 23698-23708.

Magnuson, B., Rainey, E.K., Benjamin, T., Baryshev, M., Mkrtchian, S., and Tsai, B. (2005). ERp29 triggers a conformational change in polyomavirus to stimulate membrane binding. Molecular cell 20, 289-300.

Mannova, P., and Forstova, J. (2003). Mouse polyomavirus utilizes recycling endosomes for a traffic pathway independent of COPI vesicle transport. Journal of virology 77, 1672-1681.

Marsh, M., and Helenius, A. (2006). Virus entry: open sesame. Cell 124, 729-740.

Maxfield, F.R. (1982). Weak bases and ionophores rapidly and reversibly raise the pH of endocytic vesicles in cultured mouse fibroblasts. The Journal of cell biology 95, 676-681.

Mercer, J., Schelhaas, M., Helenius, A. (2010). Virus entry by endocytosis. Annu Rev Biochem 79:803-33.

Meresse, S., Gorvel, J.P., and Chavrier, P. (1995). The rab7 GTPase resides on a vesicular compartment connected to lysosomes. Journal of cell science 108 (Pt 11), 3349-3358.

Montgomery, R.I., Warner, M.S., Lum, B.J., and Spear, P.G. (1996). Herpes simplex virus-1 entry into cells mediated by a novel member of the TNF/NGF receptor family. Cell 87, 427-436.

Nakanishi, A., Clever, J., Yamada, M., Li, P.P., and Kasamatsu, H. (1996). Association with capsid proteins promotes nuclear targeting of simian virus 40 DNA. Proceedings of the National Academy of Sciences of the United States of America 93, 96-100.

Neu, U., Woellner, K., Gauglitz, G., and Stehle, T. (2008). Structural basis of GM1 ganglioside recognition by simian virus 40. Proceedings of the National Academy of Sciences of the United States of America 105, 5219-5224.

Nielsen, D.G. (2009). The relationship of interacting immunological components in dengue pathogenesis. Virology journal 6, 211.

Oda, Y., Okada, T., Yoshida, H., Kaufman, R.J., Nagata, K., and Mori, K. (2006). Derlin-2 and Derlin-3 are regulated by the mammalian unfolded protein response and are required for ER-associated degradation. The Journal of cell biology 172, 383-393.

Otis, K.O., Thompson, K.R., and Martin, K.C. (2006). Importin-mediated nuclear transport in neurons. Current opinion in neurobiology 16, 329-335.

Pelkmans, L., Burli, T., Zerial, M., and Helenius, A. (2004). Caveolin-stabilized membrane domains as multifunctional transport and sorting devices in endocytic membrane traffic. Cell 118, 767-780.

Pelkmans, L., and Helenius, A. (2002). Endocytosis via caveolae. Traffic (Copenhagen, Denmark) 3, 311-320.

Pelkmans, L., Kartenbeck, J., and Helenius, A. (2001). Caveolar endocytosis of simian virus 40 reveals a new two-step vesicular-transport pathway to the ER. Nature cell biology 3, 473-483.

Pelkmans, L., Puntener, D., and Helenius, A. (2002). Local actin polymerization and dynamin recruitment in SV40-induced internalization of caveolae. Science (New York, NY 296, 535-539.

Pho, M.T., Ashok, A., and Atwood, W.J. (2000). JC virus enters human glial cells by clathrin-dependent receptor-mediated endocytosis. Journal of virology 74, 2288-2292.

Qian, M., Cai, D., Verhey, K.J., and Tsai, B. (2009). A lipid receptor sorts polyomavirus from the endolysosome to the endoplasmic reticulum to cause infection. PLoS pathogens 5, e1000465.

Querbes, W., Benmerah, A., Tosoni, D., Di Fiore, P.P., and Atwood, W.J. (2004). A JC virus-induced signal is required for infection of glial cells by a clathrin- and eps15-dependent pathway. Journal of virology 78, 250-256.

Querbes, W., O'Hara, B.A., Williams, G., and Atwood, W.J. (2006). Invasion of host cells by JC virus identifies a novel role for caveolae in endosomal sorting of noncaveolar ligands. Journal of virology 80, 9402-9413.

Rainey-Barger, E.K., Magnuson, B., and Tsai, B. (2007). A chaperone-activated nonenveloped virus perforates the physiologically relevant endoplasmic reticulum membrane. Journal of virology 81, 12996-13004.

Riboni, L., and Tettamanti, G. (1991). Rapid internalization and intracellular metabolic processing of exogenous ganglioside by cerebellar granule cells differentiated in culture. Journal of neurochemistry 57, 1931-1939.

Rink, J., Ghigo, E., Kalaidzidis, Y., and Zerial, M. (2005). Rab conversion as a mechanism of progression from early to late endosomes. Cell 122, 735-749.

Romer, W., Berland, L., Chambon, V., Gaus, K., Windschiegl, B., Tenza, D., Aly, M.R., Fraisier, V., Florent, J.C., Perrais, D., et al. (2007). Shiga toxin induces tubular membrane invaginations for its uptake into cells. Nature 450, 670-675.

Schelhaas, M., Malmstrom, J., Pelkmans, L., Haugstetter, J., Ellgaard, L., Grunewald, K., and Helenius, A. (2007). Simian Virus 40 depends on ER protein folding and quality control factors for entry into host cells. Cell 131, 516-529.

Schwarzmann, G. (2001). Uptake and metabolism of exogenous glycosphingolipids by cultured cells. Seminars in cell & developmental biology 12, 163-171.

Sekiguchi, K., Franke, A.J., and Baxt, B. (1982). Competition for cellular receptor sites among selected aphthoviruses. Archives of virology 74, 53-64.

Shieh, M.T., WuDunn, D., Montgomery, R.I., Esko, J.D., and Spear, P.G. (1992). Cell surface receptors for herpes simplex virus are heparan sulfate proteoglycans. The Journal of cell biology 116, 1273-1281.

Skehel, J.J., and Wiley, D.C. (2000). Receptor binding and membrane fusion in virus entry: the influenza hemagglutinin. Annual review of biochemistry 69, 531-569.

Smith, A.E., and Helenius, A. (2004). How viruses enter animal cells. Science (New York, NY 304, 237-242.

Smith, A.E., Lilie, H., and Helenius, A. (2003). Ganglioside-dependent cell attachment and endocytosis of murine polyomavirus-like particles. FEBS letters 555, 199-203.

Sonnichsen, B., De Renzis, S., Nielsen, E., Rietdorf, J., and Zerial, M. (2000). Distinct membrane domains on endosomes in the recycling pathway visualized by multicolor imaging of Rab4, Rab5, and Rab11. The Journal of cell biology 149, 901-914.

Starr, T., Ng, T.W., Wehrly, T.D., Knodler, L.A., and Celli, J. (2008). Brucella intracellular replication requires trafficking through the late endosomal/lysosomal compartment. Traffic (Copenhagen, Denmark) 9, 678-694.

Stehle, T., Gamblin, S.J., Yan, Y., and Harrison, S.C. (1996). The structure of simian virus 40 refined at 3.1 A resolution. Structure 4, 165-182.

Stehle, T., and Harrison, S.C. (1996). Crystal structures of murine polyomavirus in complex with straight-chain and branched-chain sialyloligosaccharide receptor fragments. Structure 4, 183-194.

Stehle, T., Yan, Y., Benjamin, T.L., and Harrison, S.C. (1994). Structure of murine polyomavirus complexed with an oligosaccharide receptor fragment. Nature 369, 160-163.

Stenmark, H., Parton, R.G., Steele-Mortimer, O., Lutcke, A., Gruenberg, J., and Zerial, M. (1994). Inhibition of rab5 GTPase activity stimulates membrane fusion in endocytosis. The EMBO journal 13, 1287-1296.

Tessitore, A., del, P.M.M., Sano, R., Ma, Y., Mann, L., Ingrassia, A., Laywell, E.D., Steindler, D.A., Hendershot, L.M., and d'Azzo, A. (2004). GM1-ganglioside-mediated activation of the unfolded protein response causes neuronal death in a neurodegenerative gangliosidosis. Molecular cell 15, 753-766.

Tong, G.M., Rajah, T.T., and Pento, J.T. (2000). The differential influence of EGF, IGF-I, and TGF-beta on the invasiveness of human breast cancer cells. In Vitro Cell Dev Biol Anim 36, 493-494.

Tsai, B. (2007). Penetration of nonenveloped viruses into the cytoplasm. Annual review of cell and developmental biology 23, 23-43.

Tsai, B., Gilbert, J.M., Stehle, T., Lencer, W., Benjamin, T.L., and Rapoport, T.A. (2003). Gangliosides are receptors for murine polyoma virus and SV40. The EMBO journal 22, 4346-4355.

Tsai, B., and Qian, M. Cellular Entry of Polyoma viruses. Current topics in microbiology and immunology.

Vitner, EB., Platt, FM., Futerman, AH. (2010). Common and uncommon pathogenic cascades in lysosomal storage diseases. J Biol Chem 2;285(27):20423-7.

Wang, D., Bresnahan, W., and Shenk, T. (2004). Human cytomegalovirus encodes a highly specific RANTES decoy receptor. Proceedings of the National Academy of Sciences of the United States of America 101, 16642-16647.

Whittaker, G.R. (2003). Virus nuclear import. Advanced drug delivery reviews 55, 733-747.

Whittaker, G.R., and Helenius, A. (1998). Nuclear import and export of viruses and virus genomes. Virology 246, 1-23.

Wolf, A.A., Jobling, M.G., Saslowsky, D.E., Kern, E., Drake, K.R., Kenworthy, A.K., Holmes, R.K., and Lencer, W.I. (2008). Attenuated endocytosis and toxicity of a mutant cholera toxin with decreased ability to cluster ganglioside GM1 molecules. Infection and immunity 76, 1476-1484.

Wu, S., Xie, P., Welsh, K., Li, C., Ni, C.Z., Zhu, X., Reed, J.C., Satterthwait, A.C., Bishop, G.A., and Ely, K.R. (2005). LMP1 protein from the Epstein-Barr virus is a

structural CD40 decoy in B lymphocytes for binding to TRAF3. The Journal of biological chemistry 280, 33620-33626.

Yang, W., Gelles, J., and Musser, S.M. (2004). Imaging of single-molecule translocation through nuclear pore complexes. Proceedings of the National Academy of Sciences of the United States of America 101, 12887-12892.

Zeng, Y., Pinard, M., Jaime, J., Bourget, L., Uyen Le, P., O'Connor-McCourt, M.D., Gilbert, R., and Massie, B. (2008). A ligand-pseudoreceptor system based on de novo designed peptides for the generation of adenoviral vectors with altered tropism. The journal of gene medicine 10, 355-367.

Zerial, M., and McBride, H. (2001). Rab proteins as membrane organizers. Nat Rev Mol Cell Biol 2, 107-117.

Zhuang, X. (2009). Nano-imaging with Storm. Nat Photonics 3(7): 365–367.